FACULTY OF SCIENCE AND TECHNOLOGY

MASTER'S THESIS

Study programme / specialisation: Master of Science, Structural and Mechanical Engineering / Structural Engineering	The (spring/autumn) semester, (year) Spring, 2023 Open / ~~Confidential~~
Author: Hans-Martin Ingebrigtsen Steinsvik	
Supervisor at UiS: Professor Samindi Samarakoon Co-supervisor: External supervisor(s):	
Thesis title: Study the behavior of prestressed concrete deep beams using FEM simulations	
Credits (ECTS): 30	
Keywords: Concrete Deep Beam Prestressed reinforcement Principal tensile and compressive stress Strut and Tie model	Pages: 103 + appendix: 45 Stavanger, (date) 13.06.2023

Abstract

The objective of this master‘s thesis is to study and analyze the behavior of prestressed concrete deep beams and how prestressing changes the strut and tie model.

The method used for analyzing the behavior is finite element modeling in ATENA. The strut and tie models are developed by analyzing the principal tensile and compressive stresses for the different models at yield. The models are analyzed without prestressed reinforcement, with 25 MPa prestressed reinforcement and 100 MPa prestressed reinforcement. In order to analyze how different load patterns affect the principal stresses, this paper analyzes three different load patterns.

In total, two different models are analyzed, each containing three different load patterns. The models are analyzed without prestressed reinforcement, with 25 MPa and 100 MPa prestressing. The prestressed reinforcement is placed straight and curved. One of the models is also analyzed with two openings with three different placements of the openings.

The results show a decrease in the distance between the bottom of the deep beam and the tie when adding prestressed reinforcement. A proposed equation to calculate the distance from the bottom of the deep beam to the tie is included in this thesis. The equation takes both the height of the deep beam and the amount of prestressing into account. The equation is based on the results gathered in this thesis.

Preface

This thesis is the final of a two-year master's degree program; Master of Science, Structural and Mechanical Engineering with a specialisation in Structural Engineering, at the University of Stavanger. This thesis results from the work done through the spring of 2023.

It has been both rewarding and challenging to work with this master thesis, one of the biggest challenges was to learn how to use ATENA and understand the results. It was rewarding when the models ran successfully and the development of the strut and tie models. Another challenge was that little work on this subject had been done previously.

I want to thank my supervisor Professor Samindi Samarakoon, for all the help with this master's thesis.

University of Stavanger

Stavanger, June 2023

Hans-Martin Ingebrigtsen Steinsvik

Contents

List of Figures

List of Tables

1 Introduction

The object of this master thesis is to study the behavior of prestressed concrete deep beams and how prestressing changes the strut and tie model.

1.1 Background

When designing a tall building, a challenge is to achieve free spaces in the lower story, this can be a reception, a parking garage, or a storage. The use of deep beams can help minimize the number of columns. A reinforced concrete deep beam is a structural element characterized by its height-to-span ratio. Eurocode states that the ratio is minimum three [3].

Compared to conventional reinforced concrete beams, which have a smaller height and a larger depth, a deep beam has a much larger span, while the depth (thickness) is smaller in the perpendicular direction. This unique geometry allows deep beams to resist higher bending moments and shear forces than shallow beams. This makes a deep beam an ideal choice for a long-span structure that requires a significant load-carrying capacity [4].

Reinforced concrete deep beams are commonly used for load-bearing structures that need to distribute heavy loads over long spans. They are commonly used in a variety of applications, such as pile foundation walls and shear walls which are designed to resist lateral forces. Overall, reinforced concrete deep beams offer an effective and efficient solution for a wide range of engineering and construction challenges.

The strut and tie model is an approach that represents the stress distribution in atypical elements or sections of concrete, such as deep beams, beams with openings, and others. It is a reliable tool for the treatment of discontinuity regions.

Reinforced concrete deep beams are subjected to multiple different factors, this includes the clear span-to-height ratio, loading type, location of the applied loads, type of prestressed reinforcement, amount and quality of web reinforcement, dimensions of bearing plates, and the compressive strength of the concrete. Due to the multiple numbers of variables, this thesis will have the same parameters for the type of prestressed reinforcement, quality of web reinforcement, dimensions of bearing plates, and the same compressive strength of the

concrete through all models. The parameters that will be changed are the span-to-height ratio, loading type, amount of prestressing, and how the prestressed reinforcement is placed.

1.1.1 Objectives of the thesis

The main objectives for this thesis are:

- Analyze the behavior of a prestressed concrete deep beam
- Suggest an equation for calculating the distance from the bottom of the deep beam to the tie, that includes the height of the beam and the jacking force

1.2 Scope/limitation

The scope of this master thesis is to analyze the behavior of prestressed concrete deep beams and analyze how the strut and tie model changes when adding prestressed reinforcement. In order to analyze how the strut and tie model changes when adding prestressing, the principal stresses are compared across different models. Different parameters are changed; this includes the height of the deep beam, load patterns, amount of prestressing, different curvature of the prestressed reinforcement, adding openings, and changing their positions.

A limitation of this thesis is that there are done little work on this subject previously. Ideally, it would include an actual prestressed concrete deep beam and test it with different load patterns and amounts of prestressing. ATENA does not provide a method to analyze the flow of forces through a member which would be the preferred method for analyzing the deep beams.

1.3 Method

The aim of the thesis is to develop an understanding of how the principal stresses change when adding prestressed reinforcement to a concrete deep beam. To do so, it is used finite element software ATENA.

Finite Element Method (FEM) simulations are widely used in engineering research and practice to study the behavior of structures, materials, and systems under different

scenarios. They allow researchers to investigate complex phenomena, optimize designs, and make predictions about the performance of a system. FEM simulations can also be used to evaluate the effects of design changes, assess the structural integrity of components, and analyze failure modes, among other applications [5].

Simulation based-research method is used in this thesis. Because simulation-based research is a type of research method that involves using computerized or mathematical models to simulate real-world situations, systems, or processes in order to study their behavior, make predictions, or test hypotheses [6]. FEM simulations can be considered a type of simulation-based research method. FEM is a numerical technique used in engineering and other fields to approximate and solve complex problems involving physical systems, such as structural mechanics, heat transfer, fluid dynamics, and electromagnetic fields [7].

FEM simulations typically involve defining the geometry, material properties, and boundary conditions of the system, and then using numerical methods to solve the resulting equations, such as the finite element method, finite difference method, or finite volume method. The results of FEM simulations can include stress and strain distributions, displacement fields, temperature profiles, and other relevant parameters, which can be analyzed and interpreted to draw conclusions and make recommendations.

FEM simulations can be classified as linear or nonlinear, depending on the type of material behavior or system response being modeled.

1.4 Outline of the thesis

- Chapter 1: Introduction
- Chapter 2: Theory
- Chapter 3: Material and Method
- Chapter 4: Modeling in ATENA
- Chapter 5: Results from ATENA
- Chapter 6: Discussion and Conclusion

2 Theory

2.1 Deep beam

A deep beam is defined as a member which the span is less than three times the overall section depth [8]. Deep beams can be used as a wall that is simply supported, this gives a bending moment under the wall, which is different from a regular wall which is supported under the entire wall.

2.2 Discontinuity regions

A structural member may be divided into B-regions or D-regions, in the B-region, which applies that the Bernoulli hypothesis is valid. The Bernoulli-Euler beam theory makes two primary assumptions [9]:

- Plane sections remain plain
- Deformed beam angles are small

Discontinuities regions, D-regions define areas of the structural members where the beam theory does not apply. Where the assumption of linear distribution of strains is not valid. Prior to any cracking, an elastic stress field exists; cracking interrupts the stress field, causing a change in the internal forces [1].

2.3 Lower-Bound Theorem

Lower-Bound Theorem states, "if an equilibrium distribution of stress can be found which balance the applied loads, and is everywhere below yield or at yield, the structure will not collapse or will be just at the point of collapse" [10]. The theory has different versions depending on the material. For a steel frame, the method is called the statically method, for concrete structures the method is called the strut-and-tie model method [10].

2.4 Strut and Tie modeling

Strut and tie model (STM) is an approach that efficiently represents intricate stress distributions as triangulated models. This method is founded on the truss analogy and can be employed for various components of concrete structures. It is commonly utilized to design atypical elements or sections of concrete structures, such as pile caps, corbels, deep beams, beams with openings, connections, and others, where standard beam theory may not be applicable [11].

The STM is based on the lower bound theorem of limit analysis, which provide a safe solution. The complex stress distribution in a structure is idealized as trusses carrying the imposed loading through the structure to its support. An STM consists of compression struts and tension ties. "STM is currently recognized as the most reliable tool for the treatment of discontinuity regions (D-region)" [10].

The flow of forces can be traced through the structure using the load path method, then the load path is replaced with polygons, and additional struts and ties are added to achieve equilibrium of forces. However, the STM can be simplified using elastic finite analysis and obtain the elastic stresses and principal stress direction, which is the method used in this thesis [10].

The STM consists of three elements, struts, ties, and nodes. Strut is a compression member which represents the compression field. Ties are the tension member where the force is restrained by normal reinforcement, prestressing, or the concrete tensile strength. Nodes are the point where strut and ties connect; the nodes are classified as a C-C-C node which resists three compressive forces, or a C-C-T node which resists two compressive forces and one tensile force. It could also be a C-T-T node and a T-T-T node [10].

In developing an STM, it is essential to control the equilibrium of forces in each node. That is done using the formulas $\sum F_y = 0$ and $\sum F_x = 0$. It is also an objective to design it with the least number of ties.

2.5 Analyses and Behavior of Deep Beams

There are meaningful to analyze deep beams in an elastic state prior to cracking. Cracking will occur at one-third to one-half of the ultimate load for a deep beam. After cracks develop a redistribution of the stress because there is no tension across the cracks [1].

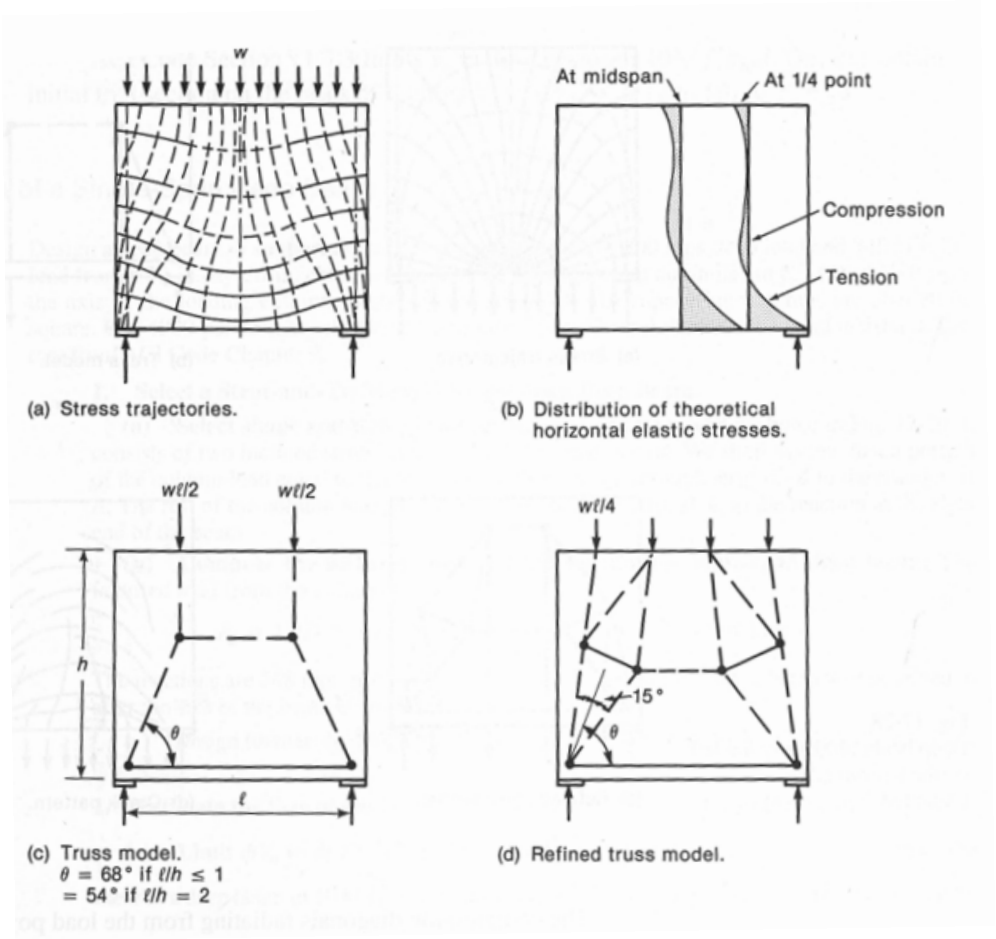

Figure 2.1: Stress trajectories [1]

In Figure 2.1 a, the dashed lines are compressive stress trajectories drawn parallel to the directions on the principal compressive stress, and solid lines are tensile stress trajectories parallel to the principal tensile stress. The stress trajectories shown in Figure 2.1a can be simplified and shown in Figure 2.1c, where the solid line represents tension ties and dashed compression struts which results in the strut and tie model.

2.5.1 Principal stress

Principal stresses of an element are, in general, maximum and minimum values of the normal stresses when the shear stress is equal to zero [12]. Normal and shear stresses are developed when the load is applied to any structure. "Due to this, applied loading concentrated on a point where all three planes, X, Y, and Z, are perpendicular to that point. The resultant stress on these planes is called principal stress" [13]. Maximum principal stress are given as σ_1, which equals:

$$\sigma_1 = (\sigma_x + \sigma_y)/2 + \sqrt{((\sigma_x - \sigma_y)/2)^2 + \tau_{xy}^2} \tag{2.1}$$

Minimum principal stress are given as σ_2 which equals:

$$\sigma_2 = (\sigma_x + \sigma_y)/2 - \sqrt{((\sigma_x - \sigma_y)/2)^2 + \tau_{xy}^2} \tag{2.2}$$

σ_x = Stress in x-direction, σ_y = Stress in y-direction, τ_{xy} = Normal shear stress.

2.6 Design guidelines

The STM is added into several design codes, the method is referred in Eurocode 2 -Design of concrete sturctures - Part 1-1: General rules for buildings [3], Appendix A of ACI 318-02 [14] and the International Federation of Structural Concrete [14].

3 Material and Methods

3.1 ATENA-GiD

ATENA is a software developed by Červenka Consulting, which is an "Advanced tool for engineering nonlinear analysis. A user-friendly software for nonlinear analysis and design of reinforced structures" [15]. ATENA simulates the real behavior of reinforced concrete, including cracking, crushing, and reinforcement yielding. ATENA focuses on reinforced concrete compared with software such as ABAQUS or ANSIS, but ATENA is in the same category of advanced analysis software.

ATENA-GiD is a finite element-based software that specifies for nonlinear analysis of reinforced concrete, where there are predefined materials with their respective material parameters. The program has three main functions[16]:

- Pre processing: Input of geometrical objects, loading, boundary condition, meshing, and solution parameters
- Analysis: Real-time monitoring of the results
- Post processing: Graphical and numerical results

GiD is used for the preparation of the data and generating the mesh, and ATENA is used for analyzing the data. GiD is a general-purpose finite element pre and post-processor that is used for data preparation for ATENA [17].

3.2 Concrete

All models in the study have been constructed using C30/37 concrete, generated via the "CC3DNonLinCementious2" model. The stress-strain relationship for this concrete is illustrated in Figure 3.1a, σ_c^{ef} is the effective stress and ε^{eq} is the uniaxial strain, while the material properties are detailed in Table 3.1. These parameters were automatically generated using EN 1992 standards within GiD. The biaxial failure function for the concrete is shown in Figure 3.1b, σ_{c1} and σ_{c2} are the principal stress in concrete, f_c' is the uniaxial cylindrical strength.

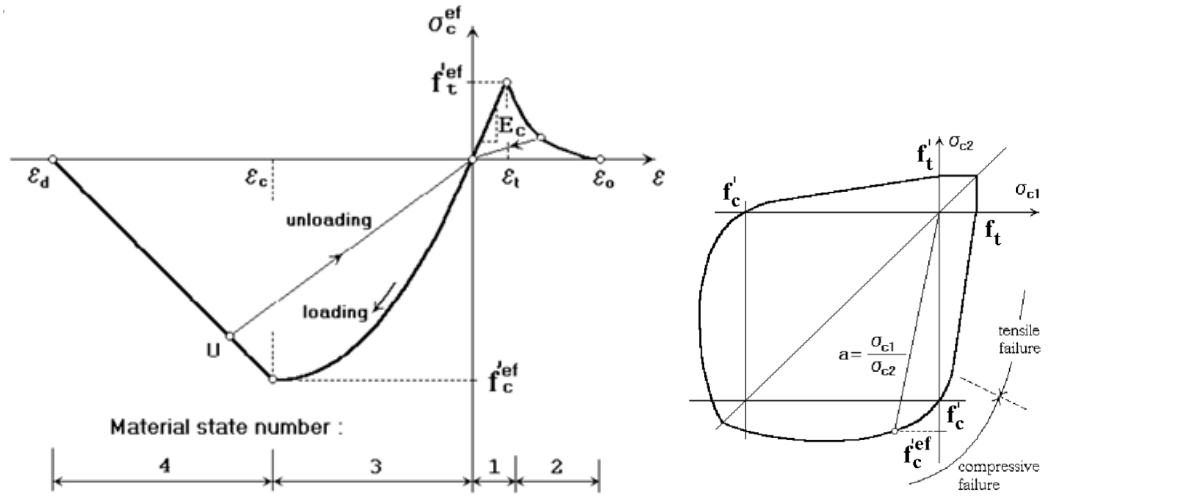

(a) Stress-strain law for concrete **(b)** Biaxial failure function for concrete

Figure 3.1: Stress-strain law and Biaxial failure function for concrete [2]

Table 3.1: Input for Concrete Deep Beam

	Deep Beam
Material	Concrete
Strength type	Cylindrical-Characteristic
Strength value	30 MPa
Safety format	Mean
Young's modulus	33550.6 MPa
Poisson ratio	0.2
Tension strength	2.9 MPa
Compression strength	-38 MPa

3.3 Steel plate and Reinforcement

The steel plates (bearing plates) were modeled using the "CC3DElastIsotropic" material recommended by ATENA, the model utilizes a Young's modulus of 200 GPa and a Poisson ratio of 0.3. The reinforcement was modeled using the "1D reinforcement" material recommended by ATENA. This model utilizes an elastic-plastic material with a yield strength of 500 MPa and a modulus of elasticity of 200 GPa.

3.3.1 Prestressed reinforcement

Prestressed reinforcement is a term used for both pre-tensioned concrete and post-tensioned concrete. When using tensioned reinforcement, you apply compression to the concrete to counteract the stresses due to the service load, which leads to reducing or even eliminating the deflection [18].

The prestressed reinforcement was modeled the same way as the reinforcement with the use of "1D reinforcement", Young's Modulus was set to 195 GPa, characteristic yield strength of 1860 MPa. In order to differentiate how the prestressed reinforcement is fixed at jacking vs after the concrete is hardened, it is necessary to define two materials with the same properties except how they are fixed at ends. Therefore Prestressed reinforcement and Prestressed reinforcement bar are added. In interval 2, the Prestressed reinforcement is added to the prestressed line and has the properties of being jacked at the start and fixed at the end. In interval 3, the conditions are set to activate the prestressed reinforcement bar for the line, and the parameters for that prestressed bar are fixed at both ends. The different intervals will be explained in Chapter 4.

Table 3.2: Input for Prestressed reinforcement and Prestressed reinforcement bar

	Prestressed reinforcement	**Prestressed reinforcement bar**
Material	Steel/Reinforcement	Steel/Reinforcement
Type of reinforcement	Reinforcement	Reinforcement
Young's Modulus	195 GPa	195 GPa
Characteristic Yield Strength	1860 MPa	1860 MPa
Class if Reinforcement	C	C
Safety Format	Mean	Mean
Geometrical Non-Linearity	Linear	Linear
Geom Type	Internal Cable	Internal Cable
Bar End	Fixed **END**	Fixed **BOTH**

3.3.1.1 Pretensioned concrete

The tendons are initially tensioned, then the concrete is casted around the tendons and cured. When the concrete has reached enough strength, the wires are released, leading to the tendons compressing the concrete. The prestress is imparted in the concrete with the bond between the concrete and the steel [18].

3.3.1.2 Post-tensioned concrete

The procedure for post-tensioned concrete is to cast the concrete around a hollow duct. Then the tendons are threaded through the ducts and jacked either from one or both sides and then anchored. The ducts with the tendons are usually filled with grout which gives a better bonding between the tendons and the concrete [18].

Within post-tensioned concrete there are two main types, it is either bonded or unbonded post-tensioned. The bonded one means that there is a bond between the tendons and the concrete, it is done by filling the ducts with grout. A bonded post-tensioned gives more control over the crack development and a higher strength for the concrete. Unbonded post-tensioned concrete allows the tendons to move freely in the longitudinal direction. Since the ducts are not filled, it is essential to apply corrosion protection to the tendons when using unbonded.

4 Modeling in ATENA

The scope of the thesis is to get an understanding of how prestressing of a concrete deep beam changes the strut and tie model. In order to get an understanding of how prestressing changes the strut and tie model, different deep beams are studied. This includes different sizes, load patterns, and amount of prestressing. In order to have a system of which deep beam is analyzed with which load pattern, the different models are named 1.1, 1.2, 1.3, 2.1, 2.2, and 2.3. The first number indicates the size of the deep beam, so Model 1.1, 1.2, and 1.3 has the same dimensions. The second number indicates which load pattern is used. 1 are two-point loads, 2 are uniformly distributed load, and 3 are one-point load off center. The deep beams are analyzed with a straight prestressed cable and a curved one, with a jacking force of 25 MPa and 100 MPa. There are four different cases, Case 1 is without prestressed reinforcement, Case 2 is with straight prestressed reinforcement, Case 3 is with curved prestressed reinforcement, and Case 4 is Model 1.1 with two openings.

4.1 Development of an accurate FEM simulation model

To make an accurate FEM simulation, the modeling needs to be correct, where all the parameters regarding dimensions, material properties, boundary conditions, and loads must be correct. The process is shown in the flow chart below (Figure 4.1):

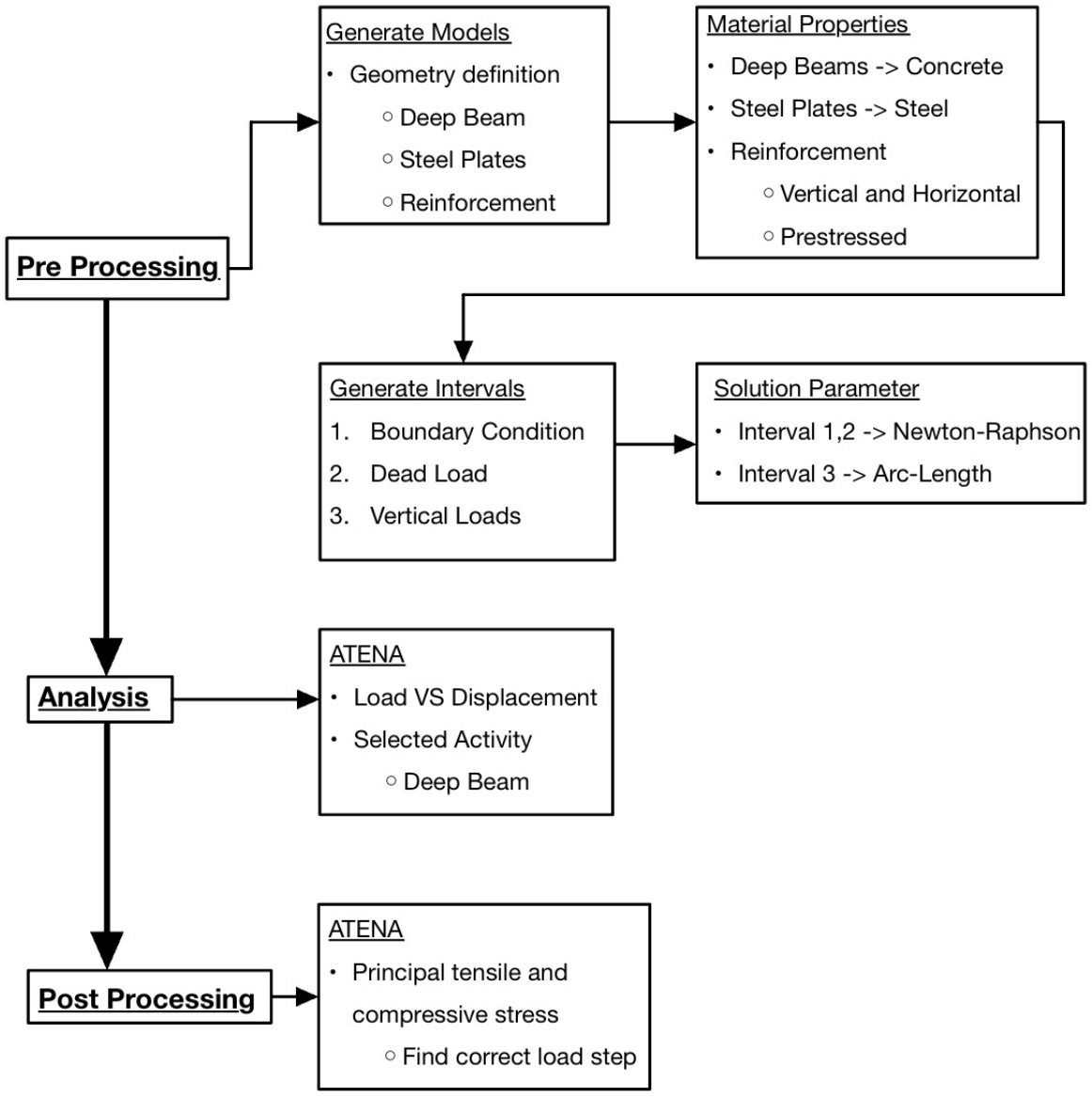

Figure 4.1: Process of generating models

4.2 Finite element method

In order to establish a good understanding of how a prestressed deep beam changes the STM compared to a regular reinforced concrete deep beam, it is necessary to use the finite element method (FEM) to get the correct answer.

4.2.1 Solution parameters in ATENA

There are several methods for analyzing and solving nonlinear equations in ATENA. All of the different methods need to solve a set of linear algebraic equations in the form:

$$A \cdot x = b \tag{4.1}$$

Where A,x,b stands for a global matrix and vectors of unknown variables and rhs of the problem [2]. For analyzing the behavior of prestressed concrete deep beam Newton-Raphson and Arc-length method is used.

4.2.1.1 Newton-Raphson method

The chosen method is Newton-Raphson (N-R) for intervals 1 and 2, which are boundary conditions and dead load, respectively. N-R can be explained as "a way of extracting a root of a polynomial" [19]. In other words, the N-R method is a quick way to find a good approximation of the root of a real-valued function. "N-R method keeps the load increment unchanged and iterates displacement until equilibrium is satisfied "[19]. The Newron-Raphson method is illustrated in Figure 4.2

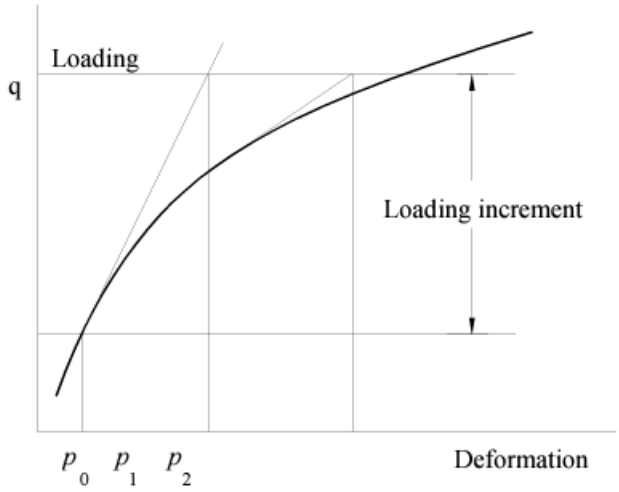

Figure 4.2: Newtons-Raphson method [2]

The N-R method employs incremental step-by-step analysis to establish the set of nonlinear equations which is given in Equations 4.2, 4.3 and 4.4.

$$\mathbf{K}(p) \cdot \Delta p = q - f(p) \tag{4.2}$$

$$f(k \cdot p) \neq k \cdot f(p) \tag{4.3}$$

$$\mathbf{K}(p) \neq \mathbf{K}(p + \Delta p) \tag{4.4}$$

- q is the vector of total applied joint loads
- $f(p)$ is the vector of internal joint forces
- Δp is the deformation increment due to the loading increment
- p is the deformations of the structure prior to load increment
- $\mathbf{K}(p)$ is the stiffness matrix, relating loading increments to deformation increments

Equation 4.2 represents the out-of-balance force during a loading increment.

4.2.1.2 Arc-length method

For interval 3 which represents the vertical load, the method for the solution parameter is Arc-Length. The Arc-Length method is a form of N-R iteration, "within each new level of external load, iterative increments of load and displacement are adjusted in such way to keep the process from doubling back on itself when the curve acquires a negative slope"[19]. The Arc-length method is illustrated in Figure 4.3

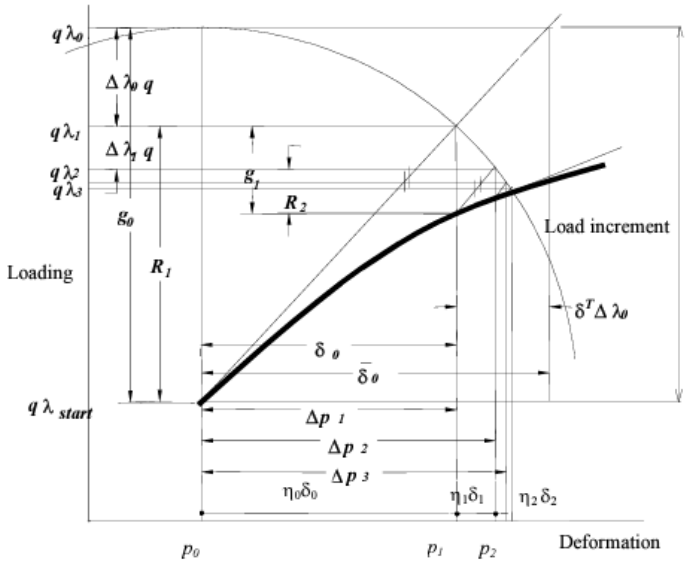

Figure 4.3: Arc-length method [2]

The following equations are a set of nonlinear equations suitable for iterative solutions for the arc-length method:

$$\mathbf{K}(p_{i-1}) \cdot \Delta P_i = \lambda \cdot q - f(p_{i-1}) = \lambda \cdot q - f_{i-1} \tag{4.5}$$

$$p_i = p_{i-1} + \Delta P_i = P_{i-1} + \eta_{i-1} \cdot \delta_{i-1} \tag{4.6}$$

$$\Delta p_i = \Delta p_{i-1} + \eta_{i-1} \cdot \delta_{i-1} \tag{4.7}$$

$$\lambda_i = \lambda_{i-1} + \Delta\lambda_{i-1} \tag{4.8}$$

- λ defines the new loading factor
- η scalar used to accelerate solutions

4.2.1.3 Convergence criterion

Equation 4.5 is nonlinear, it is therefore necessary to iterate until the convergence criterion is satisfied [2]. A convergence criterion is a criterion used to verify the convergence of a sequence, it is used to determine when an iterative method has reached a solution with sufficient accuracy [20]. ATENA supports the following possible criterion's:

$$\sqrt{\frac{\Delta p_i^T \cdot \Delta p_i}{p_i^T \cdot p_i}} \leq \varepsilon_{rel.disp} \tag{4.9}$$

$$\sqrt{\frac{(q - f(p_{i-1}))^T \cdot (q - f(p_{i-1}))}{f(p_i)^T \cdot f(p_i)}} \leq \varepsilon_{rel.force} \tag{4.10}$$

$$\sqrt{\frac{\Delta p_i^T (q - f(p_{i-1}))}{p_i^T \cdot f(p_i)}} \leq \varepsilon_{rel.energy} \tag{4.11}$$

$$\sqrt{\frac{max((q^k - f^k(p_{i-1}))) \cdot max((q^k - f^k(p_{i-1})))}{max(f^k(p_i)) \cdot max(f^k(p_i))}} \leq \varepsilon_{abs.force} \tag{4.12}$$

Condition 4.9 checks for the norm of deformation change during the last iteration, condition 4.10 checks the norm of the out-of-balance force. Condition 4.11 checks out-of-balance energy, and condition 4.12 checks the out-of-balance forces in terms of maximum components. ε is the convergence limit set to 0.01.

4.2.2 Interval data- Load steps

In GiD an assign intervals which corresponds to load steps in ATENA, the interval data defines the loading history for the structure. This includes boundary conditions, the definition of loading, and assigning the chosen solution parameters.

4.2.2.1 Interval 1

Interval 1 defines the boundary conditions, this includes the supports and how the plates are connected to the deep beam. In interval 1 the measuring points are defined, this includes external forces and displacement. The connection between the plates and the deep beam is done with the use of masters and slaves, the deep beam is defined as the master and the plates as slaves. The master-slave boundary condition specifies that "all available degrees of one finite node is equal to degrees of freedom of another node" [2]. In order to connect the nodes from different materials to each other, the master-slave connections are used. The generate multiple steps is activated with an interval multiplier of 1 and the number of load steps is 1.

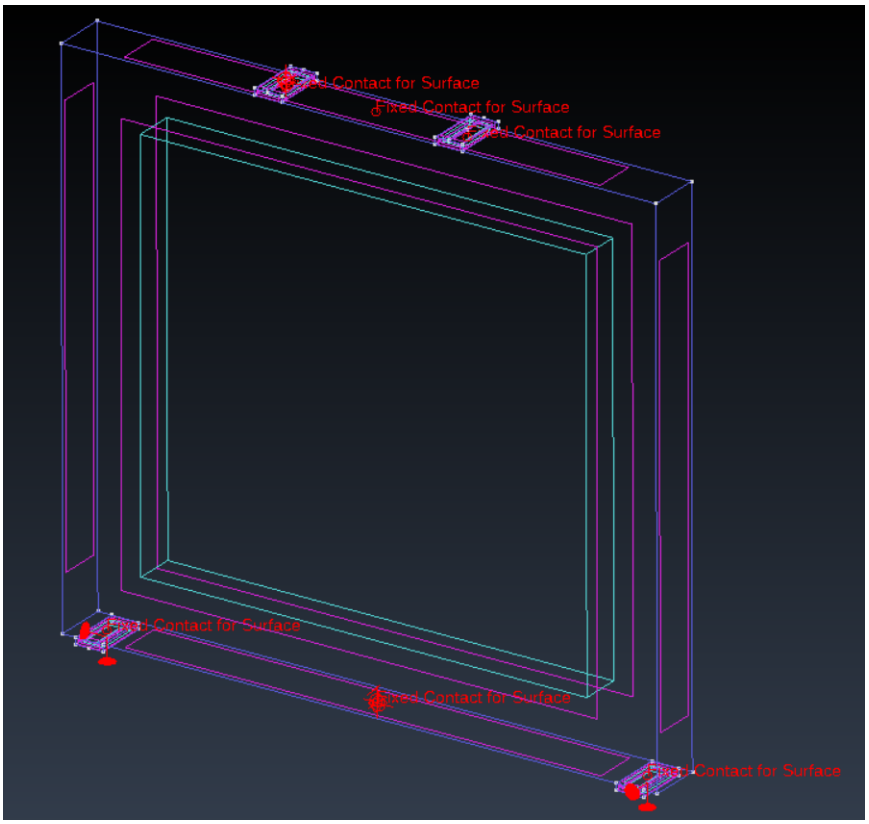

Figure 4.4: Conditions for interval 1

Figure 4.4 shows which conditions are defined in interval 1, the supports are marked with the line and circle at the bottom plates, and the master-slave connections are designated with "Fixed Contact for Surface". The measuring points are displayed with a circle with a cross in the middle, shown on the top left plate and in the middle of the bottom of the beam.

4.2.2.2 Interval 2

Interval 2 defines the dead load and the initial loads before the external loads are applied, the dead load is shown in Figure 4.5 with the red arrow and the red marks on the reinforcement. This interval takes an additional load case into account, in this case, it is load case 1. For the models with prestressed reinforcement, the initial stressing is taken into account, in order to do this, the applied force is added in this interval, shown with "Prestressing for Reinf Line". The generate multiple steps is activated with an interval multiplier of 1, and the number of load steps is 1.

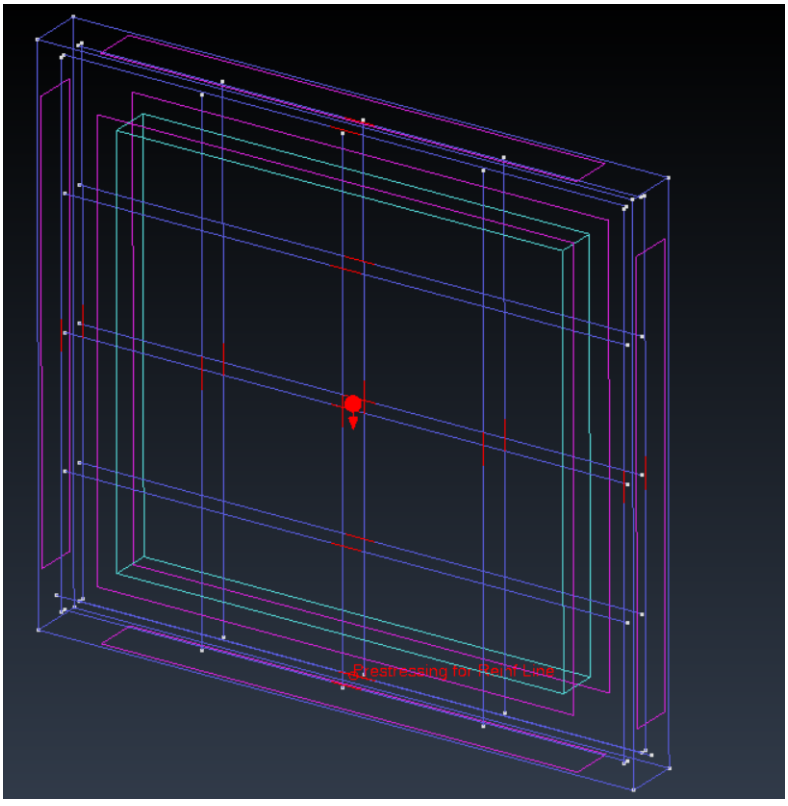

Figure 4.5: Conditions for interval 2

4.2.2.3 Interval 3

Interval 3 defines the vertical loads as external loads and how the conditions for the prestressed bar are, these conditions are shown in Figure 4.6 with the red arrows (vertical loads) and red mark at the prestressed reinforcement. In interval 3, the Prestressed reinforcement bar is activated to the prestressed reinforcement line, which is fixed at both ends. The generate multiple steps is activated with an interval multiplier of 2, and the number of load steps is 100. Interval 3 takes an additional load case into account, this is load case 1. The solution parameters are also activated, the solution parameter for interval 3 is arc length, the optimized band is Sloan, the stiffness type is Elastic Predictor and the solver is Pardiso.

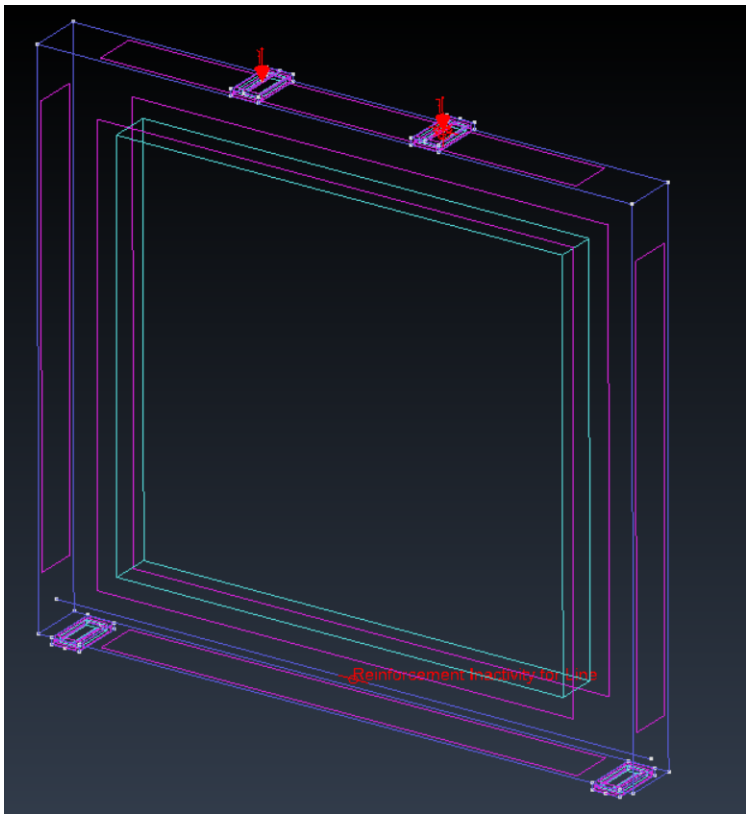

Figure 4.6: Conditions for interval 3

4.2.3 Meshing

In order to accurately simulate the behavior of the concrete a three-dimensional eight-node hexahedral isoparametric element with a mesh size of 20mm was used.

4.3 Model 1

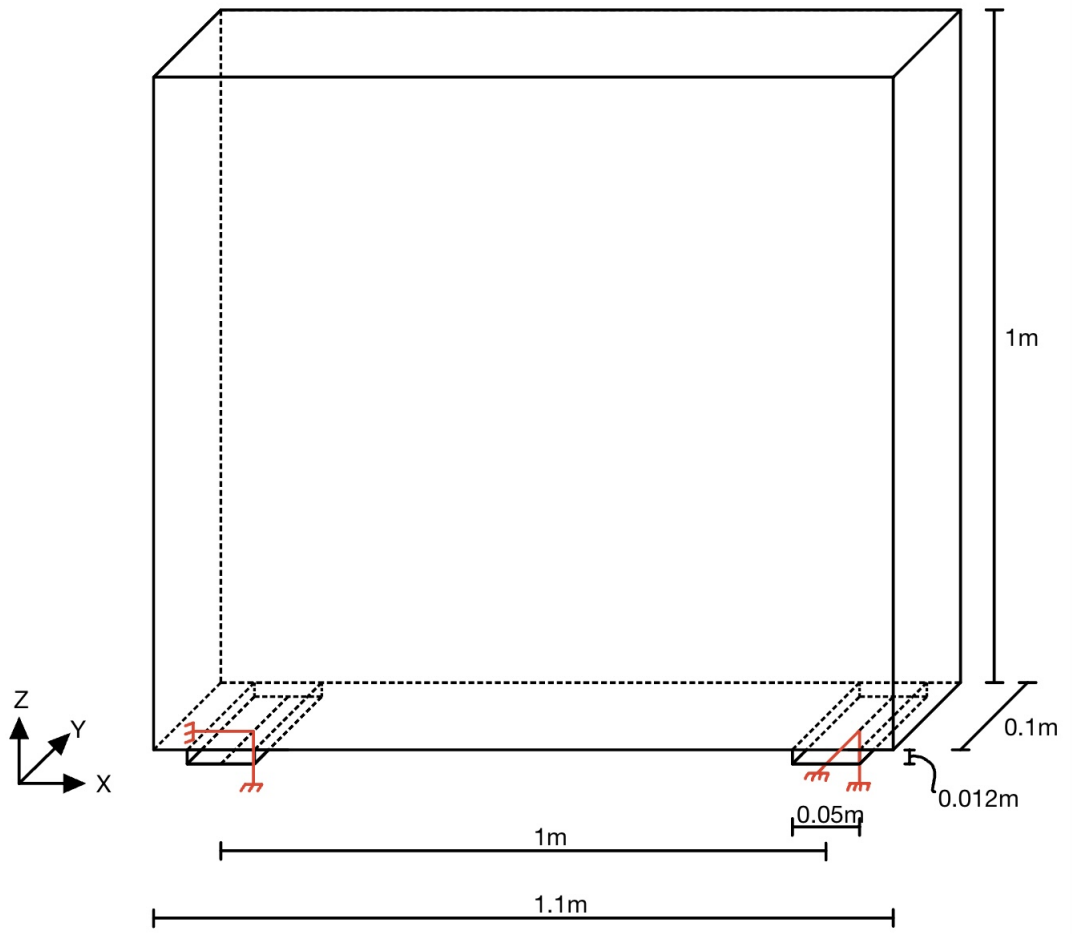

Figure 4.7: Dimensions of Model 1

Figure 4.7 shows the dimensions of Model 1. Model 1 is a deep beam with the dimensions of a height of 1m, a length of 1.1m, a distance between supports of 1m, and a depth of 0.1m. The deep beam is supported at two plates, for the plate to the left it is supported in Z-and X-direction, and for the plate to the right is supported in the Z- and Y-direction. The plates have the dimensions of height of 0.012m, length of 0.05m, and depth of 0.1m.

Model 1 is reinforced with longitudinal reinforcement of ø10 c260 on both sides, horizontal reinforcement is ø10 c235. The prestressed reinforcement is tendons with a diameter of 12.5mm.

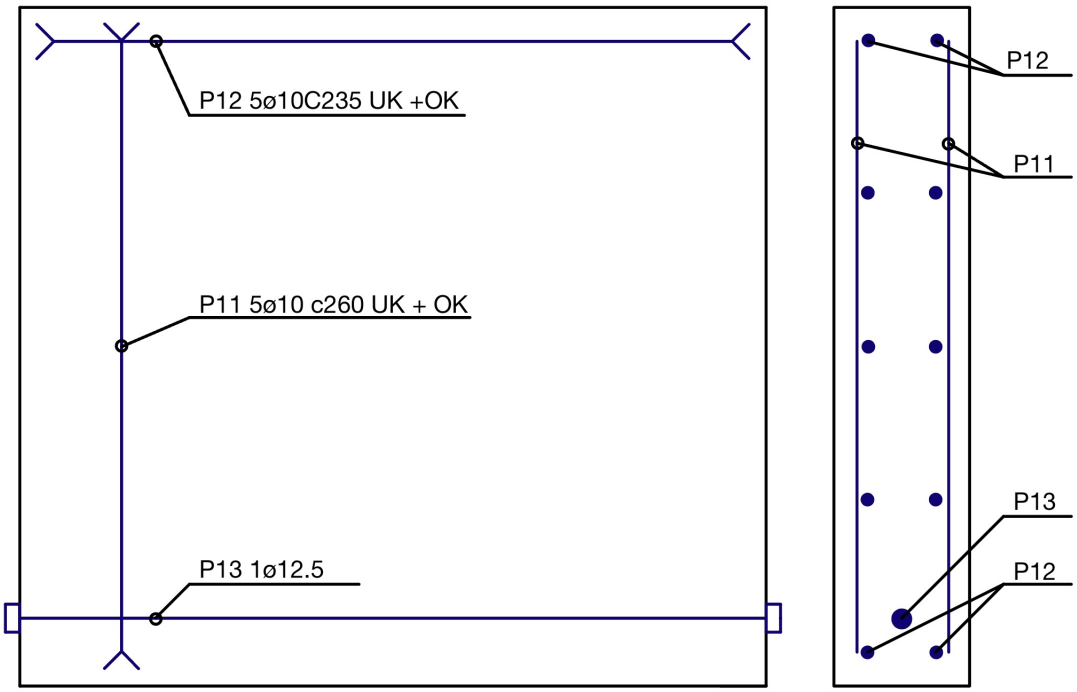

Figure 4.8: Reinforcement drawing of Model 1

Figure 4.8 shows the reinforcement drawing for Model 1 with a straight prestressed reinforcement. P11 is the vertical reinforcement, P12 is the horizontal reinforcement and P13 is the prestressed reinforcement.

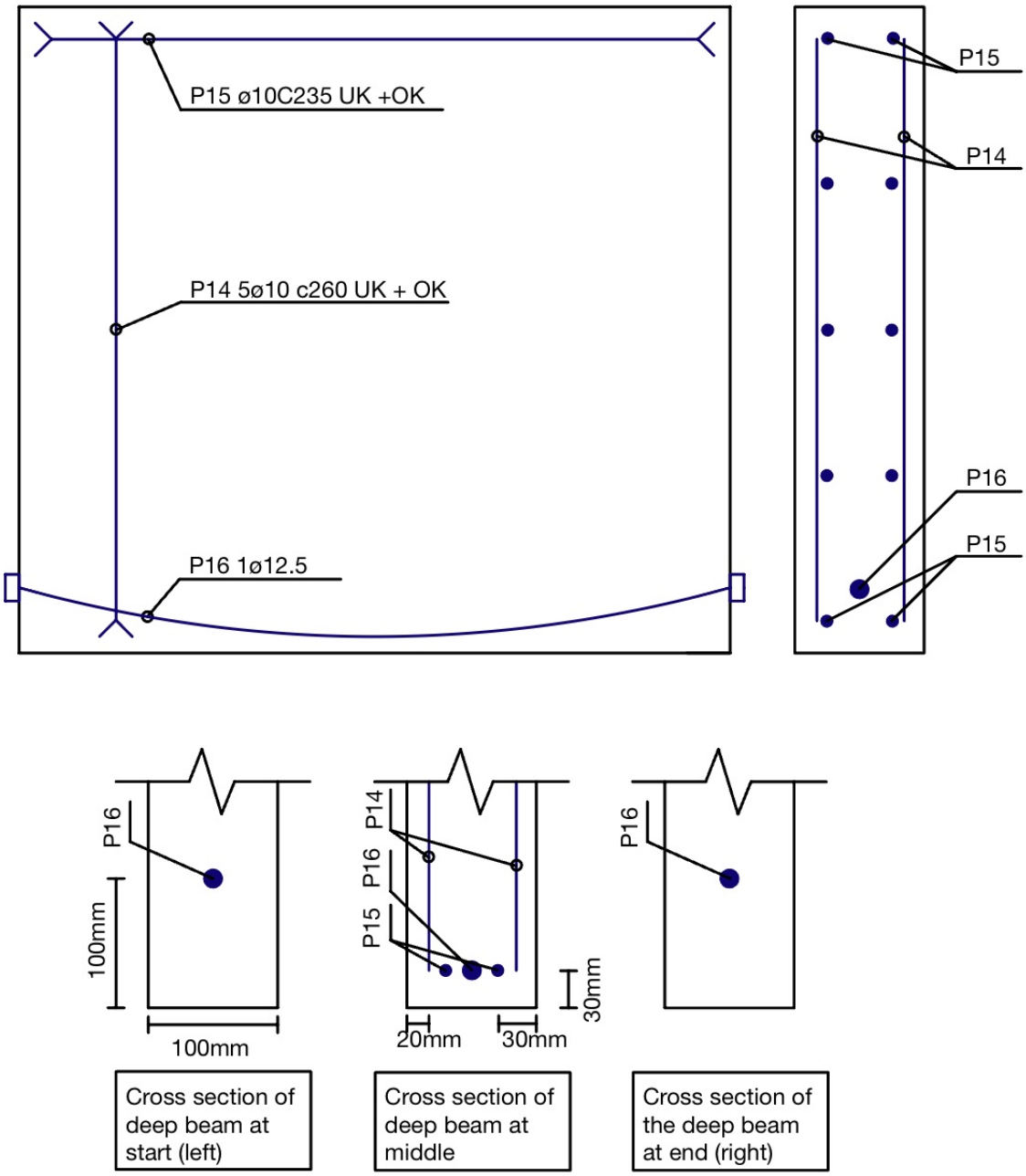

Figure 4.9: Reinforcement drawing of Model 1 with curved prestressed reinforcement

Figure 4.9 shows the reinforcement drawing for Model 1 with a curved prestressed reinforcement. P14 is the vertical reinforcement, P15 is the horizontal reinforcement, and P16 is the curved prestressed reinforcement with an eccentricity of 70mm. The same parameters for both the web reinforcement and the prestressed reinforcement are used for the one with curved and straight prestressed reinforcement.

Eurocode 2 states the minimum and maximum reinforcement for a deep beam in Chapter 9.7 [3]. The calculations for maximum and minimum vertical reinforcement are as follows: $A_{s.vmin} = 0.002 \cdot A_c$ and $A_{s.vmax} = 0.04 \cdot A_c$

- $A_c = 10 \cdot 10^4 mm^2/m$: Square section per meter
- $A_{s.vmin}$: Minimum vertical reinforcement
- $A_{s.vmax}$: Maximum vertical reinforcement

The spacing between the vertical bars is $min(3 \cdot b_v, 400mm)$, where b_v is the depth of the deep beam. The calculations give a minimum steel reinforcement area of $A_{s.vmin} = 200mm^2/m$ for both sides and a maximum of $4000mm^2/m$. Therefore the chosen vertical reinforcement for Model 1 is ø10c260 which equals a cross-section area of $A_{s.v} = 302mm^2/m$.

The calculations for minimum horizontal reinforcement for a deep beam are as follows: $A_{s.hmin} = max(0.025 \cdot A_{s.vmin}; 0.3 \cdot A_c \cdot \frac{f_{ctm}}{f_{yk}})$

- $A_{s.vmin} = 200mm^2/m$: Minimum vertical reinforcement
- $f_{ctm} = 2.9\text{MPa}$: Mean value of axial tensile strength of concrete
- $f_{yk} = 500\text{MPa}$: Characteristic yield strength of reinforcement

The maximum spacing for the horizontal reinforcement is equal to $300mm$. The chosen horizontal reinforcement for Model 1 is ø10c235 which leads to $A_{s.h} = 334mm^2/m$.

4.3.1 Model 1.1

Model 1.1 is Model 1 with two-point loads (P) on top of the deep beam which is shown in Figure 4.10. The two-point loads are located in the middle of the loading plates. The loading plates have the same dimensions as the support plates, length is 0.05m, depth is 0.1m, and height is 0.012m.

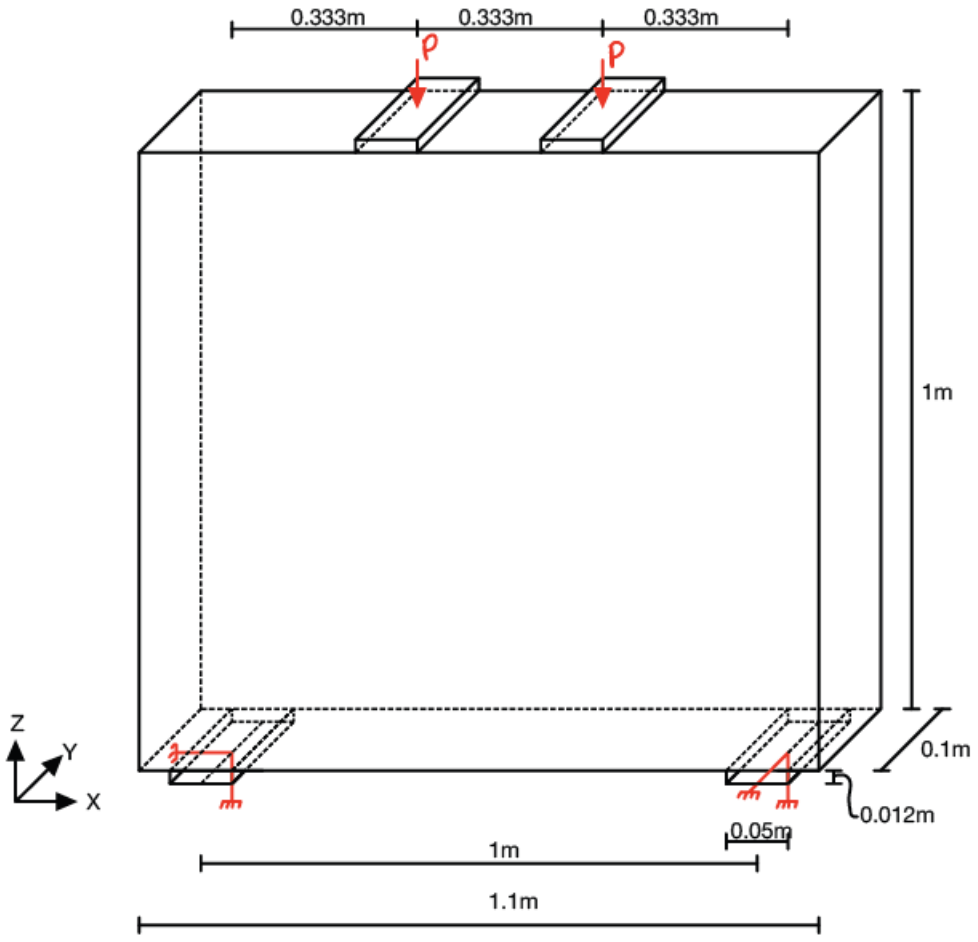

Figure 4.10: Model 1.1

4.3.2 Model 1.2

Model 1.2 is Model 1 with a uniform distributed load (q) along the top of the deep beam shown in Figure 4.11. The loading plate has the same length and depth as the top of the beam, height is 0.012m

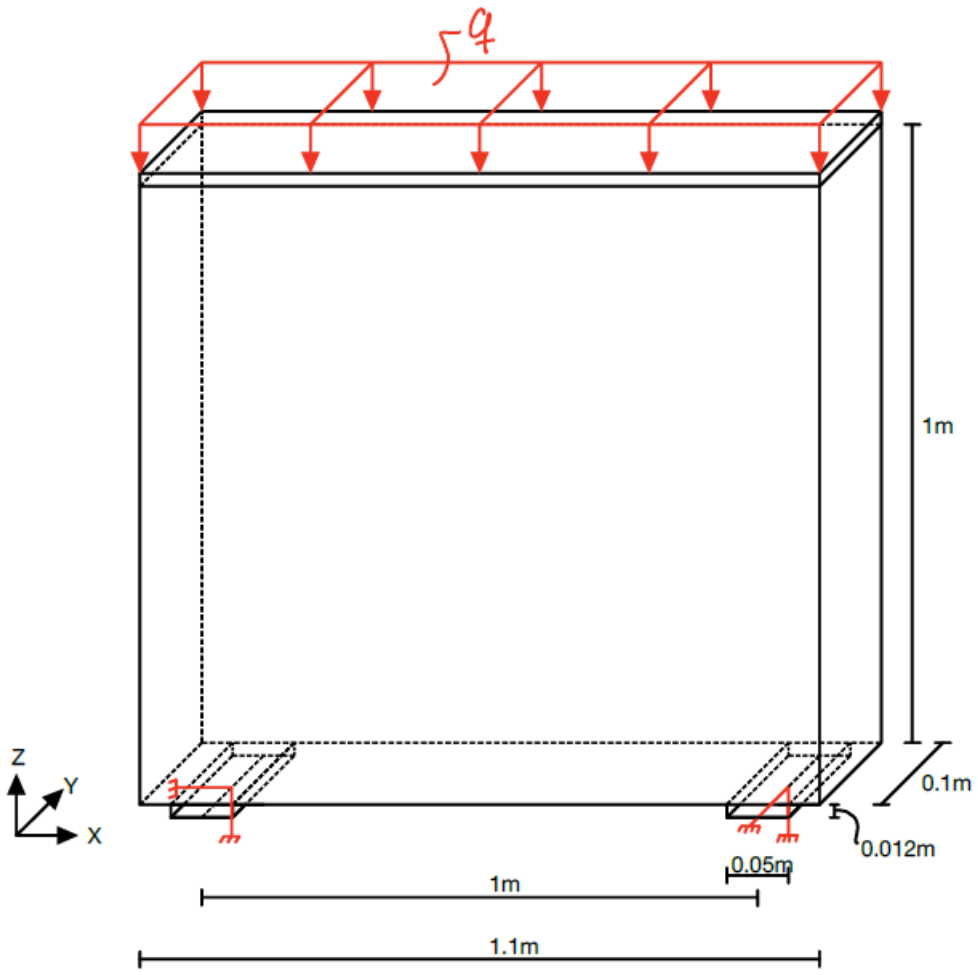

Figure 4.11: Model 1.2

4.3.3 Model 1.3

Model 1.3 is Model 1 with one point load off center, Figure 4.12 shows the placement of the point load (P). The placement of the point load is the same for Model 1.3 as the point load to the left for Model 1.1.

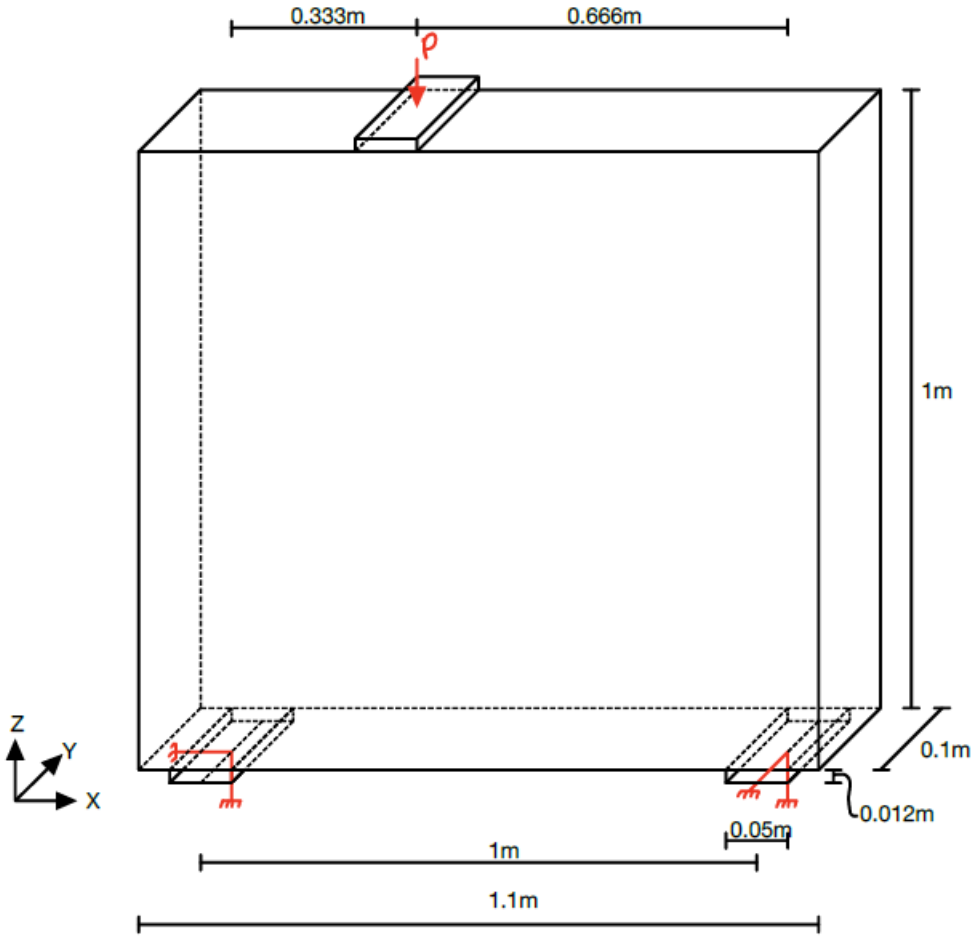

Figure 4.12: Model 1.3

4.4 Model 2

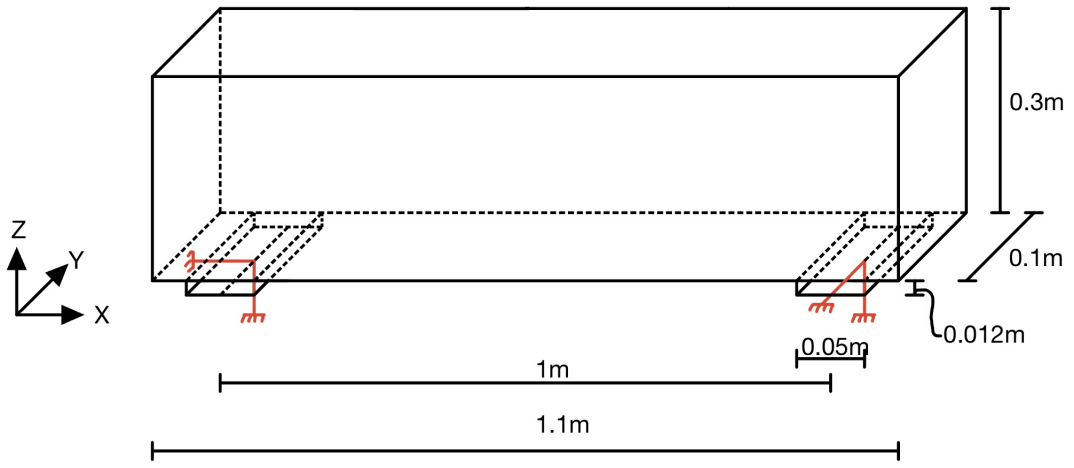

Figure 4.13: Dimensions of Model 2

Figure 4.13 shows the dimensions of Model 2. Model 2 has a length of 1.1m, a height of 0.3m, and a depth of 0.1m. It is supported at the two plates, where the right plate are supported in X and Z direction. The right plate is supported in Y and Z directions.

The minimum reinforcement for Model 2 is the same as for Model 1 because it has the same depth, concrete type (C30/37), and reinforcement type (B500NC). Therefore the vertical reinforcement chosen for Model 2 is ø10c260. The maximum spacing for the horizontal reinforcement is 300mm, and the horizontal reinforcement selected for Model 2 is ø10 in each corner.

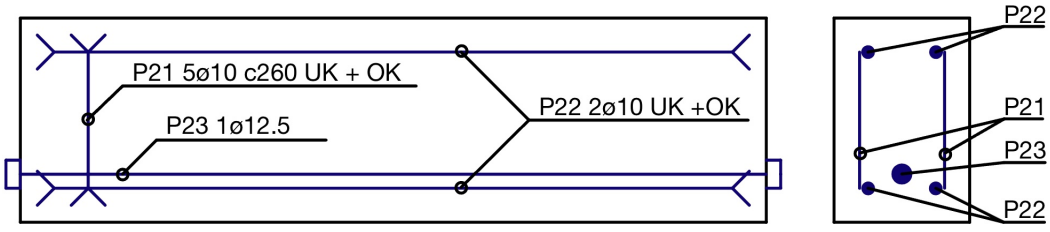

Figure 4.14: Reinforcement drawing of Model 2 with straight prestressed reinforcement

Figure 4.14 shows the reinforcement drawing for Model 2 with a straight prestressed reinforcement. P21 is the vertical reinforcement, P22 is the horizontal reinforcement and P23 is the prestressed reinforcement.

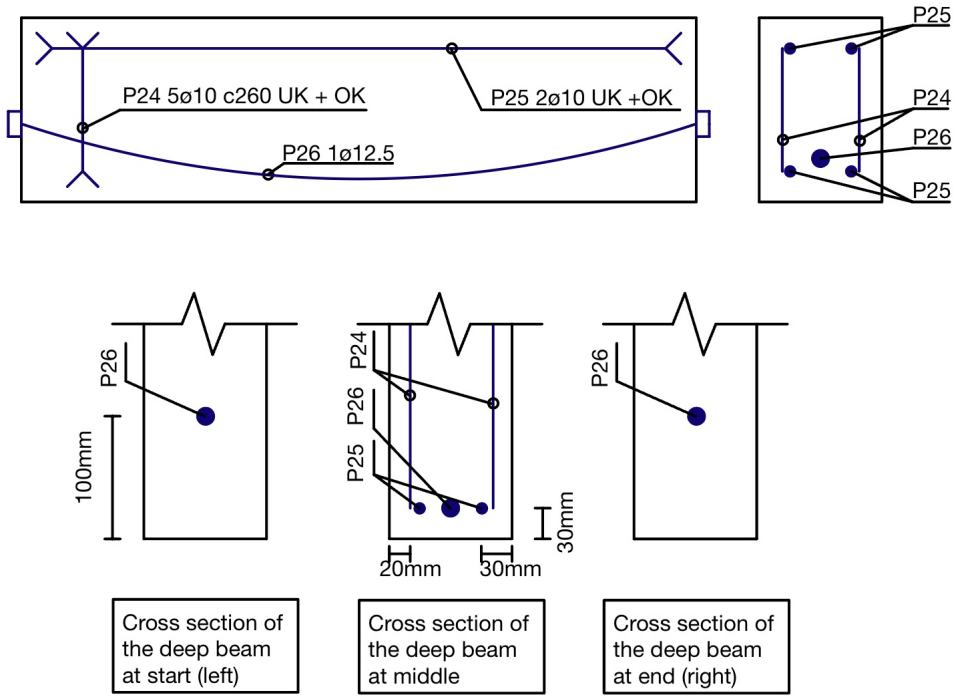

Figure 4.15: Reinforcement drawing of Model 2 with curved prestressed reinforcement

Figure 4.15 shows the reinforcement drawing of Model 2 with a curved prestressed reinforcement. P24 is the horizontal reinforcement, P25 is the horizontal reinforcement and P26 is the prestressed reinforcement with an eccentricity of 70mm.

4.4.1 Model 2.1

Model 2.1 is Model 2 with two point loads (P), Figure 4.16 shows where they are located.

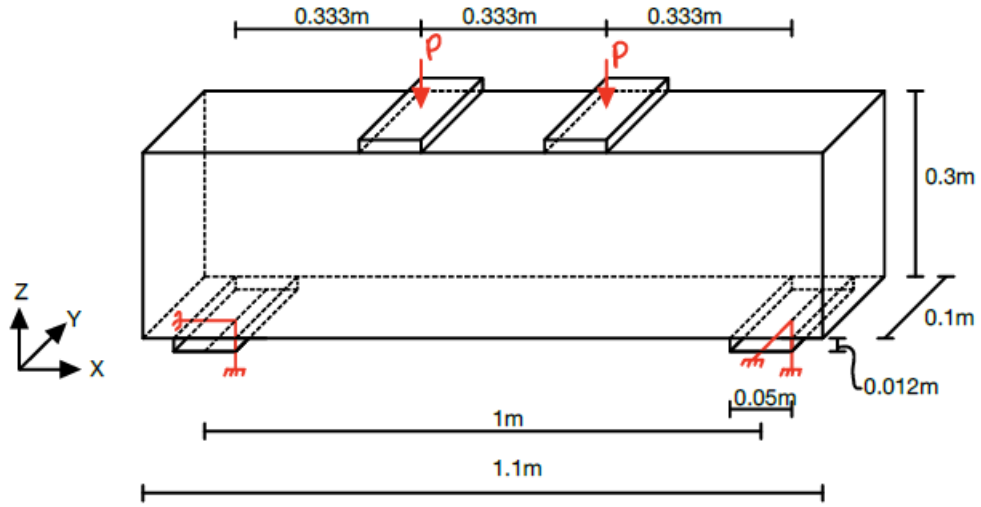

Figure 4.16: Model 2.1

4.4.2 Model 2.2

Model 2.2 is Model 2 with a uniform distributed load (q) over the entire top of the deep beam, Figure 4.17 shows Model 2.2.

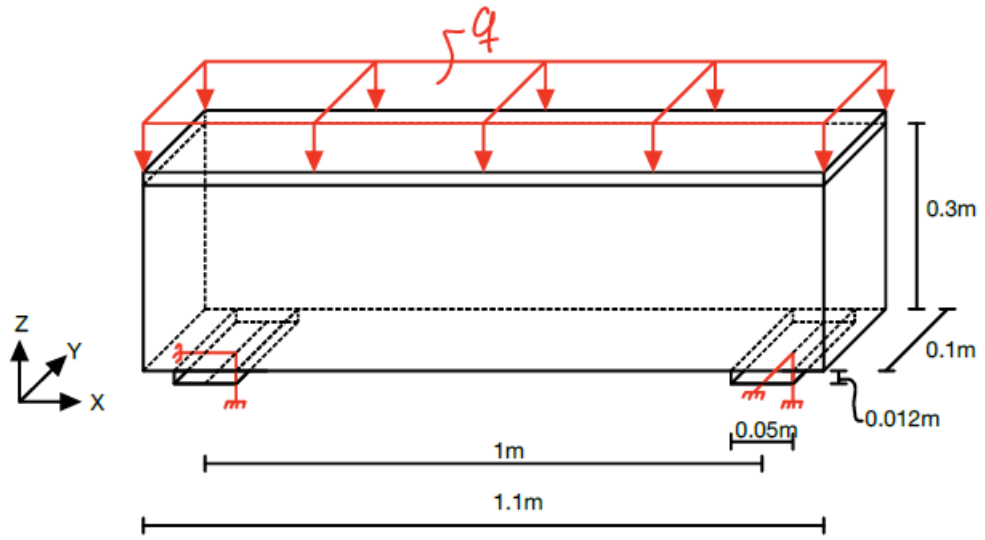

Figure 4.17: Model 2.2

4.4.3 Model 2.3

Model 2.3 is Model 2 with one point load off center, Figure 4.18 shows the placement of the point load (P).

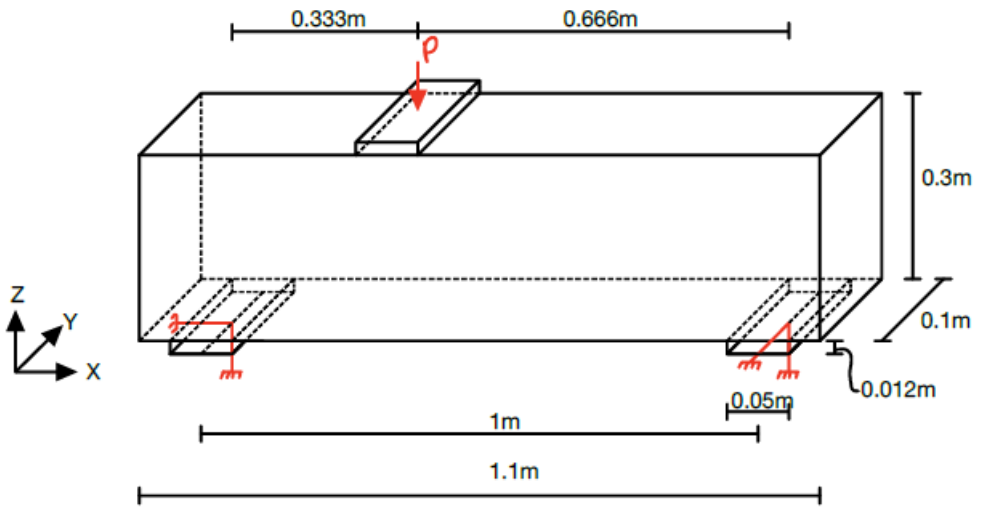

Figure 4.18: Model 2.3

4.5 Model 1.1 with openings

Model 1.1 with openings contains three different scenarios, case 4.1, case 4.2, and case 4.3. The positions of the openings are different, but the size of the openings remains the same. The dimensions, boundary conditions, reinforcement, and load pattern are the same as Model 1.1, which contains two-point loads. The openings have the dimensions of length of 0.2m, height of 0.16m, and depth equal to the beam (0.1m) each.

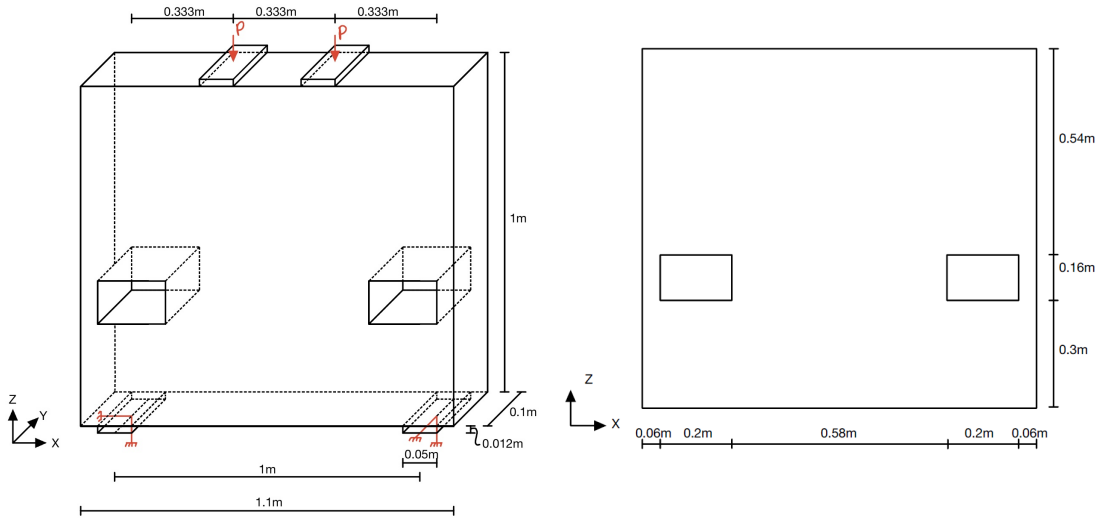

Figure 4.19: Case 4.1

Figure 4.19 shows the placements of the two openings in Model 1.1, in the analysis this Model is case 4.1. The two openings are located 0.3m from the bottom of the beam and 0.06m from the side of the beam.

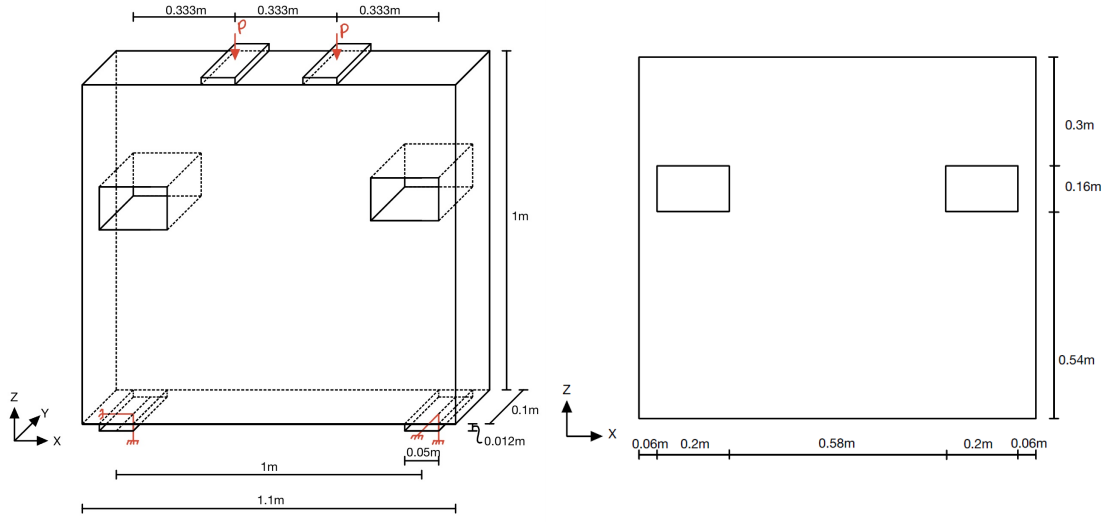

Figure 4.20: Case 4.2

Figure 4.20 shows the placements of the openings for case 4.2, where the openings are located 0.54m from the bottom of the beam to the bottom of the opening. The x-positions remain the same for case 4.2 as for case 4.1.

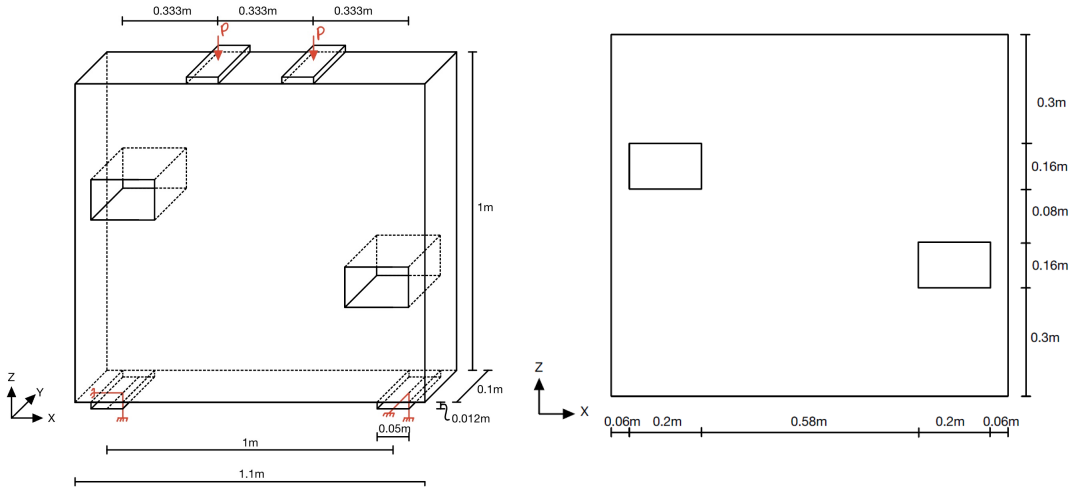

Figure 4.21: Case 4.3

Figure 4.21 shows the placements of the two openings; for case 4.3, the openings are unlike cases 4.1 and 4.2, not placed at the same height. The opening on the left is set 0.54m from the bottom, and the opening on the right is located 0.3m from the bottom.

The reason for analyzing a deep beam with openings is because in many situations there are necessary, it could be for windows, electrical installations, ventilation, or pipes. In order to find out if prestressed reinforcement will change the STM the analyses will regard Model 1.1 with different locations of the two openings.

4.6 Case description

The results are categorized into different cases, case 1 to case 4.

4.6.1 Case 1

Case 1 regards all the models without prestressed reinforcement. For Model 1, the longitudinal reinforcement is ø10 c260 (both sides), and the horizontal reinforcement of ø10 c235 (both sides). For Model 2, the longitudinal reinforcement is the same as for Model 1 (ø10 c260), and the horizontal is ø10 in each corner.

4.6.2 Case 2

Case 2 regards all the models with a straight prestressed reinforcement, for Model 1, Figure 4.8 shows the placement of the reinforcement. Figure 4.14 shows the placement of the reinforcement for Model 2. The models are analyzed with 25 MPa and 100 MPa prestressing.

4.6.3 Case 3

Case 3 regards all the models with a curved prestressed reinforcement, Figures 4.9 and 4.15 show the reinforcement drawings for Model 1 and 2, respectively. The models are analyzed with 25 MPa and 100 MPa prestressing.

4.6.4 Case 4

Case 4 regards Model 1.1 with two openings, this case includes without prestressed reinforcement, 25 MPa straight prestressed reinforcement, and 100 MPa straight prestressed reinforcement. The openings are placed in three different positions, as shown in Figures 4.19, 4.20, and 4.21. The models are reinforced similarly to cases 1 and 2, without prestressed reinforcement and with straight prestressed reinforcement, respectively.

5 Results from ATENA

5.1 Behavior of deep beams using FEM simulations

In order to find out if prestressed reinforcement changes the strut and tie model for a concrete deep beam, this thesis will look at how the principal stresses change when adding prestressing and increasing it. For the tensile part, ATENA defines it as maximum principal stress, and the compression part is defined as minimum principal stress. The results take the height of principal tensile stress at the load step just before yielding (lower bound theory).

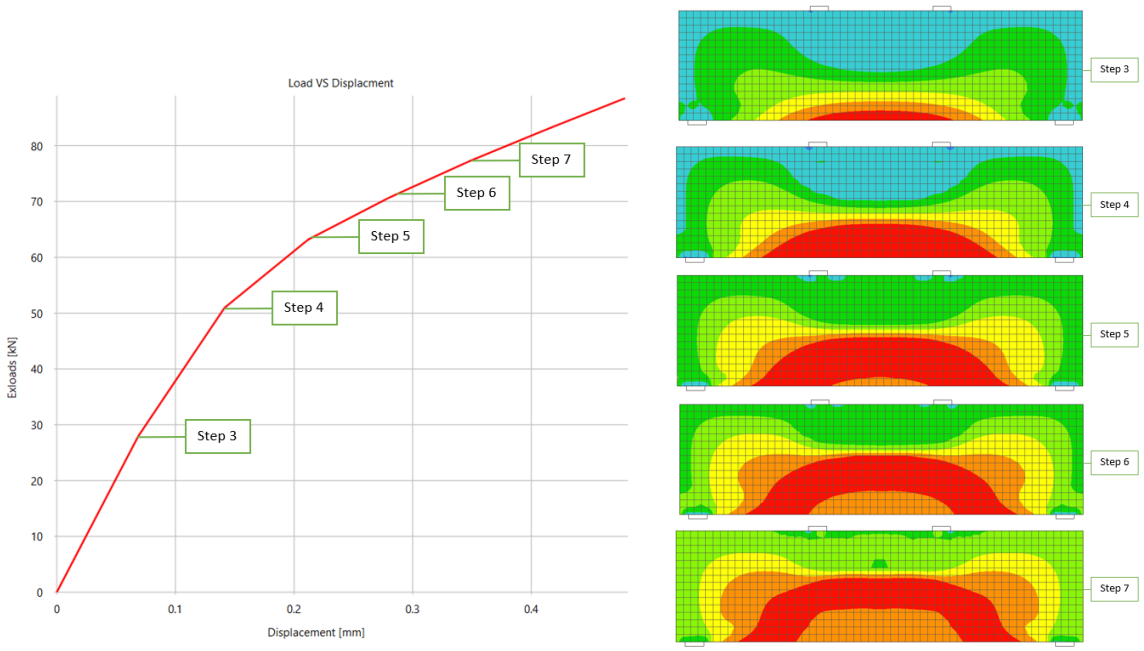

Figure 5.1: Load VS Displacement step 3-7 (left), Principal tensile stress development for Model 2.1 (right)

Figure 5.1 shows the load vs displacement from start to step 7 and how the principal tension stress develops when further loading. From steps 4 to 5, there is a significant difference in stress at the bottom of the beam; step 5 shows a decrease in stress at the middle bottom, which indicates a crack propagation. Therefore for Model 2.1, step 4 is just before yielding, and the results are taken into account. The load vs displacement diagram indicates where the yield start, after step 4, the graph goes from a linear to a curved form. The reason step 1 and 2 are not displayed is that they are taken into account in interval 1 and 2, where the external load is not yet applied.

The following results show the principal tensile and compressive stresses for all the models right before yielding. It also shows a proposed strut and tie model from the principal stress results. The color scale on the principal tensile stress is not the same as for principal compressive stress. For the principal tensile stress, the red area is equal to 1.4 to 2.9 MPa, for the principal compressive stress, the red zone is equal to 0 to -3.3 MPa. Therefore the color scale can not be compared between tensile and compressive stresses.

5.2 Case 1

Case 1 involves the models which do not contain prestressed reinforcement, the models are used as a reference, and the results will be compared to the ones with prestressed reinforcement.

5.2.1 Model 1

The dimensions of Model 1 are shown in Figure 4.7.

5.2.1.1 Model 1.1

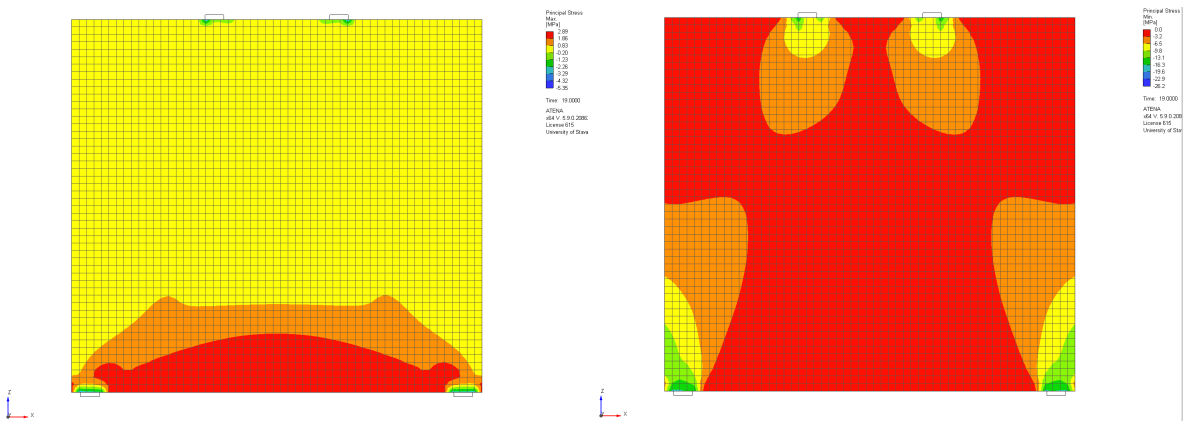

Figure 5.2: Principal tensile stress (left), principal compressive stress (right) for Model 1.1 without prestressing

Figure 5.2 shows the principal tensile and compressive stress for Model 1.1 without prestressed reinforcement. When analyzing the results, the peak of the red area for the principal tensile stress (Figure on the left) is measured which equals a. For the principal compressive stress (Figure on the right), the height of the top yellow area is measured, which equals b. The reason for taking only the yellow area into account is because it

propagates close to straight unlike the orange area, which propagates with an angle towards the supports. The peak of the principal tensile stress area is equal to 7.9 meshes which equals 158mm (a). The height of the yellow area of the principal compressive stress (b) is equal to 106mm.

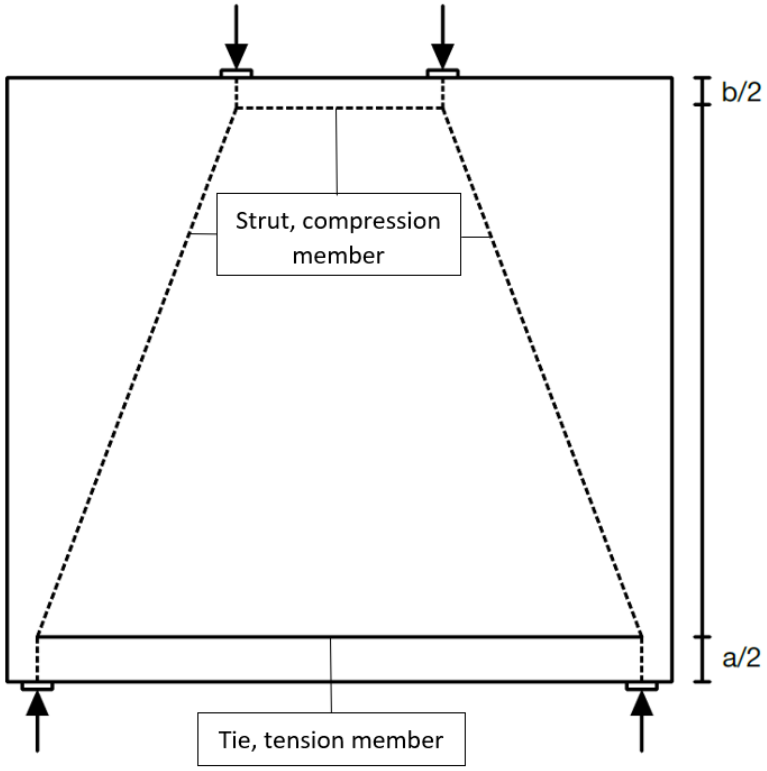

Figure 5.3: STM for Model 1.1 without prestressed reinforcement

The strut and tie models are developed from the principal compressive and tensile stresses. The locations of the strut and ties are at the center of the principal stresses. Therefore, the distance a/2 equals the distance from the bottom of the deep beam to the center of the peak of the principal tensile stress. The same rule applies to the distance b/2, which equals the distance from the top of the deep beam to the center of the principal compressive stress, which equals the distance from the top of the beam to the top strut.

Figure 5.3 shows the strut and tie model for Model 1.1 without prestressing. The solid line represents the tie, and the dotted lines represent the struts. The distance a/2 equals 79mm from the bottom of the beam to the tie. The distance b/2 between the strut and the top of the beam is equal to 53mm. The two vertical struts are placed directly under the two-point loads, the same for the two vertical struts at the bottom for the support loads.

5.2.1.2 Model 1.2

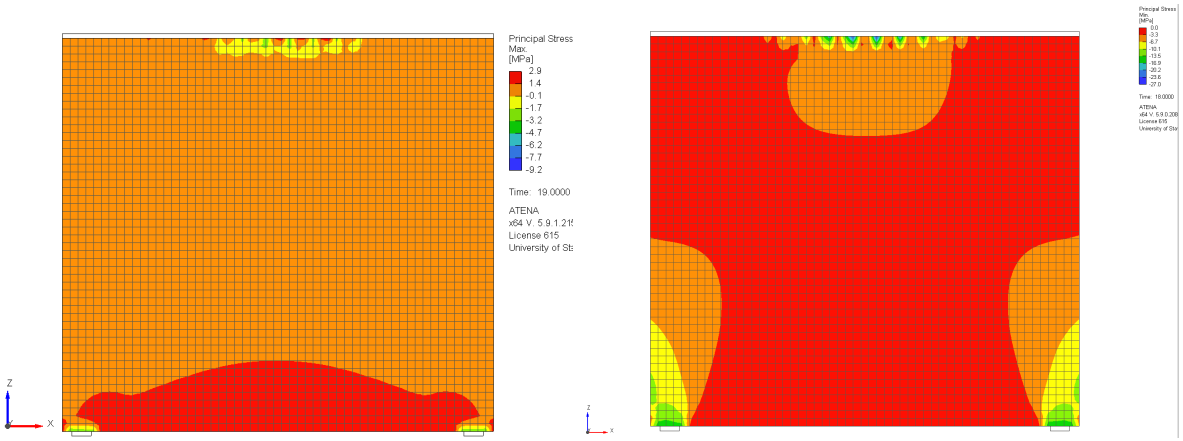

Figure 5.4: Principal tensile stress (left), principal compressive stress (right) for Model 1.2 without prestressing

Figure 5.4 shows the principal tensile and compressive stresses for Model 1.2 without prestressed reinforcement. The height of the maximum principal tensile stress (a) is 164 mm.

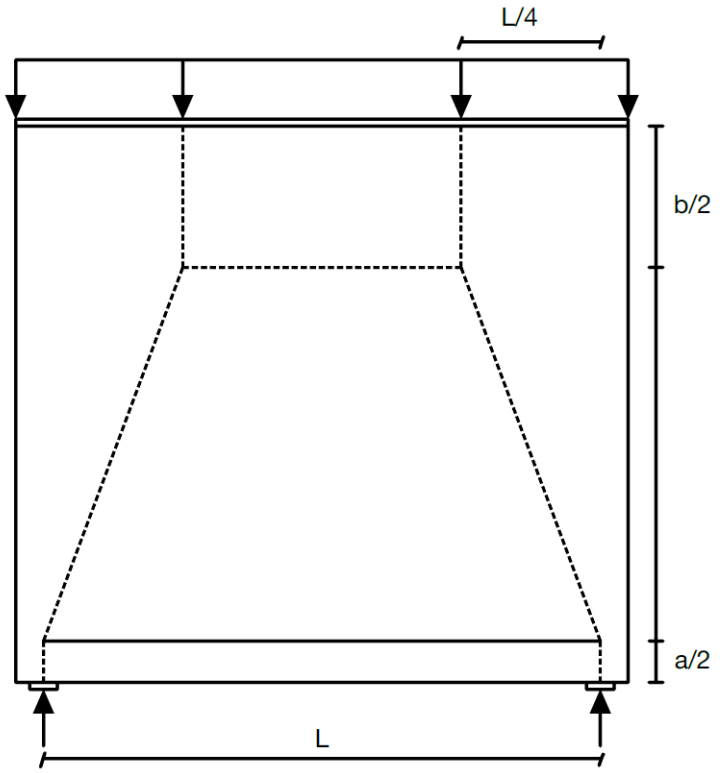

Figure 5.5: Strut and Tie Model for Model 1.2

Figure 5.5 shows the strut and tie model for Model 1.2, which does not involve prestressed

reinforcement. The value of a/2 is 82mm, while b/2 is equal to 260mm. The distance between the tie and the strut is 658mm. According to "Betongkonstruksjoner, [21]" the z-value for a deep beam, where h=l and a uniformly distributed load $z = 0.62 \cdot h$. However, for Model 1.2, the z-value is 0.658, which is slightly higher than expected. This could be due to how ATENA applies the load. If a finer load step is chosen (i.e., more steps), the increase in load with each step would be lower, and the correct load step would be selected just before yield. By using a finer load step evaluation, a and b values would increase while z would decrease.

5.2.1.3 Model 1.3

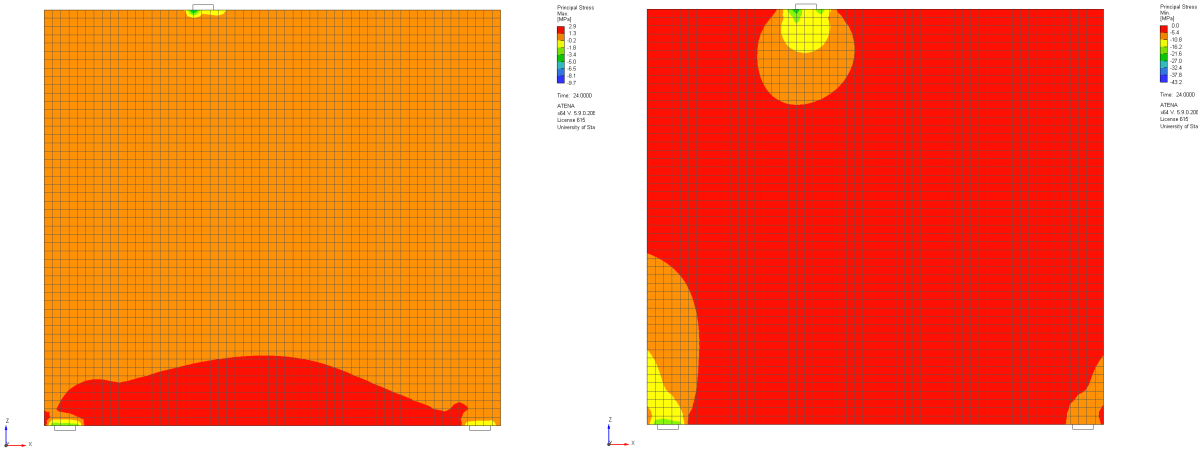

Figure 5.6: Principal tensile stress (left), principal compressive stress (right) for Model 1.3 without prestressing

Figure 5.6 shows the principal tensile and compressive stress for Model 1.3 which does not have prestressed reinforcement. The values for a and b are 168mm and 106mm respectively, they are measured the same way as Model 1.1. Regarding the principal tensile stress as Figure 5.6 on the left shows the stress development is uneven compared to both Model 1.1 and 1.2, the reason for this is the placement of the vertical load is off center to the left.

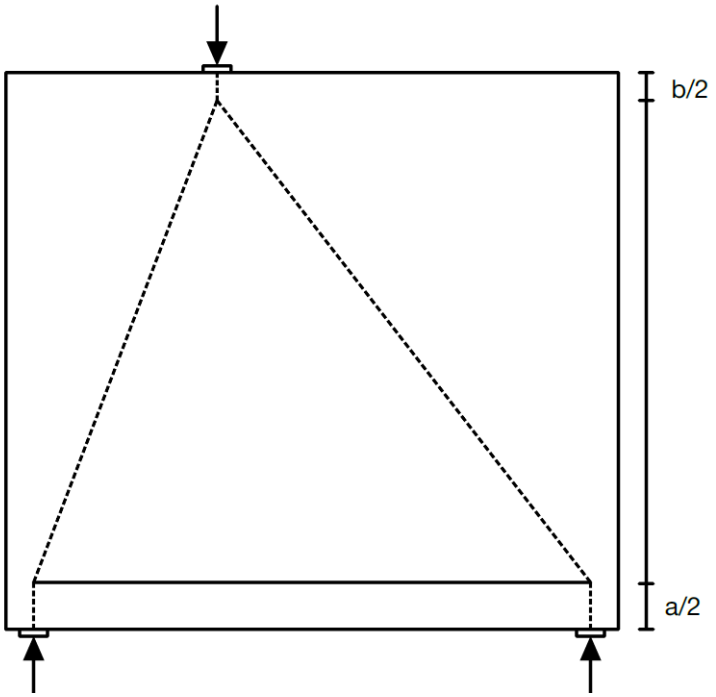

Figure 5.7: Strut and Tie Model for Model 1.3

Figure 5.7 shows the proposed strut and tie model for Model 1.3 without prestressed reinforcement, a/2 is equal to 84mm, and b/2 is equal to 53mm. The distance between the top node and the top of the beam (b/2) remains the same for Models 1.1 and 1.3.

5.2.2 Model 2

The dimensions of Model 2 are shown in Figure 4.13.

5.2.2.1 Model 2.1

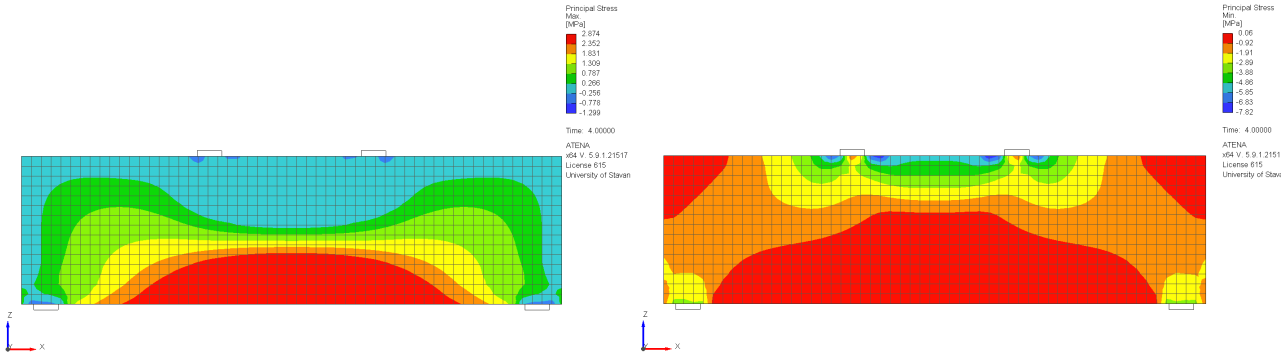

Figure 5.8: Principal tensile stress (left), principal compressive stress (right) for Model 2.1 without prestressing

Figure 5.8 shows the principal tensile and compressive stress for Model 2.1 without prestressed reinforcement. The analyses of the results give the distance a is equal to 102mm, and b is equal to 80mm. When comparing the principal compressive stress from Model 2.1 with 1.1, there is a difference in how the compressive stress develops through the deep beam. For Model 2.1, the orange area propagates through the beam to the area around the supports. For Model 1.1, the orange area almost connects, the reason for this is the height difference and the compressive area don't go all the way through the beam.

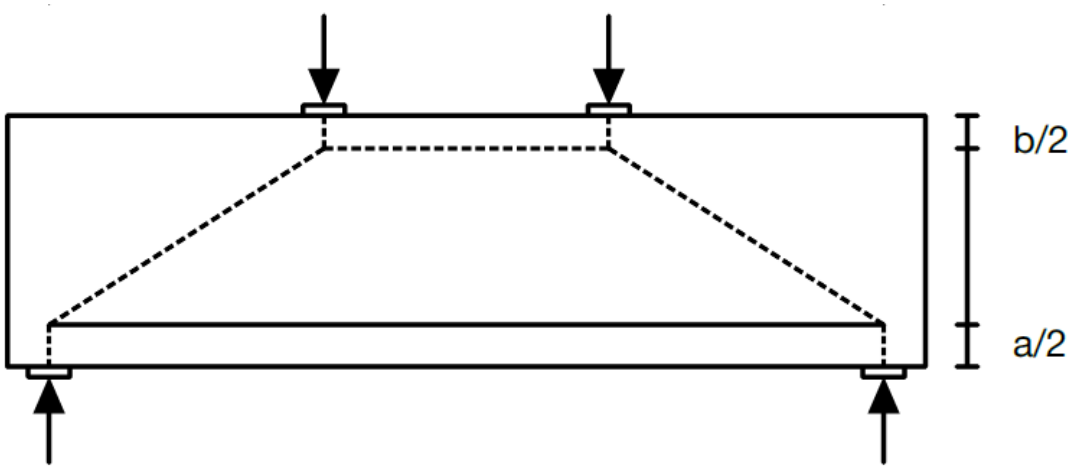

Figure 5.9: Strut and Tie model for Model 2.1 without prestressed reinforcement

Figure 5.9 is the proposed strut and tie model for Model 2.1 without prestressed

reinforcement, developed from the principal tensile and compressive stresses shown in Figure 5.8. The distance between the bottom of the beam and the tie (a/2) is equal to 51mm, and the distance between the strut and the top of the beam (b/2) is equal to 40mm.

5.2.2.2 Model 2.2

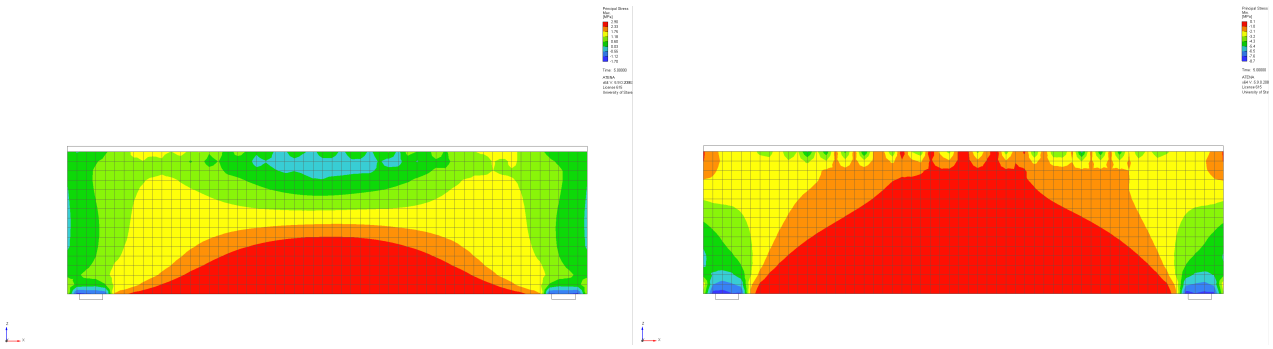

Figure 5.10: Principal tensile stress (left), principal compressive stress (right) for Model 2.2 without prestressing

Figure 5.10 shows the principal tensile and compressive stresses for Model 2.2 without prestressed reinforcement. When comparing the principal tensile stress, the distribution is similar to Model 1.2, on the other hand, the principal compressive stress develops differently. The red area for the principal compressive stress ranges from 0 to -1 MPa, thereby the smallest. The principal compressive stress for Model 1.2 has a compressive area in the middle of the top of the beam, with a form close to a rectangle. The compressive stress distribution for Model 2.2 is larger further from the center. A reason for this could be that the beam for Model 2.2 is lower than Model 1.2, this gives a more significant deflection which provides tension between the supports, which propagates all the way through the beam. Therefore the distance b is measured from the top of the beam to where the red area straightens out, which equals 60mm. The peak of the principal tensile stress (a) is equal to 120mm.

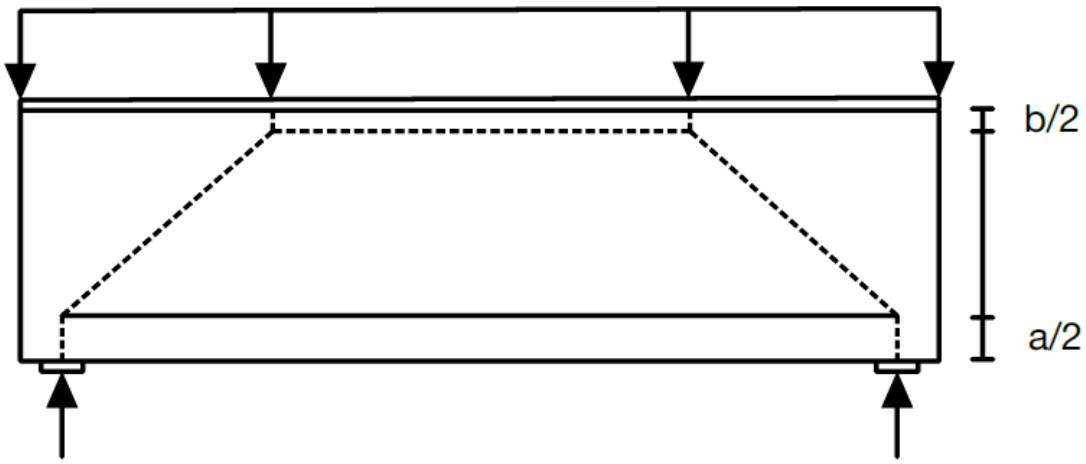

Figure 5.11: Strut and Tie model for Model 2.2 without prestressed reinforcement

Figure 5.11 shows the strut and tie model for Model 2.2 without prestressed reinforcement, a/2 is equal to 60mm, and b/2 is equal to 30mm.

5.2.2.3 Model 2.3

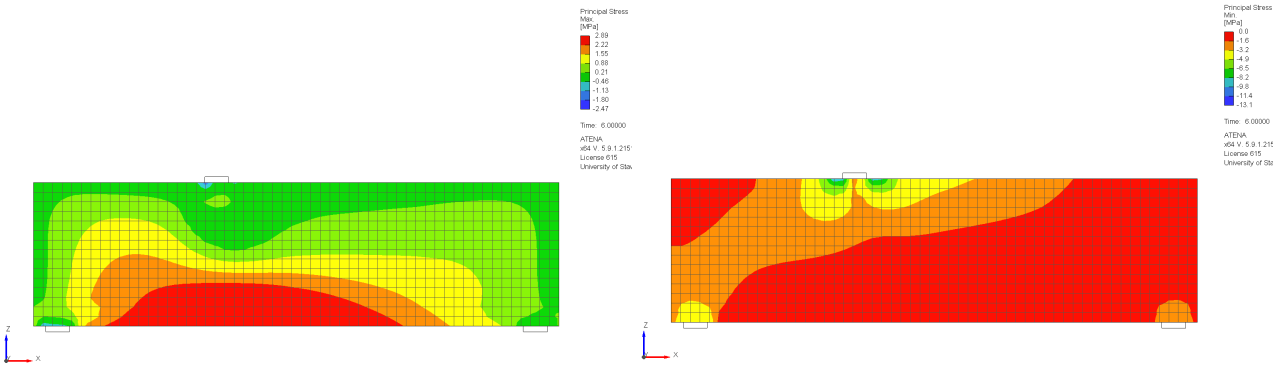

Figure 5.12: Principal tensile stress (left), principal compressive stress (right) for Model 2.3 without prestressing

Figure 5.12 shows the principal tensile and compressive stress for Model 2.3 without prestressed reinforcement. There is an uneven stress development for both tensile and compressive stress, this is because there is only one point load which is placed off center of the top of the beam as in Model 1.3. The height of the maximum principal tensile stress (a) is equal to 90mm, and the height of the principal compressive stress (b) is equal to 86mm.

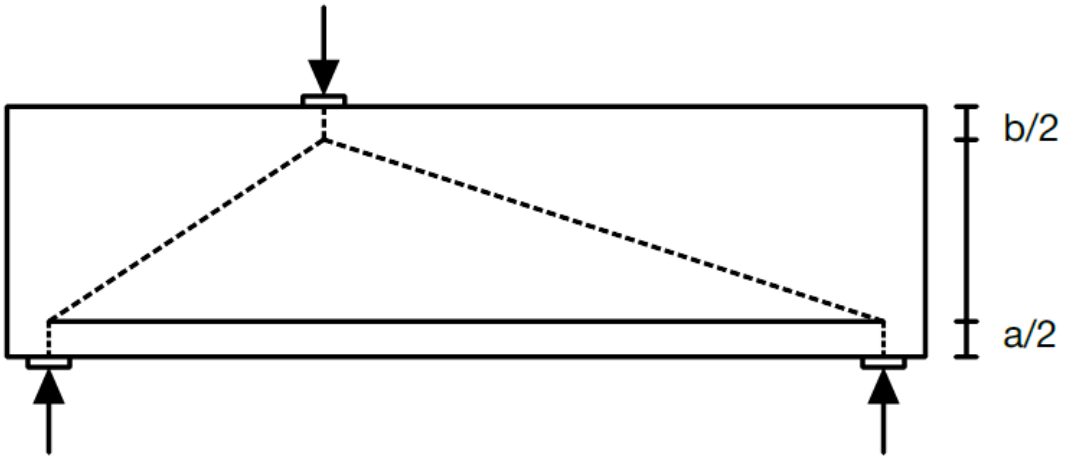

Figure 5.13: Strut and Tie model for Model 2.3 without prestressing

Figure 5.13 shows the strut and tie model for Model 2.3 without prestressing, developed from the principal tensile and compressive stresses shown in Figure 5.6. The distances a/2 are equal to 45mm and b/2 are equal to 43mm.

5.3 Case 2

Case 2 involves all models with a straight prestressed reinforcement. The strut and tie model is drawn with the color red and green. Red represents the models with 25 MPa prestressing and green represents the models with 100 MPa prestressing.

5.3.1 Model 1

The dimensions of Model 1 are shown in Figure 4.7 and the reinforcement drawing for Model 1 with a straight prestressed reinforcement is shown in Figure 4.8.

5.3.1.1 Model 1.1 with 25 MPa prestressing

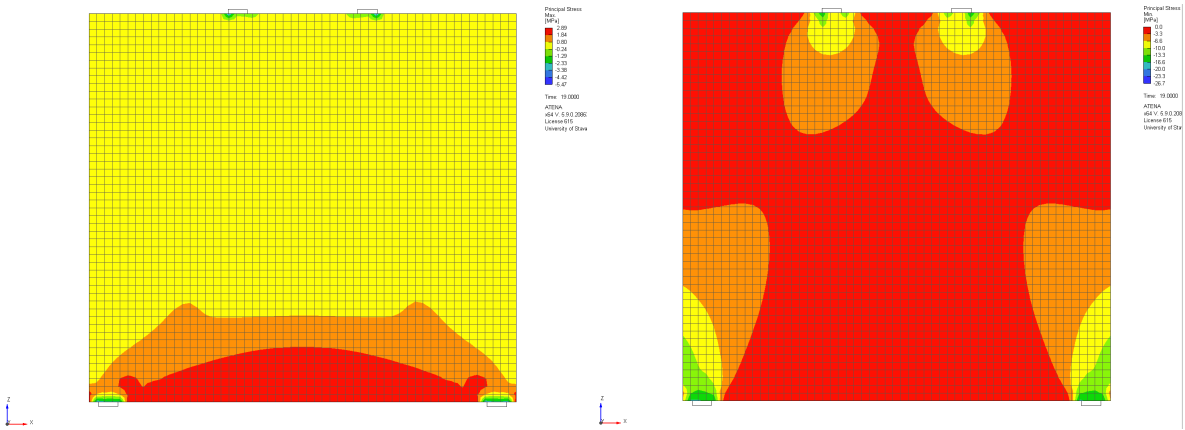

Figure 5.14: Principal tensile stress (left), principal compressive stress (right) for Model 1.1 with 25 MPa prestressing

Figure 5.14 shows the principal tensile and compressive stresses for Model 1.1 with a straight 25 MPa prestressed reinforcement. The height of the principal tensile stress area (a) is equal to 140mm. There is a decrease in the height of the maximum principal tensile stress when comparing Model 1.1 without prestressing and this one, the difference is 18mm. The height of the yellow area for the principal compressive stress is the same for the two models, b is equal to 106mm.

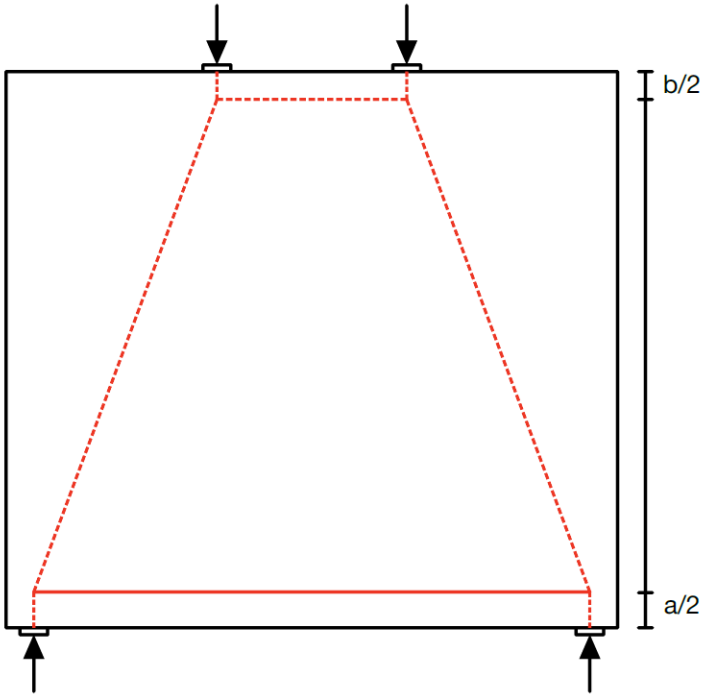

Figure 5.15: STM for Model 1.1 with 25 MPa straight prestressed reinforcement

Figure 5.15 shows the strut and tie model for Model 1.1 with a straight prestressed reinforcement with 25 MPa prestressing. From analyzing the results of the principal stresses, the development of the STM is done. The distance a/2 is equal to 70mm, and b/2 is equal to 53mm. The results show no change in the placement of the top strut compared to Model 1.1 without prestressing, but the placement of the tie has decreased by 9mm.

5.3.1.2 Model 1.1 with 100 MPa prestressing

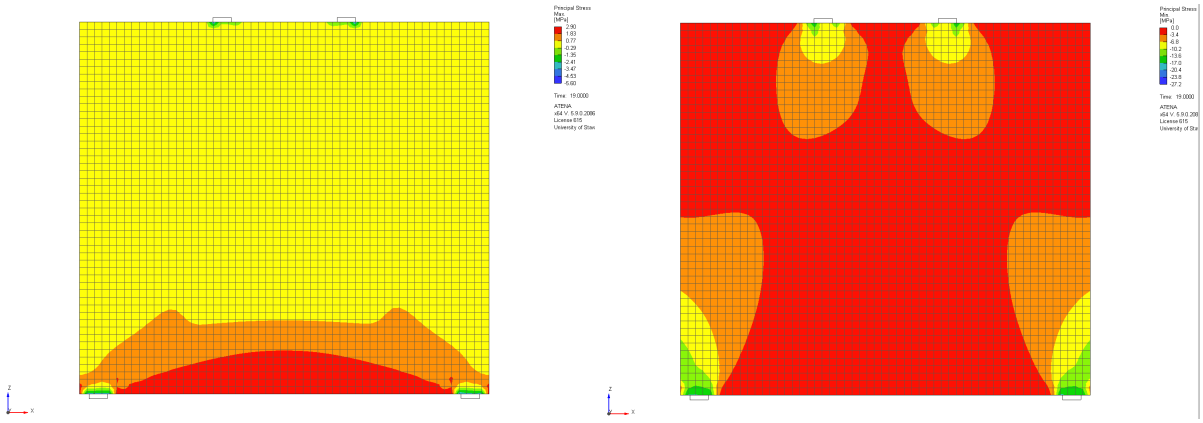

Figure 5.16: Principal tensile stress (left), principal compressive stress (right) for Model 1.1 with 100 MPa prestressing

Figure 5.16 shows the principal tensile and compressive stress for Model 1.1 with 100 MPa straight prestressed reinforcement. The distance a is equal to 118mm, and b is equal to 106mm.

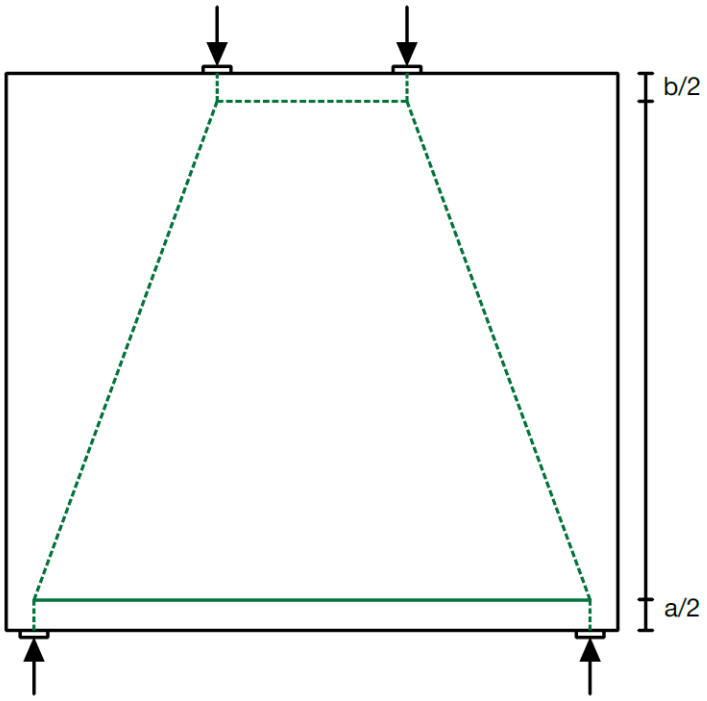

Figure 5.17: Strut and Tie model for Model 1.1 with 100 MPa straight prestressing

Figure 5.17 is the strut and tie model for Model 1.1 with 100 MPa prestressing in a straight line. The distance between the bottom of the beam and the tie (a/2) is equal to 59mm, there is a decrease of 20mm compared to Model 1.1 without prestressed reinforcement and a reduction of 11mm compared to Model 1.1 with 25 MPa prestressing. The distance b/2 remains the same which equals 53mm.

5.3.1.3 Model 1.2 with 25 MPa prestressing

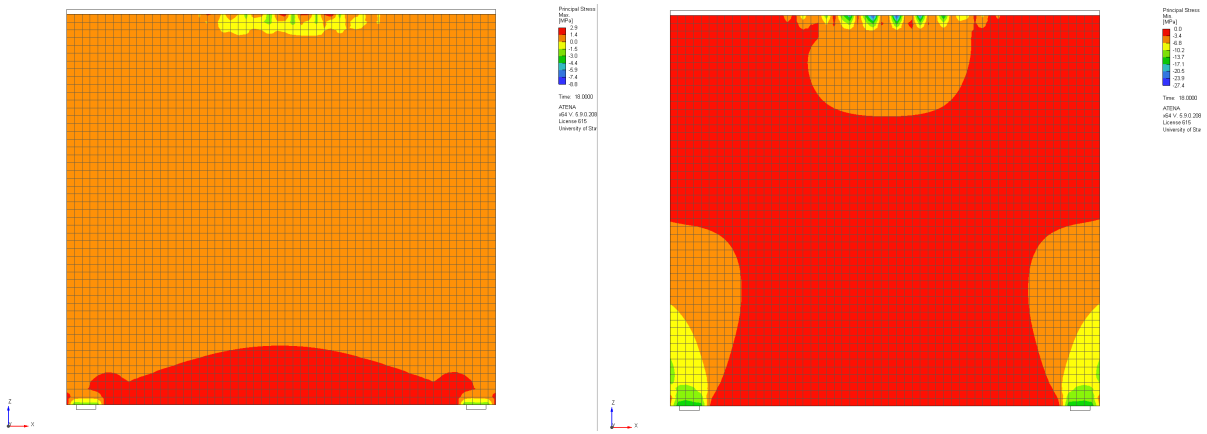

Figure 5.18: Principal tensile stress (left), principal compressive stress (right) for Model 1.2 with 25 MPa prestressing

Figure 5.18 shows the principal tensile and compressive stress for Model 2.2 with 25 MPa straight prestressed reinforcement. The tensile and compressive stress distribution is quite similar to Model 2.2 without prestressing, but the height of the maximum principal tensile stress (a) has decreased to 152mm, which is a decrease of 6mm.

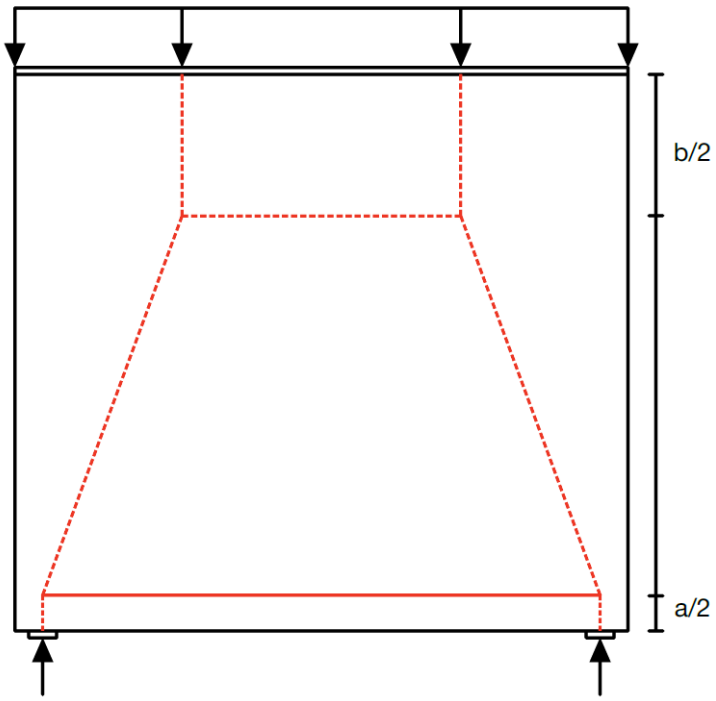

Figure 5.19: Strut and Tie model for Model 1.2 with 25 MPa straight prestressing

Figure 5.19 is the Strut and Tie model for Model 1.2 with 25 MPa straight prestressed

reinforcement. The distance between the tie and the bottom of the beam (a/2) is equal to 76mm, and the distance b/2 is equal to 260mm.

5.3.1.4 Model 1.2 with 100 MPa prestressing

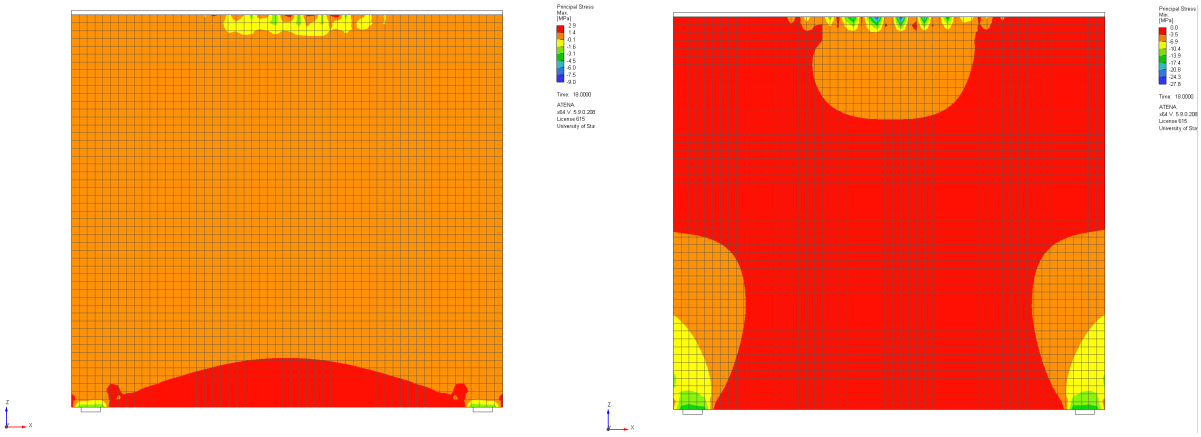

Figure 5.20: Principal tensile stress (left), principal compressive stress (right) for Model 1.2 with 100 MPa prestressing

Model 1.2 with 100 MPa straight prestressed reinforcement shows the principal tensile and compressive stress, as illustrated in Figure 5.20. The values of a and b are 124mm and 260mm, respectively. Notably, the height of the tensile stress (a) has reduced further compared to Model 1.2 with 25 MPa prestressing and Model 1.2 without any prestressing.

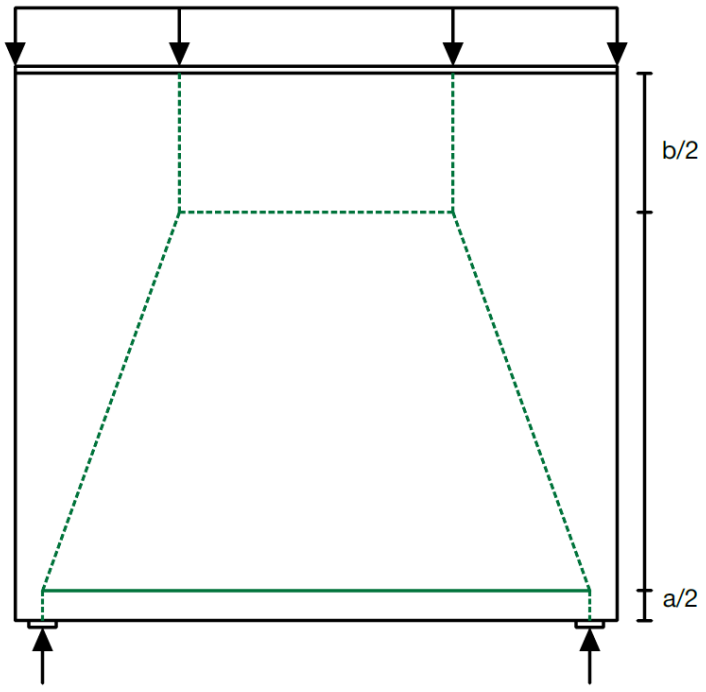

Figure 5.21: Strut and Tie model for Model 1.2 with 100 MPa straight prestressing

The strut and tie model for Model 1.2 with 100 MPa straight prestressing is shown in Figure 5.21. The distance between the bottom of the beam and the tie (a/2) is equal to 64mm, and b/2 is equal to 260mm.

5.3.1.5 Model 1.3 with 25 MPa prestressing

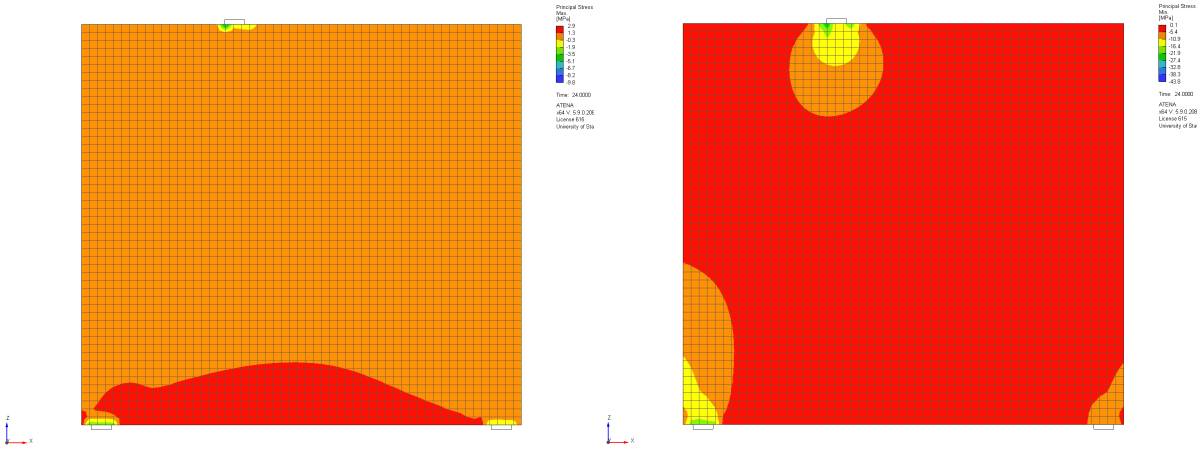

Figure 5.22: Principal tensile stress (left), principal compressive stress (right) for Model 1.3 with 25 MPa prestressing

Figure 5.22 shows the principal tensile and compressive stress for Model 1.3 with 25 MPa straight prestressed reinforcement. The distance a is equal to 158mm and b is equal to 106mm.

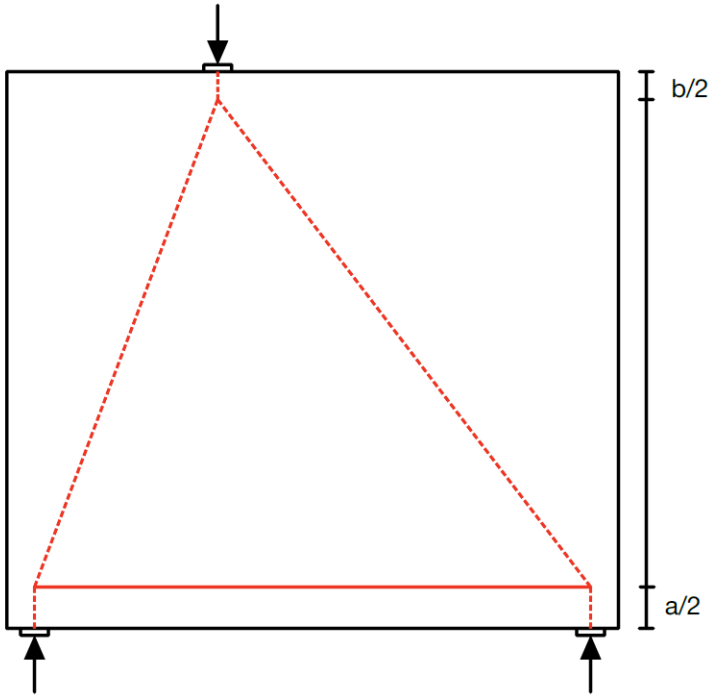

Figure 5.23: Strut and Tie model for Model 1.3 with 25 MPa straight prestressing

The strut and tie model for Model 1.3 with 25 MPa straight prestressing is shown in Figure 5.23. The distance (a/2) is equal to 79mm and b/2 is equal to 53mm.

5.3.1.6 Model 1.3 with 100 MPa prestressing

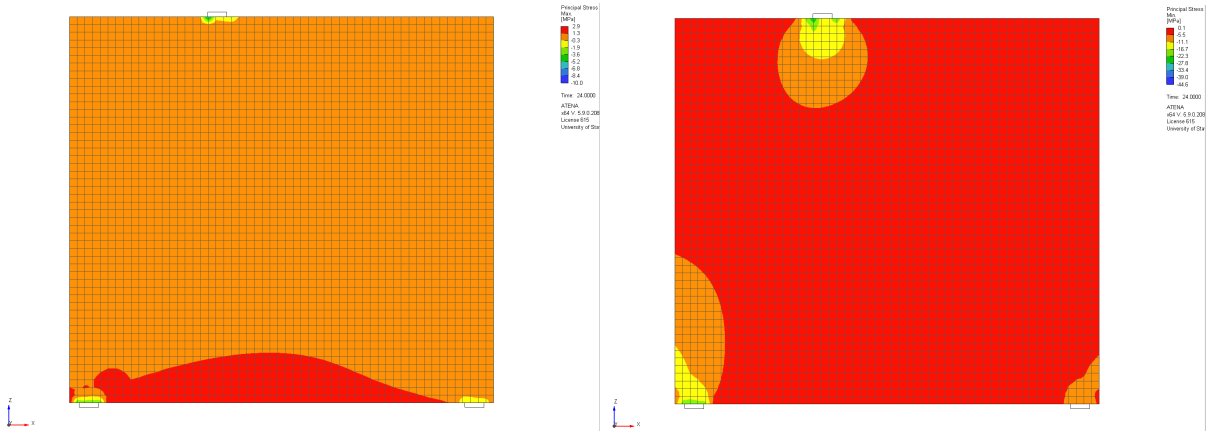

Figure 5.24: Principal tensile stress (left), principal compressive stress (right) for Model 1.3 with 100 MPa prestressing

The principal tensile and compressive stress for Model 1.3 with 100 MPa straight prestressed reinforcement at yield is shown in Figure 5.24. The peak of the principal tensile stress (a) is equal to 128mm, and the distance b is equal to 106mm. The stress distribution has the same form as Model 1.3 with 25 MPa prestressing and Model 1.3 without prestressing.

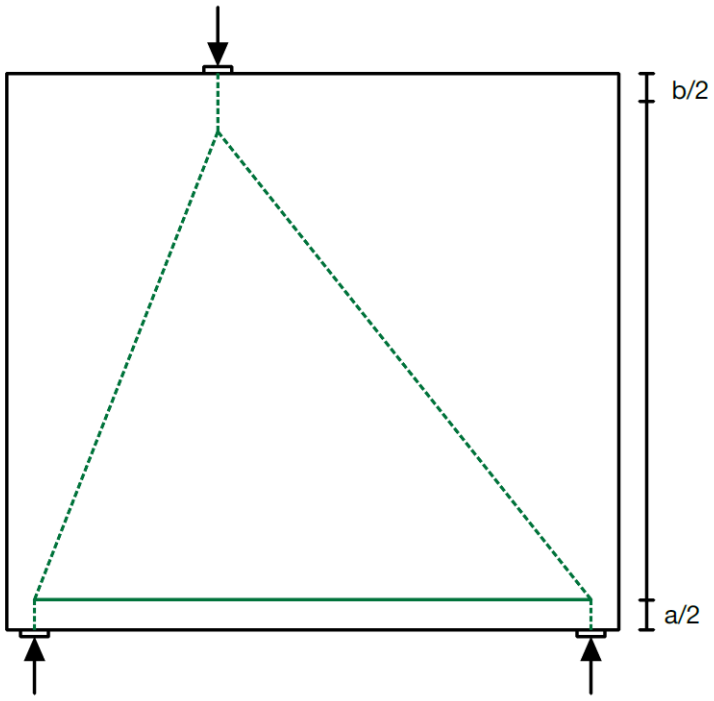

Figure 5.25: Strut and Tie model for Model 1.3 with 100 MPa straight prestressing

The strut and tie model for Model 1.3 with 100 MPa prestressing is developed from the results of the principal tensile and compressive stress is shown in Figure 5.25. The distance a/2 is equal to 64mm and b/2 is equal to 53mm. The distance a/2 has decreased by 20mm compared with Model 1.3 without prestressed reinforcement.

5.3.2 Model 2

The dimensions of Model 2 are shown in Figure 4.13 and the reinforcement drawing for Model 2 with a straight prestressed reinforcement is shown in Figure 4.15.

5.3.2.1 Model 2.1 with 25 MPa prestressing

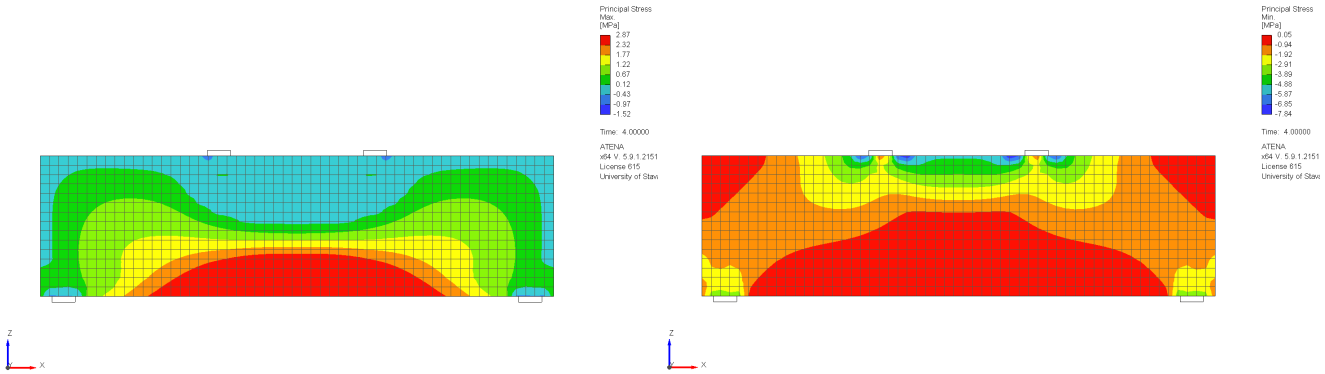

Figure 5.26: Principal tensile stress (left), principal compressive stress (right) for Model 2.1 with 25 MPa prestressing

The principal tensile and compressive stress for Model 2.1 with 25 MPa straight prestressing is shown in Figure 5.26. The principal tensile stress distribution has a similar distribution as Model 1.1, which has the same load pattern (two-point loads). The height of the maximum principal tensile stress (red-area) (a) is equal to 90mm. The principal compressive stress distribution develops in a similar way as Model 2.1 without prestressing, where the compressive stress develops through the beam from the external load to the support. The distance b is equal to 80mm.

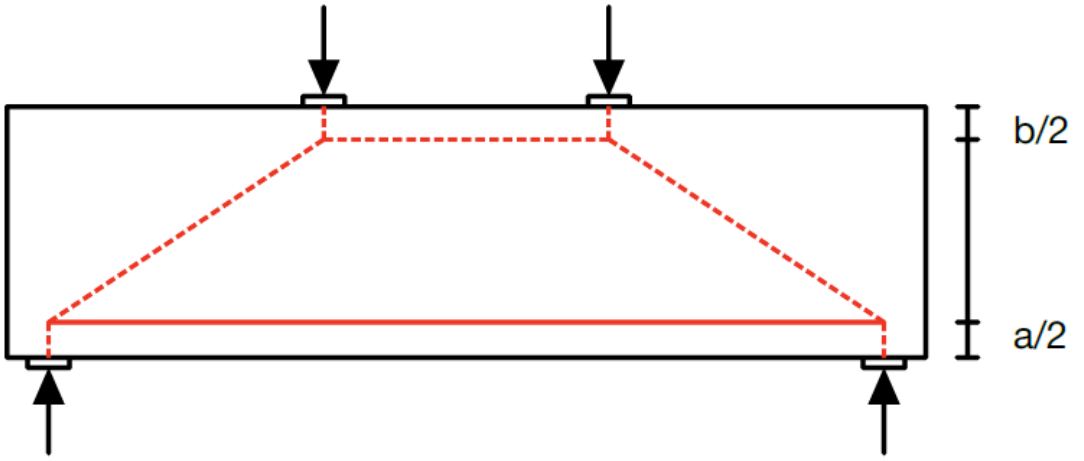

Figure 5.27: Strut and Tie model for Model 2.1 with 25 MPa straight prestressing

The Strut and Tie model for Model 2.1 is shown in Figure 5.27, a/2 are equal to 45mm and b/2 are equal to 40mm. The distance a/2 has decreased by 6mm compared to Model 2.1 without prestressed reinforcement.

5.3.2.2 Model 2.1 with 100 MPa prestressing

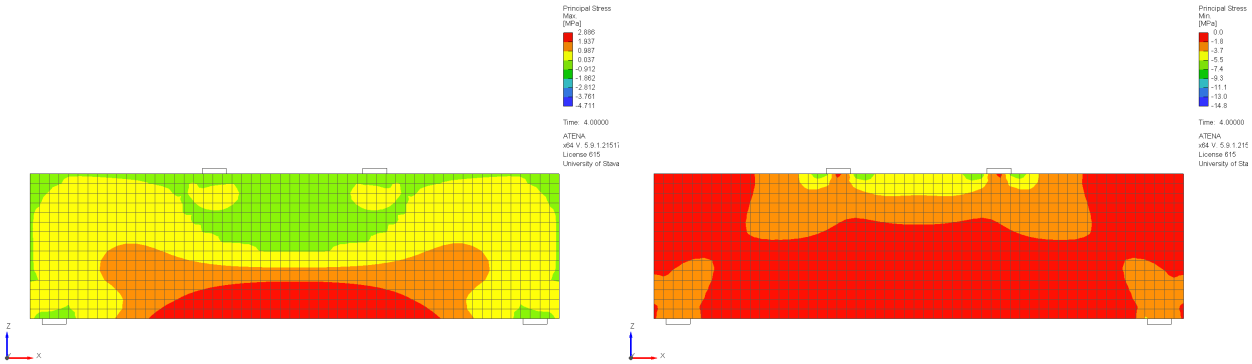

Figure 5.28: Principal tensile stress (left), principal compressive stress (right) for Model 2.1 with 100 MPa prestressing

Figure 5.28 shows the principal tensile and compressive stress for Model 2.1 with 100 MPa straight prestressing. The maximum principal tensile stress distribution has a similar shape as Model 2.1 with 25 MPa prestressing and without prestressing, on the other hand, the principal compressive stress distribution is not. The compressive area does not go all the way through the beam, it has a similar distribution as Model 1.1. The reason for this is the amount of prestressing. The peak of the principal tensile stress (a) is equal to 78mm and the peak of the principal compressive stress (b) is equal to 80mm.

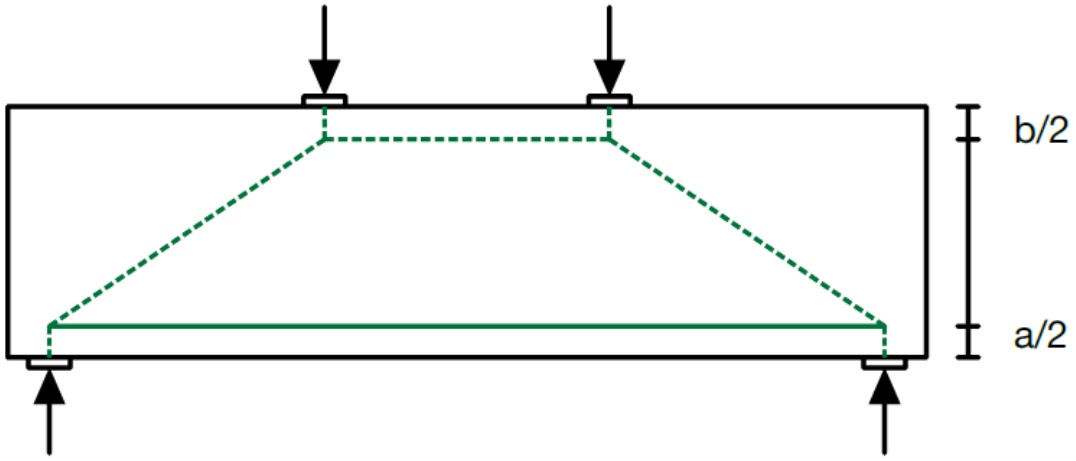

Figure 5.29: Strut and Tie model for Model 2.1 with 100 MPa straight prestressing

The strut and tie model for Model 2.1 with 100 MPa prestressing developed from the principal tensile and compressive stresses are shown in Figure 5.29. The distance a/2 is equal to 39mm, which is a decrease of 12mm and b/2 is equal to 40mm.

5.3.2.3 Model 2.2 with 25 MPa prestressing

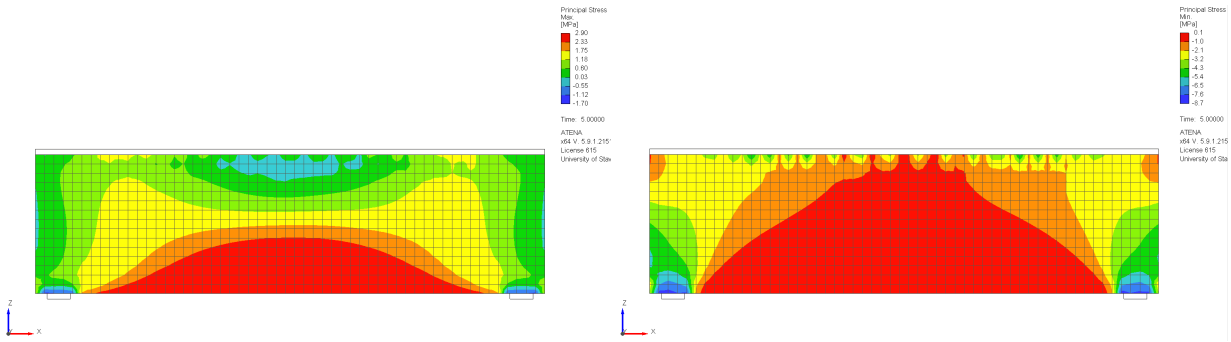

Figure 5.30: Principal tensile stress (left), principal compressive stress (right) for Model 2.2 with 25 MPa prestressing

Figure 5.30 shows the principal tensile and compressive stress for Model 2.2 with 25 MPa straight prestressing. The peak of the principal tensile stress (a) is equal to 118mm for Model 2.2 with 25 MPa straight prestressed reinforcement, and the distance from the top of the beam to where the principal compressive stress straightens out (b) is equal to 44mm. The distance b is measured the same way as Model 2.2 without prestressed reinforcement.

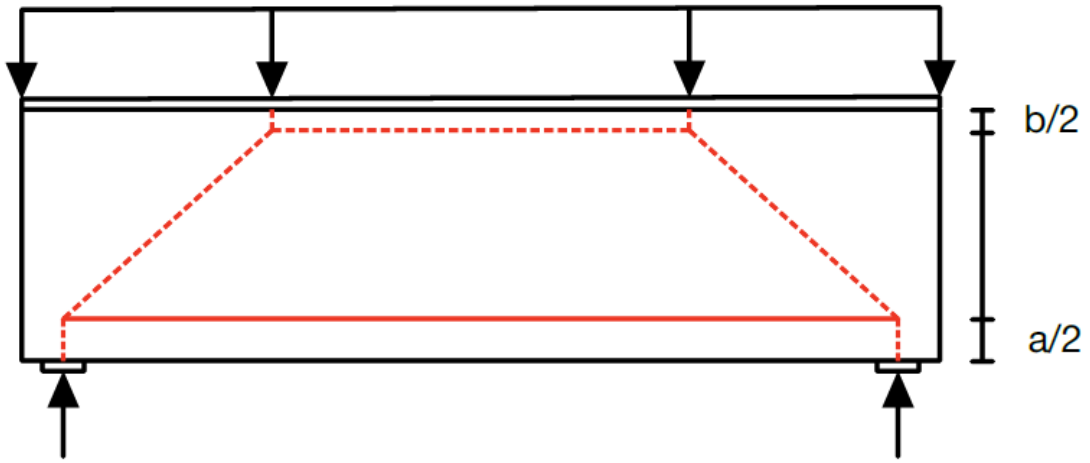

Figure 5.31: Strut and Tie model for Model 2.2 with 25 MPa prestressed reinforcement

Figure 5.31 shows the strut and tie model which is developed from the principal tensile and compressive stress. The distance a/2 is equal to 59mm, and the distance b/2 is

equal to 22mm. The distance a/2 has reduced by 1mm compared to Model 2.2 without prestressed reinforcement, and b/2 remains the same.

5.3.2.4 Model 2.2 with 100 MPa prestressing

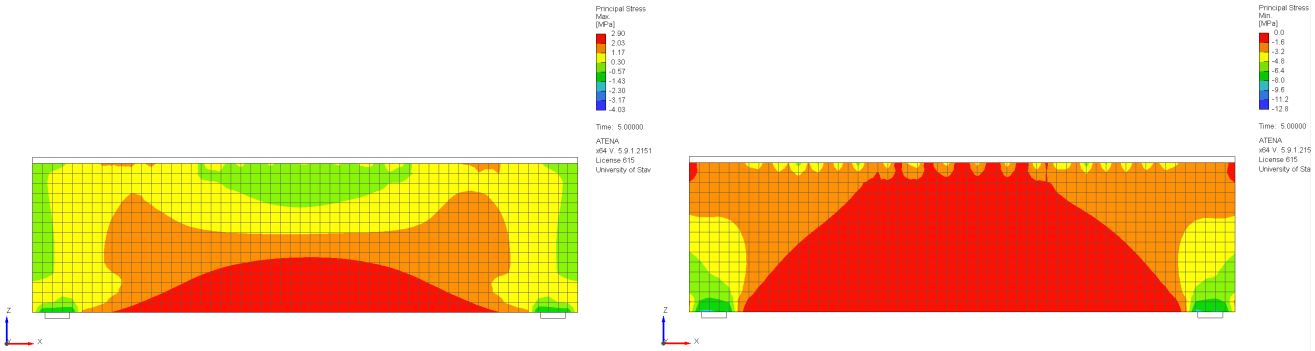

Figure 5.32: Principal tensile stress (left), principal compressive stress (right) for Model 2.2 with 100 MPa prestressing

The principal tensile and compressive stress for Model 2.2 with 100 MPa straight prestressed reinforcement is shown in Figure 5.32. The peak of the principal tensile stress is measured similarly to the previous model, a is equal to 108mm and b is equal to 44mm.

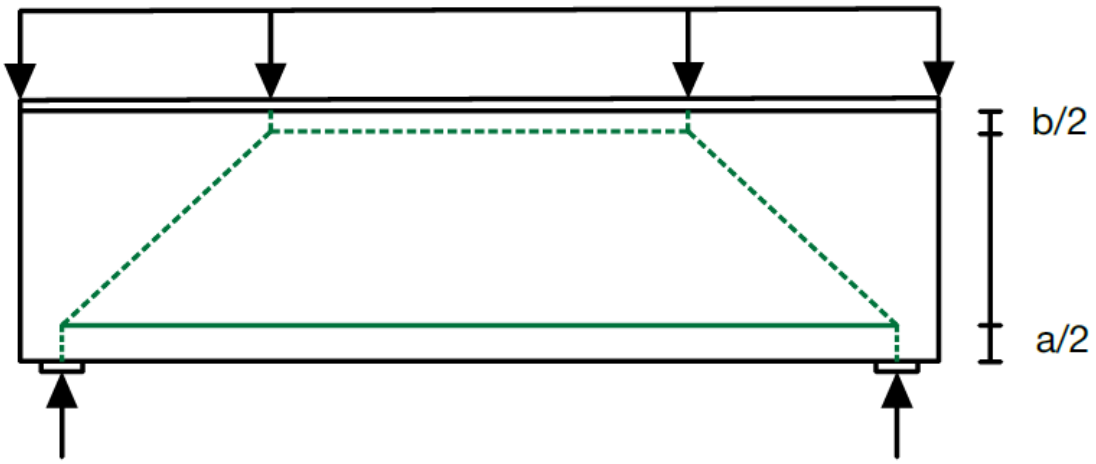

Figure 5.33: Strut and Tie model for Model 2.2 with 100 MPa straight prestressing

The proposed strut and tie model for Model 2.2 with 100 MPa prestressing is shown in Figure 5.33. The distance a/2 is equal to 54mm and b/2 is equal to 22mm. Compared to the STM for model 2.2 without prestressed reinforcement, the distance a/2 has decreased by 6mm.

5.3.2.5 Model 2.3 with 25 MPa prestressing

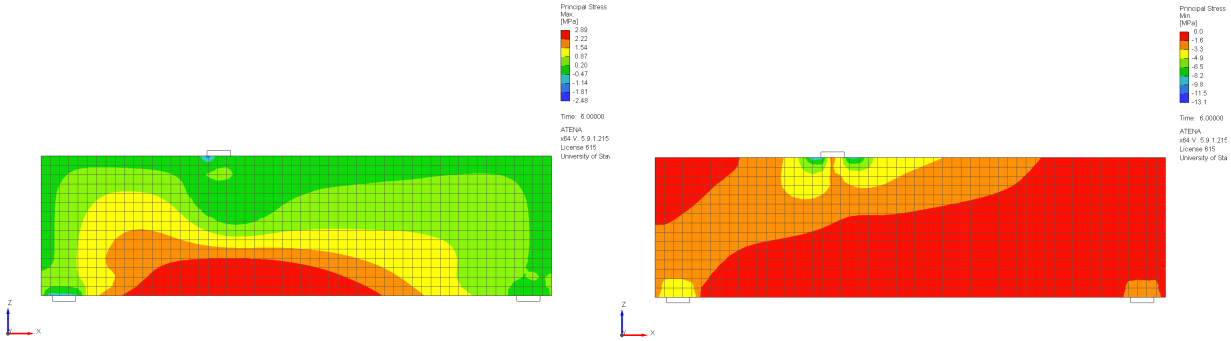

Figure 5.34: Principal tensile stress (left), principal compressive stress (right) for Model 2.3 with 25 MPa prestressing

The principal tensile and compressive stress at yield for Model 2.3 with 25 MPa straight prestressed reinforcement is shown in Figure 5.34. The distance from the bottom of the beam to the peak of the maximum principal tensile stress (a) is equal to 80mm. The principal compressive stress distributes the same way as Model 2.2 without prestressing, the distance from the top of the beam to the yellow area (b) is equal to 86mm.

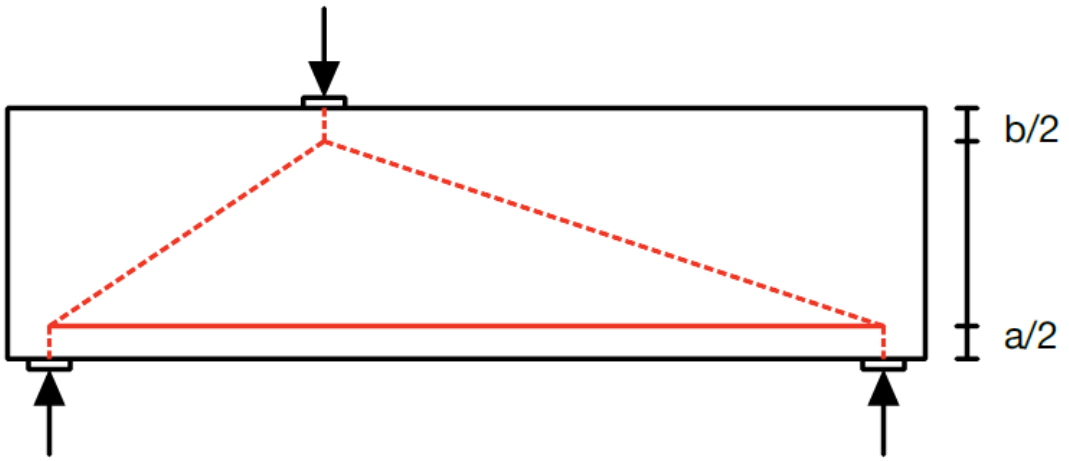

Figure 5.35: Strut and Tie model for Model 2.3 with 25 MPa straight prestressed reinforcement

The strut and tie model for Model 2.3 is displayed in Figure 5.35, a/2 are equal to 40mm and b/2 are equal to 43mm. The distance a/2 has been reduced by 5mm compared to Model 2.3 without prestressed reinforcement.

5.3.2.6 Model 2.3 with 100 MPa prestressing

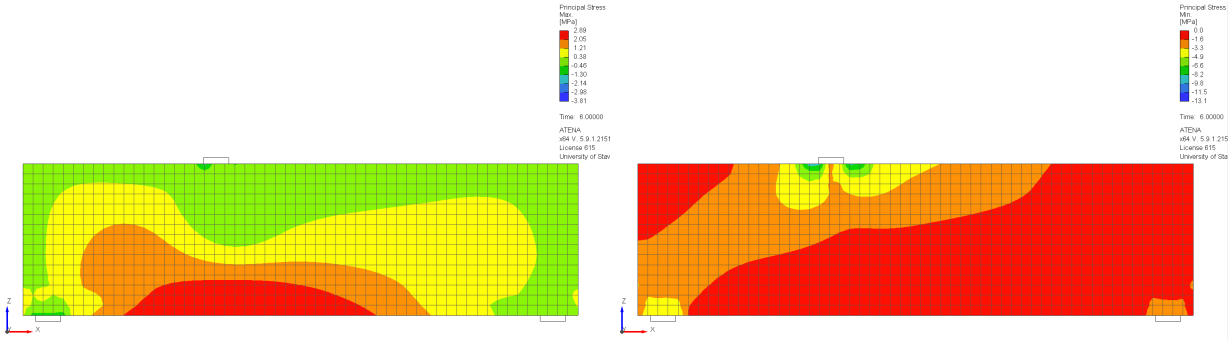

Figure 5.36: Principal tensile stress (left), principal compressive stress (right) for Model 2.3 with 100 MPa prestressing

Figure 5.36 shows the principal tensile and compressive stress for Model 2.3 with 100 MPa straight prestressed reinforcement. The peak of the principal tensile stress is equal to 70mm, and the distance b is equal to 86mm.

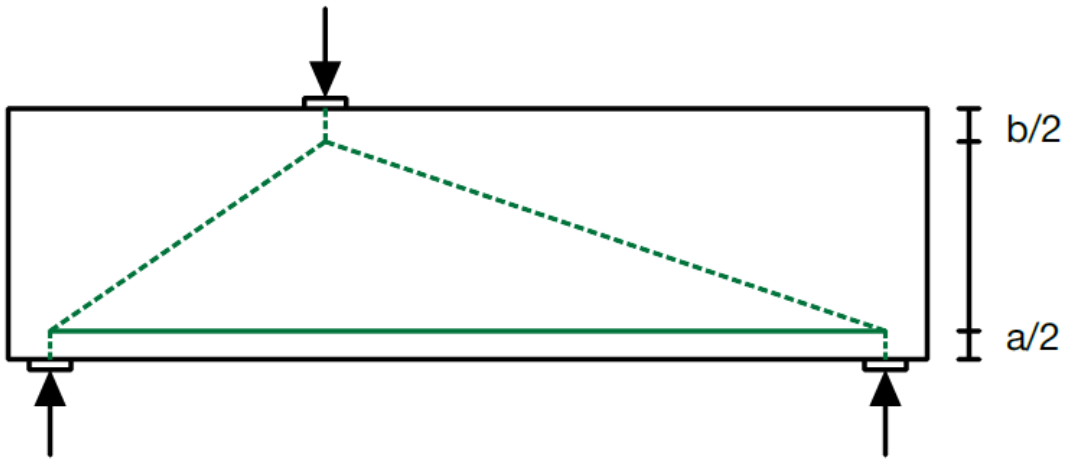

Figure 5.37: Strut and Tie model for Model 2.3 with 100 MPa straight prestressed reinforcement

Figure 5.37 displays the STM for Model 2.3 with 100 MPa straight prestressed reinforcement. The distance a/2 is equal to 35mm, it has decreased by 10mm and b/2 is equal to 43mm.

5.4 Case 3

Case 3 regards all models with curved prestressed reinforcement. The strut and tie models are drawn with red and green colors that represent the amount of prestressing, red is 25 MPa and green is 100 MPa.

5.4.1 Model 1

The reinforcement drawing for Model 1 with a curved prestressed reinforcement is shown in Figure 4.9.

5.4.1.1 Model 1.1 with 25 MPa prestressing

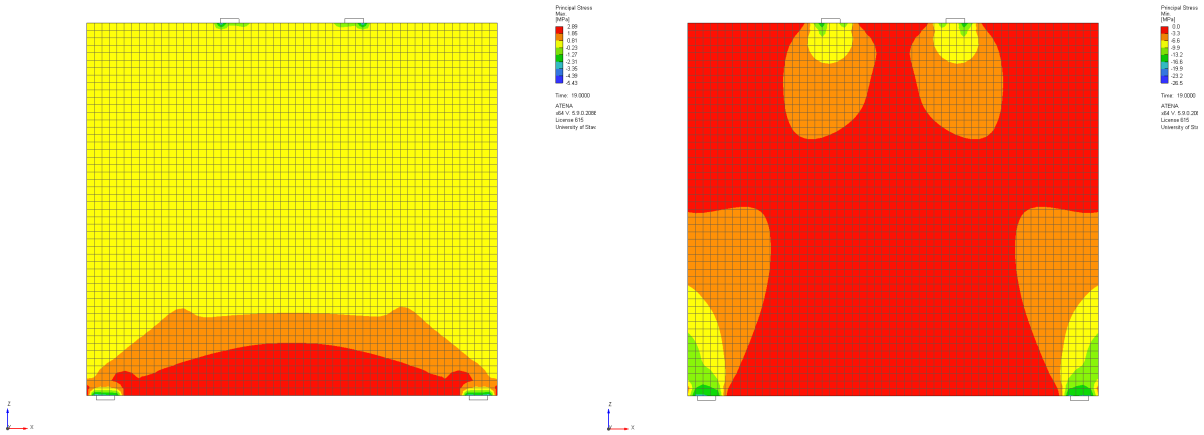

Figure 5.38: Principal tensile stress (left), principal compressive stress (right) for Model 1.1 with 25 MPa prestressing (curved)

Figure 5.38 shows the results of the principal tensile and compressive stresses for Model 1.1 with 25 MPa curved prestressed reinforcement. The results of the principal stresses show no change in the height of the stress development compared to Model 1.1 with 25 MPa straight prestressed reinforcement.

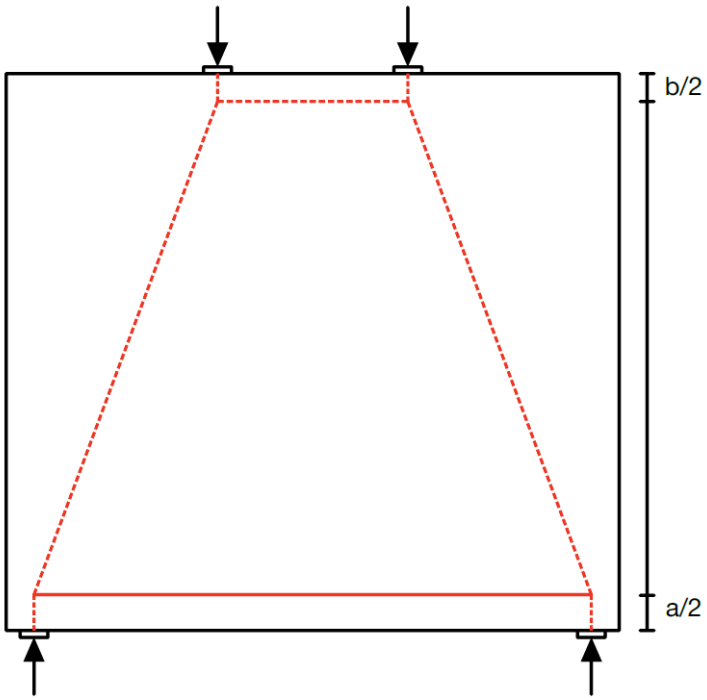

Figure 5.39: STM for Model 1.1 with 25 MPa curved prestressed reinforcement

Figure 5.39 is the strut and tie model developed from the results of principal tensile and compressive stresses shown in Figure 5.38. The distance from the bottom of the beam to the tie is 70mm and the distance from the top of the beam to the top strut is 53mm. The distance a/2 remains the same compared to Model 1.1 with 25 MPa straight prestressed reinforcement and decreases with 9mm compared to Model 1.1 without prestressed reinforcement.

5.4.1.2 Model 1.1 with 100 MPa prestressing

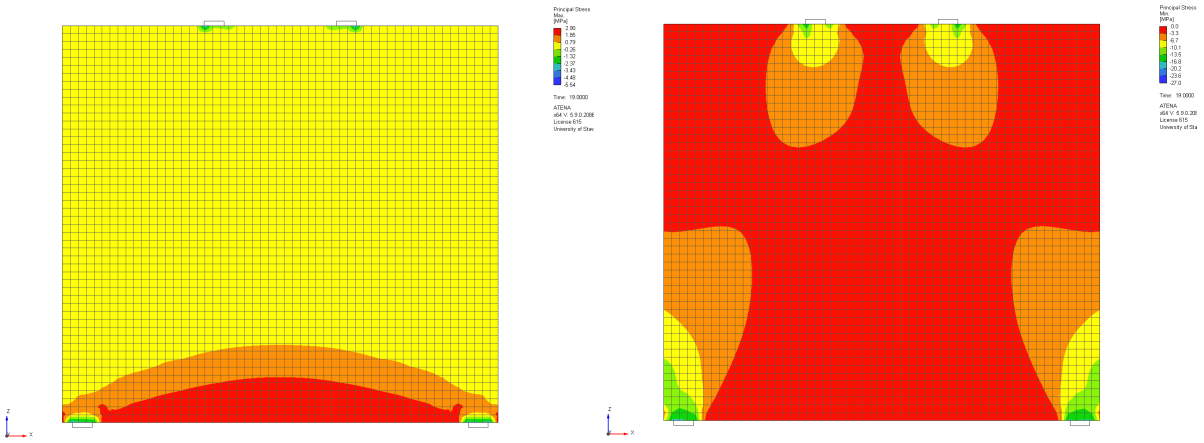

Figure 5.40: Principal tensile stress (left), principal compressive stress (right) for Model 1.1 with 100 MPa prestressing (curved)

Figure 5.40 shows the principal tensile and compressive stress for Model 1.1 with 100 MPa curved prestressed reinforcement. The height of a and b are measured the same way, a is equal to 112mm and b is equal to 106mm. The distance between the top of the beam to the strut remains the same for all Models 1.1.

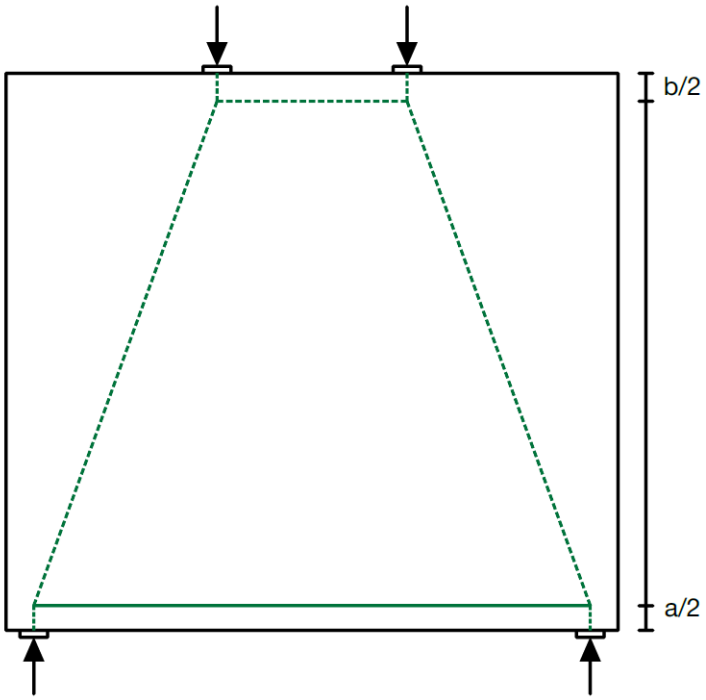

Figure 5.41: Strut and Tie model for Model 1.1 with 100 MPa curved prestressed reinforcement

Figure 5.41 shows the strut and tie model for Model 1.1 with 100 MPa curved prestressed reinforcement. The distance from the bottom of the beam to the tie (a/2) is equal to 56mm, this is a decrease of 2mm compared to Model 1.1 with 100 MPa straight prestressed reinforcement. Compared to Model 1.1 without prestressed reinforcement a/2 has decreased by 23mm. The distance b/2 is equal to 53mm.

5.4.1.3 Model 1.2 with 25 MPa prestressing

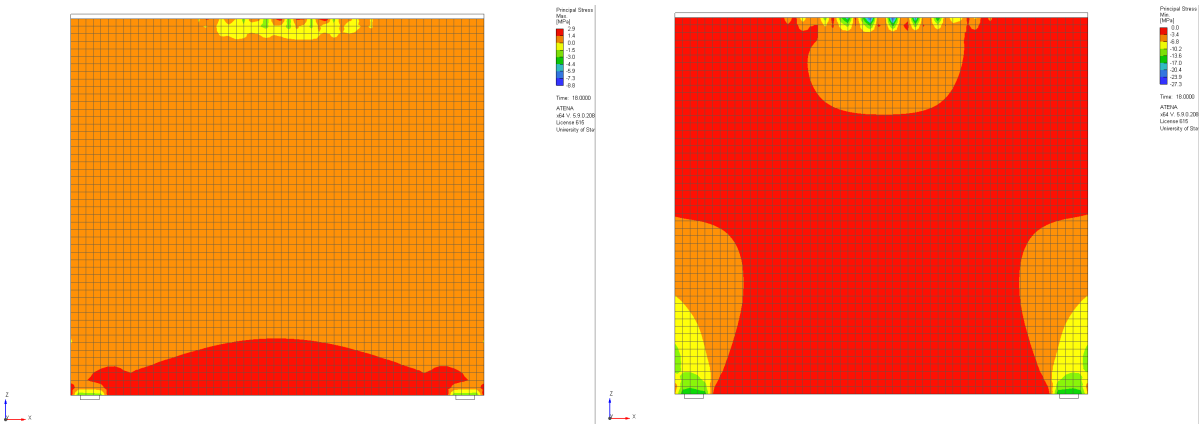

Figure 5.42: Principal tensile stress (left), principal compressive stress (right) for Model 1.2 with 25 MPa prestressing (curved)

The principal stresses for Model 1.2 with 25 MPa curved prestressing are displayed in Figure 5.42. The stress development is similar to Model 1.2 with straight prestressing. The distance a is equal to 150mm.

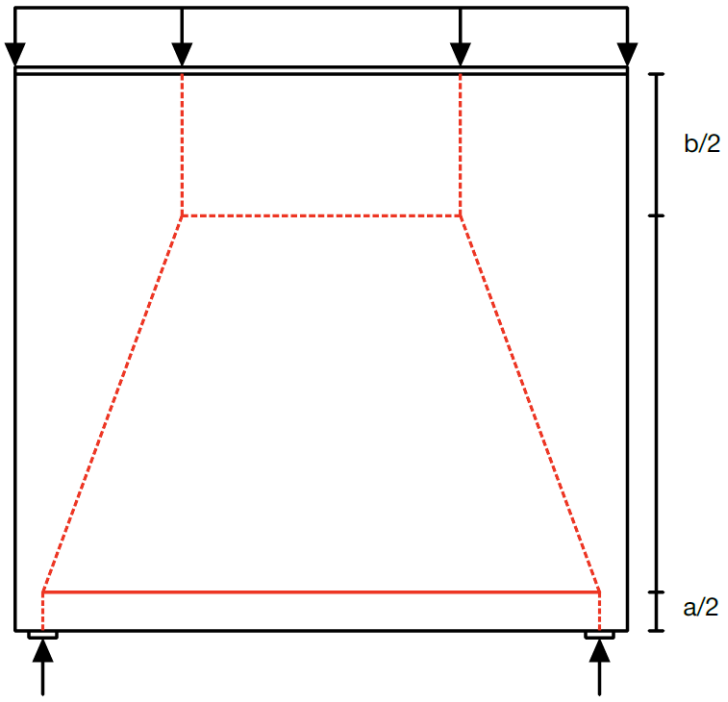

Figure 5.43: Strut and Tie model for Model 1.2 with 25 MPa curved prestressed reinforcement

Figure 5.43 is the strut and tie model for Model 1.2 with a curved prestressed reinforcement. The distance between the tie and the bottom of the beam a/2 is equal to 75mm, compared

to Model 1.2 with 25 MPa straight prestressing it is an decrease of 1mm. The distance b/2 is equal to 260mm.

5.4.1.4 Model 1.2 with 100 MPa prestressing

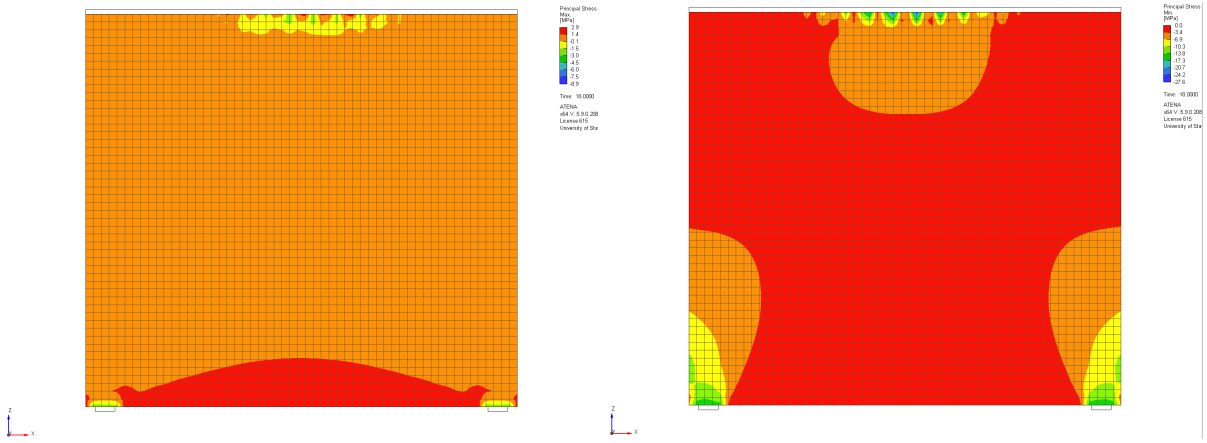

Figure 5.44: Principal tensile stress (left), principal compressive stress (right) for Model 1.2 with 100 MPa prestressing (curved)

The principal tensile and compressive stress for Model 1.2 with 100 MPa curved prestressing is shown in Figure 5.44. The distance a is equal to 122mm, and b remains the same.

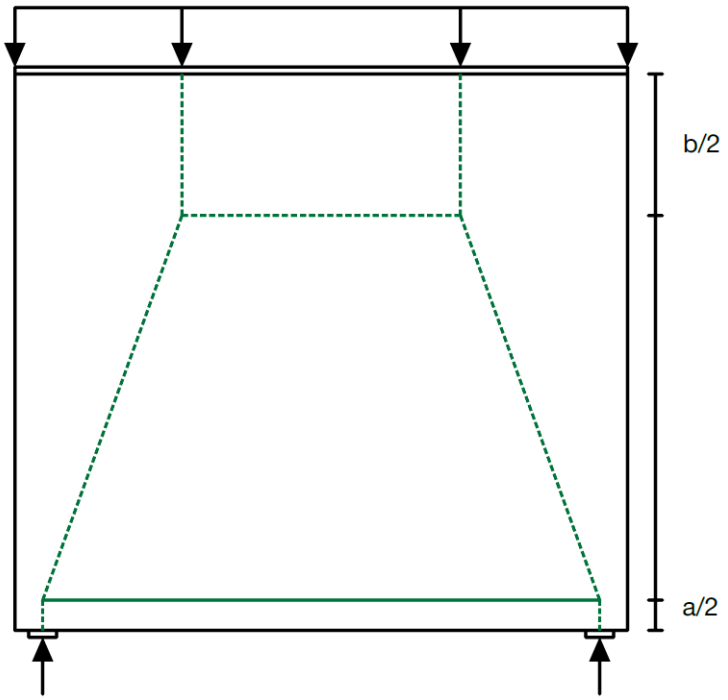

Figure 5.45: Strut and Tie model for Model 1.2 with 100 MPa curved prestressed reinforcement

The strut and tie model for Model 1.2 with 100 MPa curved prestressed reinforcement, developed from the principal tension and compression stress results is shown in Figure 5.45. The distance (a/2) is equal to 61mm, compared to Model 1.2 with straight prestressing which is a decrease of 1mm and compared to Model 1.2 without prestressed reinforcement a/2 has decreased by 7mm.

5.4.1.5 Model 1.3 with 25 MPa prestressing

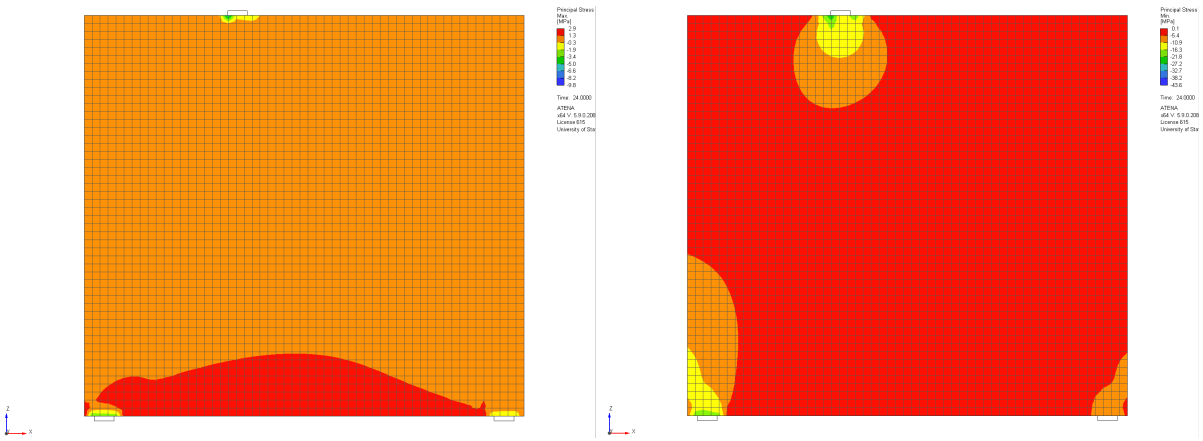

Figure 5.46: Principal tensile stress (left), principal compressive stress (right) for Model 1.3 with 25 MPa prestressing (curved)

Figure 5.46 shows the principal tensile and compressive stresses for Model 1.3 with 25 MPa curved prestressed reinforcement. The peak of the principal tensile stress (a) is equal to 156mm and b is equal to 106mm.

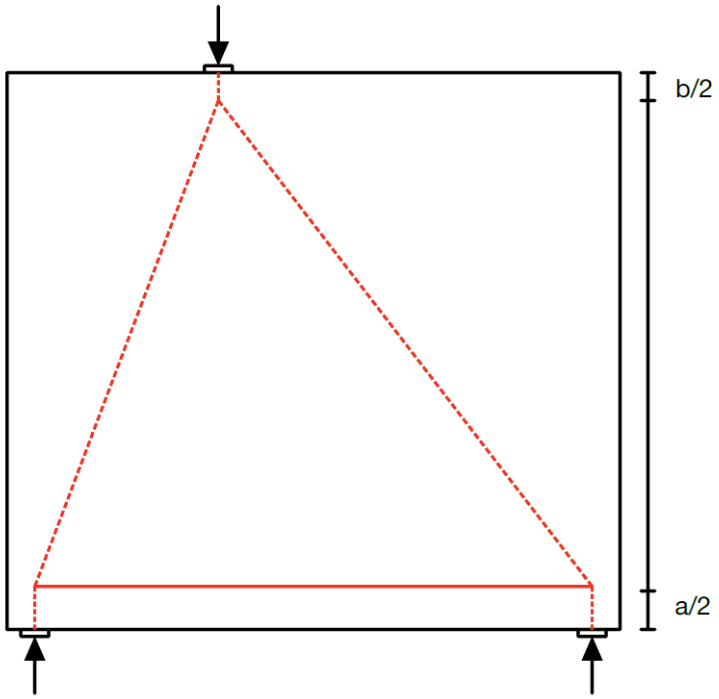

Figure 5.47: Strut and Tie model for Model 1.3 with 25 MPa curved prestressed reinforcement

The strut and tie model for Model 1.3 with 25 MPa curved prestressed reinforcement are shown in Figure 5.47. The distance a/2 is equal to 78mm, which is a decrease of 1mm compared to Model 1.3 with 25 MPa straight prestressed reinforcement. The distance b/2 is equal to 53mm.

5.4.1.6 Model 1.3 with 100 MPa prestressing

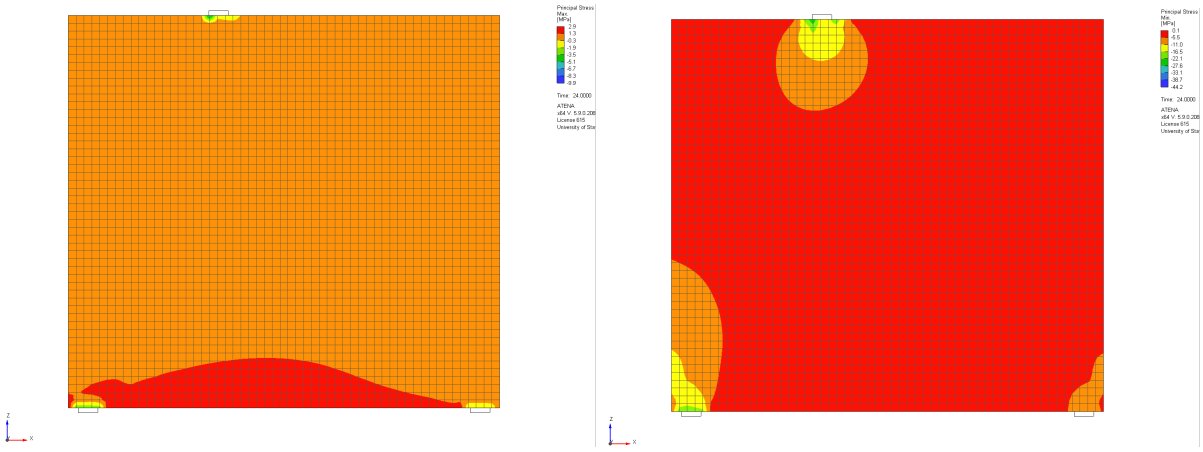

Figure 5.48: Principal tensile stress (left), principal compressive stress (right) for Model 1.3 with 100 MPa prestressing (curved)

The principal tensile and compressive stress for Model 1.3 with 100 MPa curved prestressed reinforcement is shown in Figure 5.48. The maximum stress development at yield has a similar shape to the other Model 1.3, but the maximum height of the principal tension stress (a) has decreased to 126mm. The distance b remains the same at 106mm.

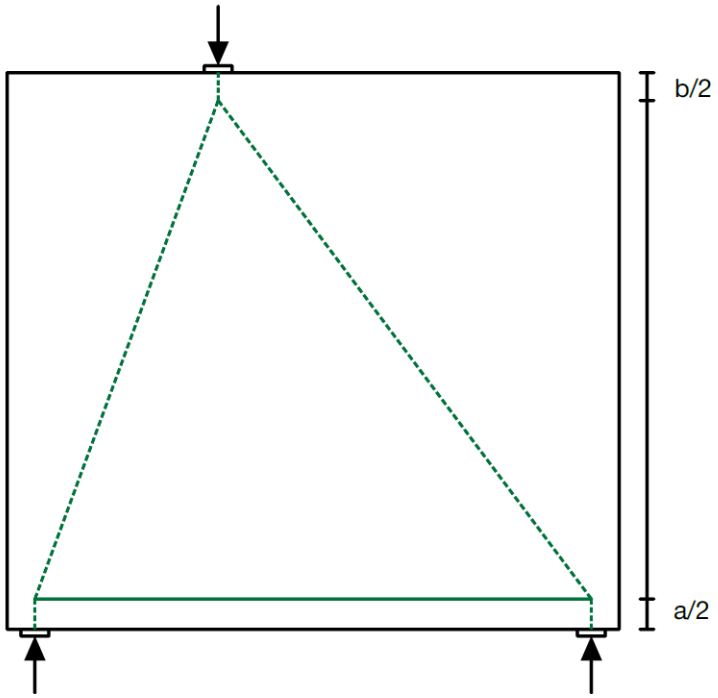

Figure 5.49: Strut and Tie model for Model 1.3 with 100 MPa curved prestressed reinforcement

The proposed strut and tie model for Model 1.3 with 100 MPa curved prestressed reinforcement are developed from the principal tensile and compressive stresses as shown in Figure 5.49. The distance from the bottom of the beam to the tie (a/2) is equal to 63mm. That equals a decrease of 1mm compared to Model 1.3 with 100 MPa straight prestressed reinforcement and a decrease of 21mm compared to Model 1.3 without prestressed reinforcement. The distance from the top of the beam to the top node (b/2) is equal to 53mm.

5.4.2 Model 2

The dimensions of Model 2 are shown in Figure 4.13 and reinforcement drawing for Model 2 with a curved prestressed reinforcement are shown in Figure 4.15.

5.4.2.1 Model 2.1 with 25 MPa prestressing

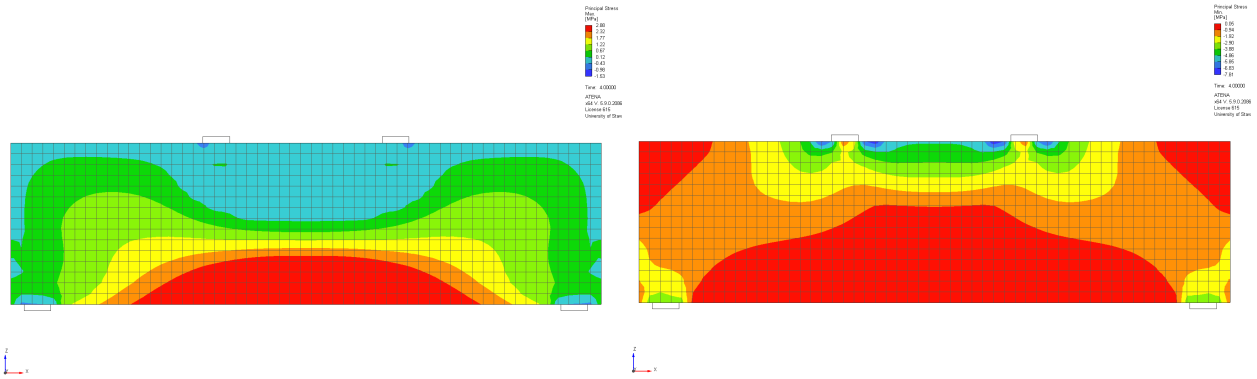

Figure 5.50: Principal tensile stress (left), principal compressive stress (right) for Model 2.1 with 25 MPa prestressing (curved)

The peak of the principal tensile stress is equal to 90mm for Model 2.1 with 25 MPa curved prestressed reinforcement. The height of the yellow area from the principal compressive stress (b) is equal to 80mm.

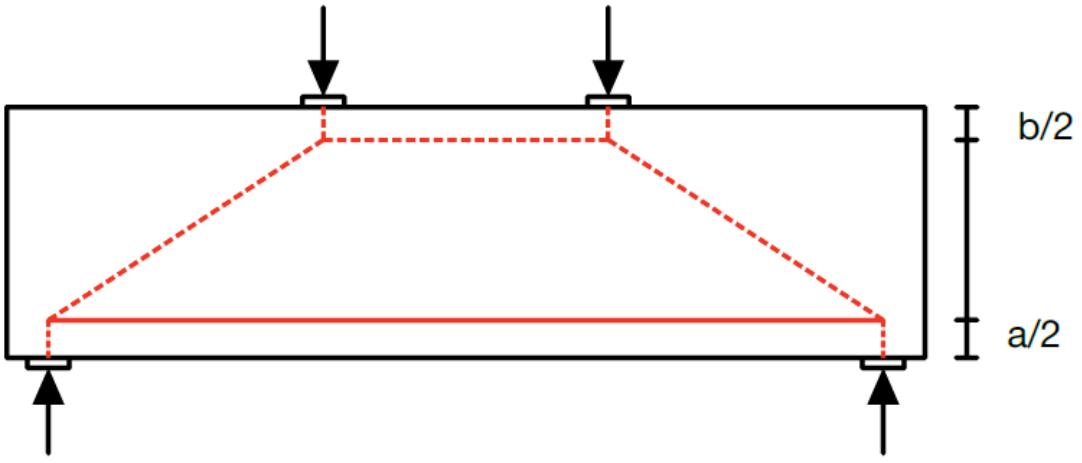

Figure 5.51: Strut and Tie model for Model 2.1 with 25 MPa curved prestressed reinforcement

Figure 5.51 illustrates the proposed strut and tie model of Model 2.1, with 25 MPa curved prestressed reinforcement. The tie is placed at a distance of 45mm from the bottom of the

beam (a/2), while the strut is located at a distance of 40mm from the top of the beam. Compared to Model 2.1 with 25 MPa straight prestressed reinforcement, the distance b/2 has not changed.

5.4.2.2 Model 2.1 with 100 MPa prestressing

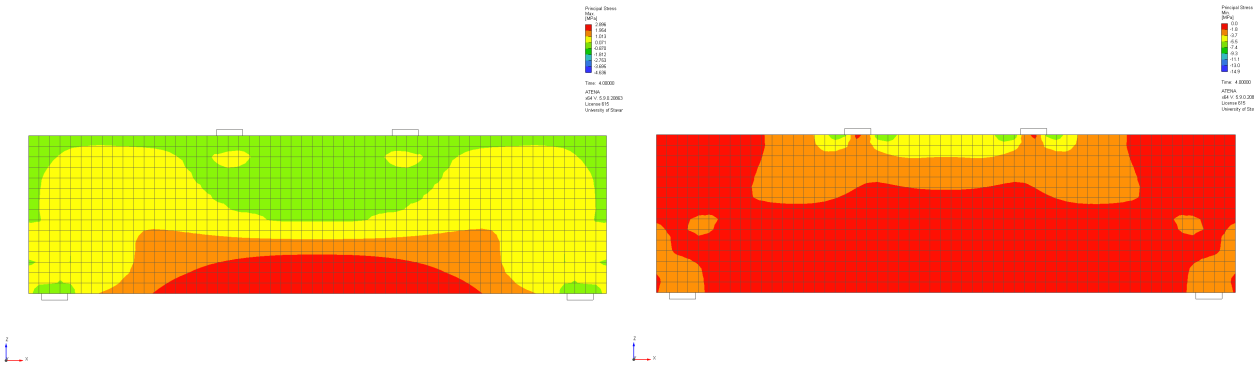

Figure 5.52: Principal tensile stress (left), principal compressive stress (right) for Model 2.1 with 100 MPa prestressing (curved)

The principal tensile and compressive stresses for Model 2.1 with 100 MPa curved prestressed reinforcement, are shown in Figure 5.52. The height of the peak of the principal tensile stress (a) is 74mm, while the height (b) of the yellow area representing the principal compressive stress is 80mm.

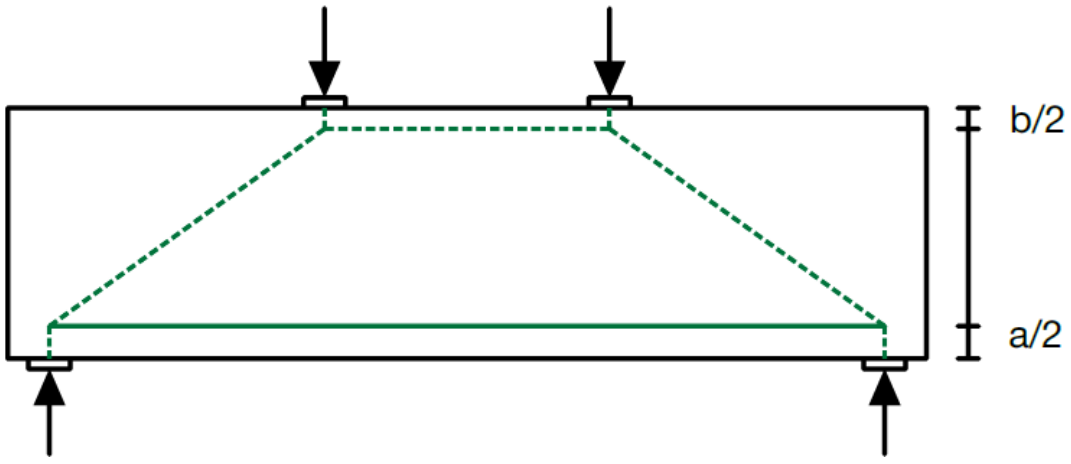

Figure 5.53: Strut and Tie model for Model 2.1 with 100 MPa curved prestressed reinforcement

The strut and tie model for Model 2.1 with 100 MPa curved prestressing are shown in Figure 5.53. The distance a/2 is equal to 37 mm and b/2 is equal to 40mm. The distance

a/2 has been reduced by 2mm compared to Model 2.1 with 100 MPa straight prestressed reinforcement.

5.4.2.3 Model 2.2 with 25 MPa prestressing

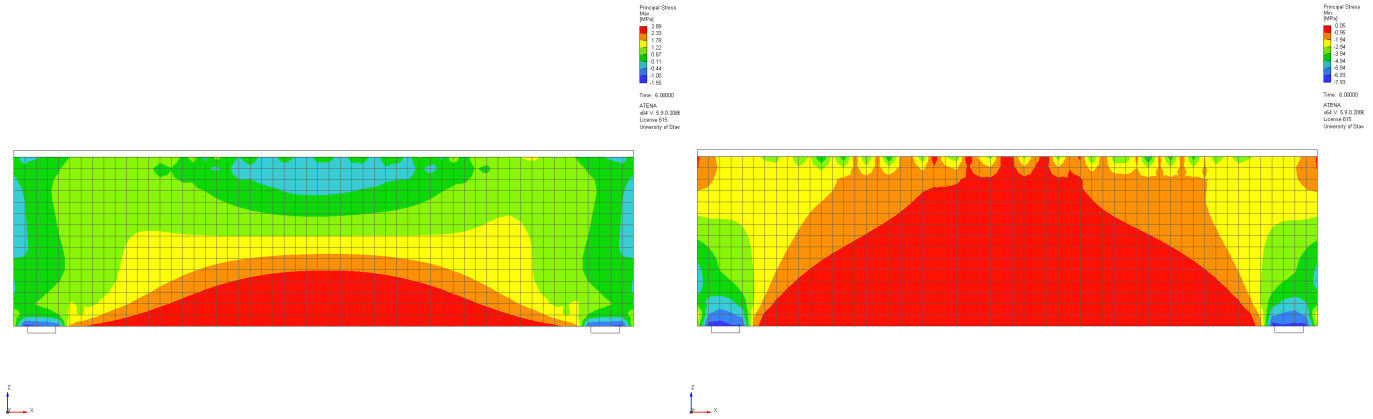

Figure 5.54: Principal tensile stress (left), principal compressive stress (right) for Model 2.2 with 25 MPa prestressing (curved)

Figure 5.54 shows the principal tensile and compressive stress for Model 2.2 with 25 MPa curved prestressed reinforcement. The peak of the principal tensile stress is equal to 98mm, and the distance b is measured the same way as Model 2.2 without prestressing and straight prestressed reinforcement and equals 40mm. The principal compressive stress development has the same propagation as Model 2.2.

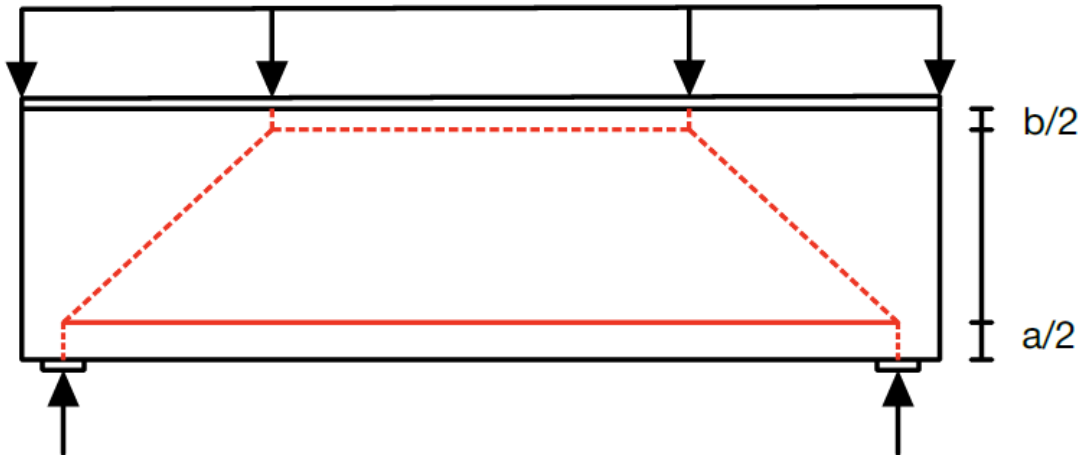

Figure 5.55: Strut and Tie model for Model 2.2 with 100 MPa curved prestressed reinforcement

The distance a/2 equals 49mm and b/2 equals 22mm, and the strut and tie model for Model 2.2 with 25 MPa curved prestressed reinforcement are shown in Figure 5.55.

5.4.2.4 Model 2.2 with 100 MPa prestressing

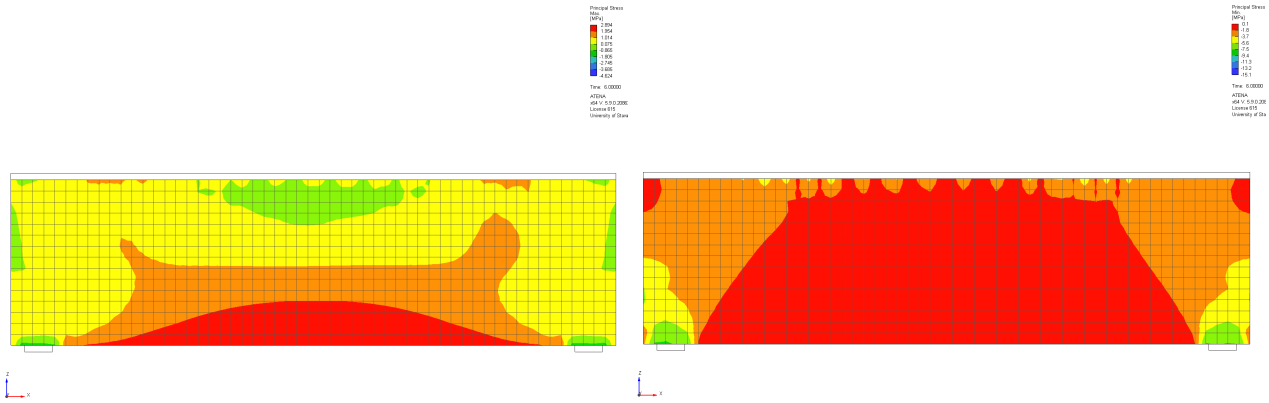

Figure 5.56: Principal tensile stress (left), principal compressive stress (right) for Model 2.2 with 100 MPa prestressing (curved)

The peak of the principal tensile stress is equal to 80mm for Model 2.2 with 100 MPa curved prestressed reinforcement shown in Figure 5.56, and the distance b is equal to 44mm.

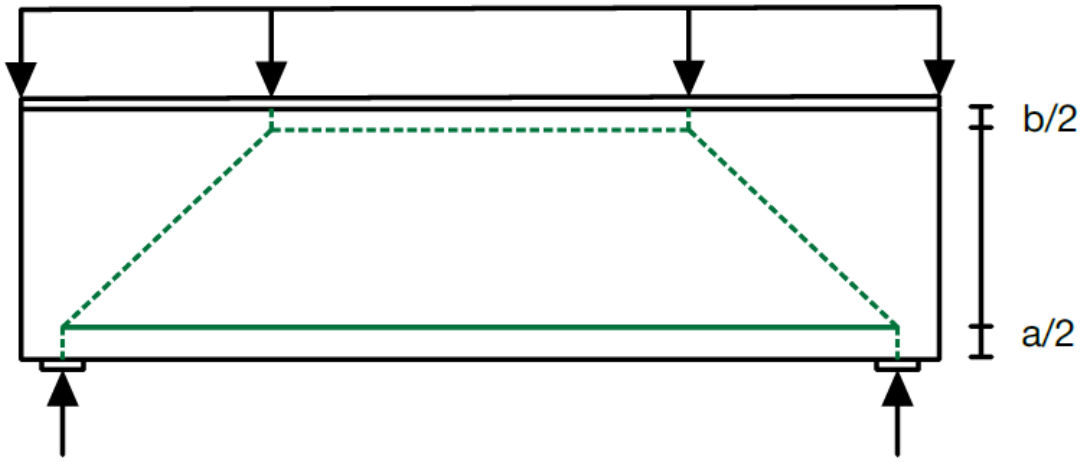

Figure 5.57: Strut and Tie model for Model 2.2 with 100 MPa curved prestressed reinforcement

The strut and tie model for Model 2.2 with 100 MPa curved prestressed reinforcement is displayed in Figure 5.57. The distance a/2 is equal to 40mm and b/2 is equal to 22mm.

5.4.2.5 Model 2.3 with 25 MPa prestressing

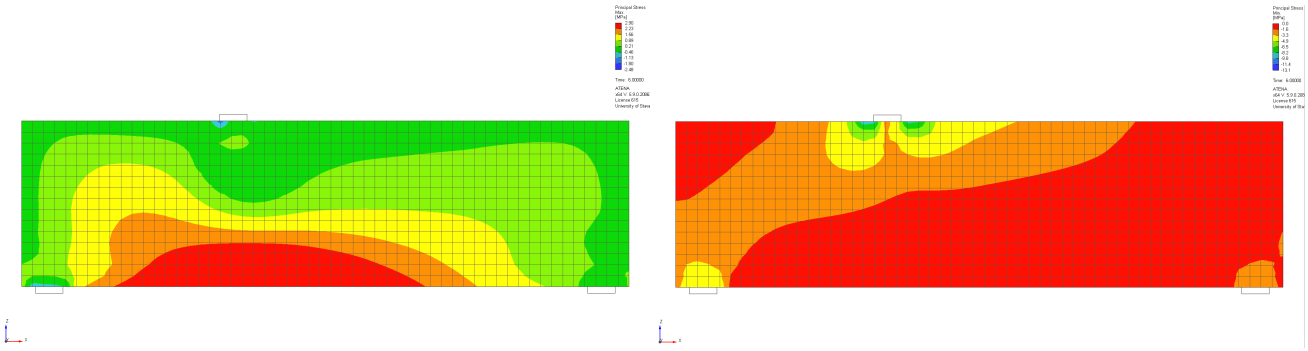

Figure 5.58: Principal tensile stress (left), principal compressive stress (right) for Model 2.3 with 25 MPa prestressing (curved)

Figure 5.58 displays the principal tensile and compressive stress for Model 2.3 with 25 MPa curved prestressed reinforcement. The peak of the principal tensile stress (a) is equal to 80mm, and the height of the yellow area for the principal compressive stress (b) is equal to 86mm.

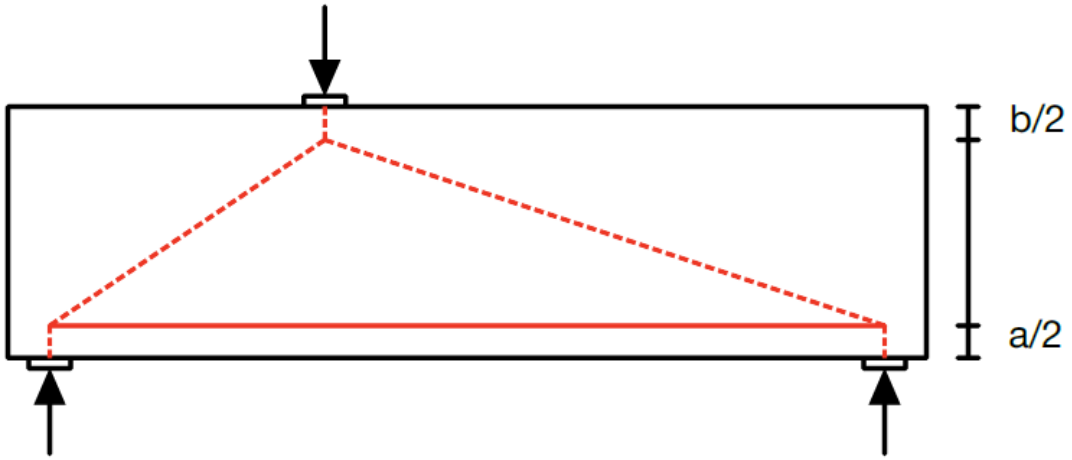

Figure 5.59: Strut and Tie model for Model 2.3 with 25 MPa curved prestressed reinforcement

The distance from the bottom of the beam to the tie a/2 is equal to 40mm and the distance from the top of the beam to the top node (b/2) is equal to 43mm. The proposed STM for Model 2.3 with 25 MPa curved prestressed reinforcement is shown in Figure 5.59. a/2 has decreased by 3mm compared to Model 2.3 with 100 MPa straight prestressed reinforcement and 10mm compared to Model 2.3 without prestressing.

5.4.2.6 Model 2.3 with 100 MPa prestressing

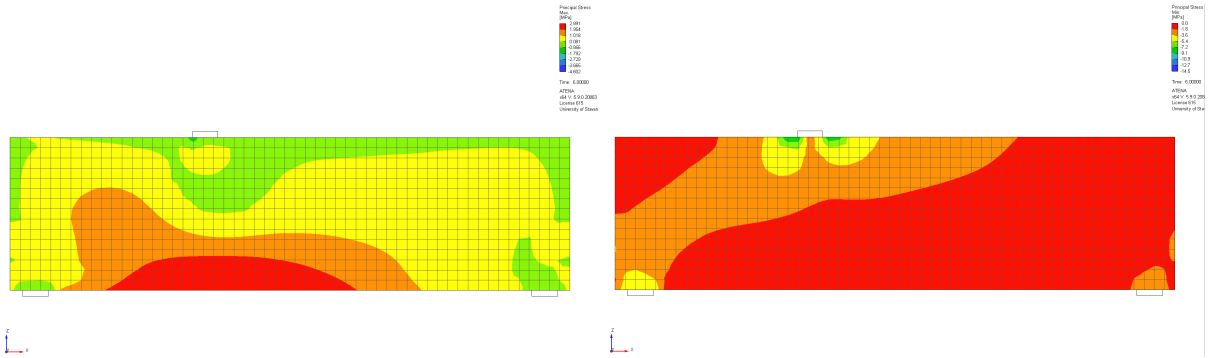

Figure 5.60: Principal tensile stress (left), principal compressive stress (right) for Model 2.3 with 100 MPa prestressing (curved)

The peak of the principal tensile stress is equal to 68mm for Model 2.3 with 100 MPa curved prestressed reinforcement. The height of the yellow area for the principal compressive stress (b) is equal to 86mm.

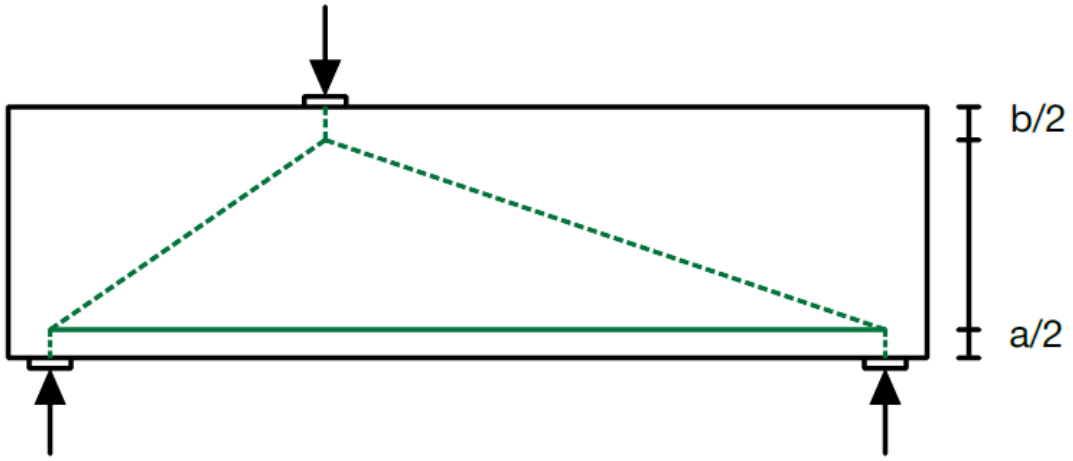

Figure 5.61: STM for Model 2.3 with 100 MPa curved prestressed reinforcement

Figure 5.61 shows the strut and tie model for Model 2.3 with 100 MPa curved prestressing developed from the principal tensile and compressive stress. The distance a/2 is equal to 34mm and b/2 is equal to 43mm.

5.5 Summary of the results for cases 1, 2, and 3

Table 5.1: Table of the distances a/2 for all cases with all models

		a/2 [mm]					
		Model 1.1	Model 1.2	Model 1.3	Model 2.1	Model 2.2	Model 2.3
0 MPa	Case 1	79	82	84	51	60	45
25 MPa	Case 2	70	76	79	45	59	40
	Case 3	70	75	78	45	49	40
100 MPa	Case 2	59	64	64	39	54	35
	Case 3	56	61	63	37	40	38

Table 5.1 shows all the results for the distance a/2 which represents the distance from the bottom of the beam to the tie.

The results from Model 1.1 shows a decrease in the height a/2 from case 1 through case 3 with 100 MPa prestressing. The results show a decrease of 9mm from case 1 to cases 2 and 3 with 25 MPa prestressing. It is a further decrease from case 1 to case 2 with 100 MPa with the value of 20mm and 23mm from case 1 to case 3 with 100 MPa prestressing. The same development is for Models 1.2 and 1.3 where there is a decrease in the height a/2 when adding prestressing and increasing the jacking force. The results show that the curved prestressed reinforcement changes the distance a/2 slightly more than the straight prestressed reinforcement.

The results from Model 2.1 shows a similar evolution as Model 1.1 where the decrease from case 1 to case 2 with 25 MPa prestressing is 6mm, the result shows no change in a/2 from case 2 to case 3 with 25 MPa. Further, the decrease from case 1 to case 2 with 100 MPa is 12mm and from case 1 to case 3 with 100 MPa the decrease is 14mm.

The following Equation 5.1 is a proposed equation for calculating the distance a/2, it consists of a number of different variables, H is the height of the deep beam and J is the jacking force for the prestressed reinforcement.

$$a/2 = b + c \cdot H + d \cdot J + e \cdot H^2 + f \cdot H \cdot J + g \cdot J^2 + h \cdot H \cdot J^2 + i \cdot H^2 \cdot J^2 \qquad (5.1)$$

- H: Height of deep beam [mm]
- J: Jacking force [MPa]

Equation 5.1 is developed with multivariate regression, based on the results given in Table 5.1. A multivariate regression model establishes a relationship between a dependent variable and more than one independent variable [22]. The dependent variable is a/2 and the independent variables are H and J. This equation is valid for cases 1 to 3, for a deep beam with a height of 1000mm and one with a height of 300mm.

The input parameters that vary on behalf of which load case is applied are b, c, d, e, f, g, h, and i. The calculations for the input parameters are shown in the appendix. The input parameters are shown in Table 5.2 and 5.3.

Table 5.2: Parameters for calculating a/2 for all models for cases 1 and 2

	Two-point loads	**Uniform distributed load**	**One-point load**
b	0	0	0
c	0.209	0.25057	0.17829
d	0.23429	0.06381	-0.24762
e	-0.00013	-0.00016857	-9.4286e-05
f	-0.000647762	-0.00032381	4.7619e-05
g	0	0	0
h	-8.5333e-06	-1.6127e-06	6.3492e-06
i	1.0667e-08	2.4127e-09	-6.3492e-09

Table 5.2 shows the values of b to i for all the models for cases 1 and 2, which are the models without prestressed reinforcement and with a straight prestressed reinforcement.

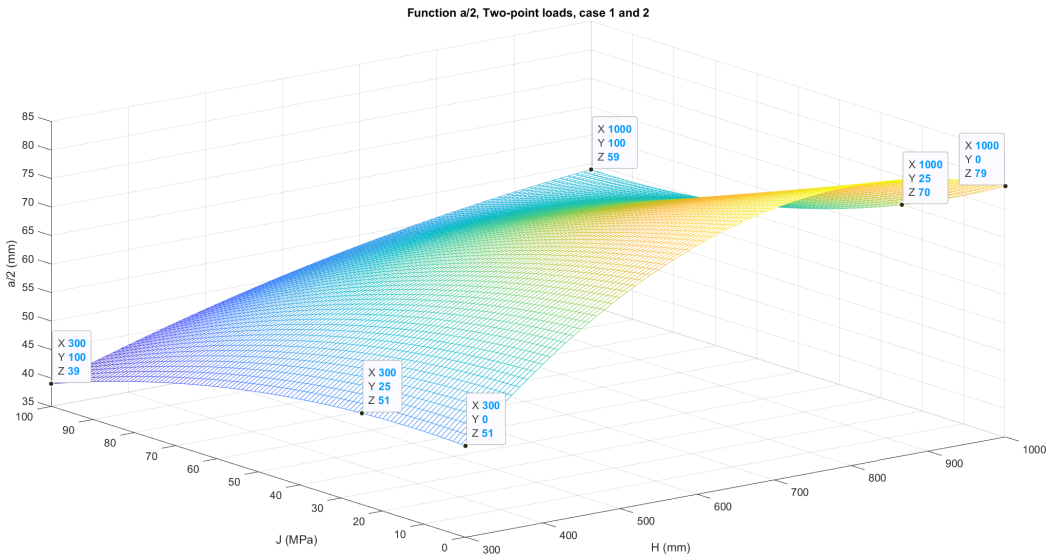

Figure 5.62: Plot of function a/2, two-point loads for cases 1 and 2

Figure 5.62 shows the plot of Equation 5.1 with the input parameters for two-point

loads shown in Table 5.2 for cases 1 and 2. The coordinates marked on the function are the results of a/2 with the different heights and jacking force, shown in Table 5.1. X-coordinates represent the height of the beam [mm], Y-coordinates represent the jacking force [MPa] and Z-coordinates represent the distance a/2 [mm].

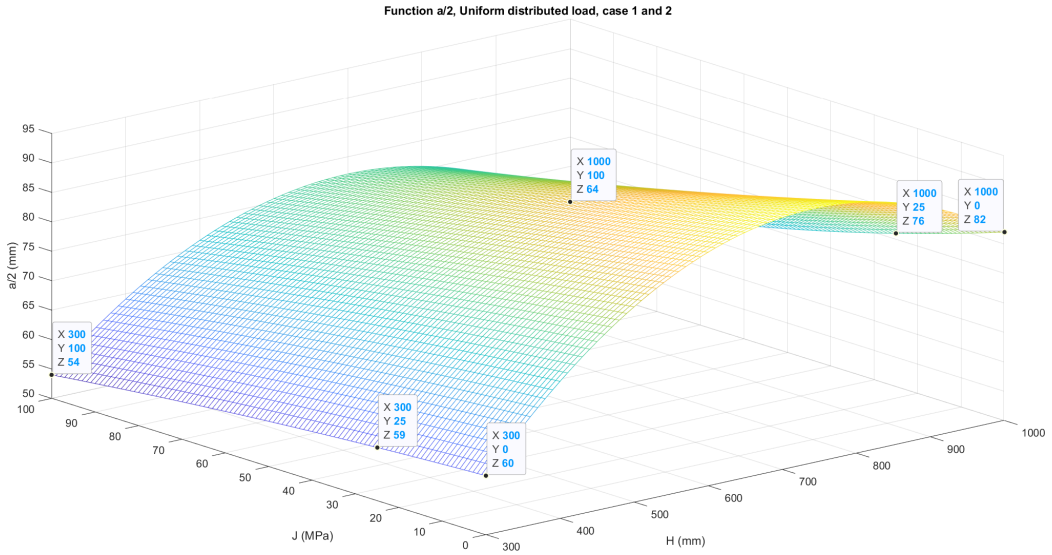

Figure 5.63: Plot of function a/2, uniform distributed load for cases 1 and 2

Figure 5.63 shows the plot of the Equation 5.1 with the input parameters for uniform distributed load shown in Table 5.2 for load cases 1 and 2.

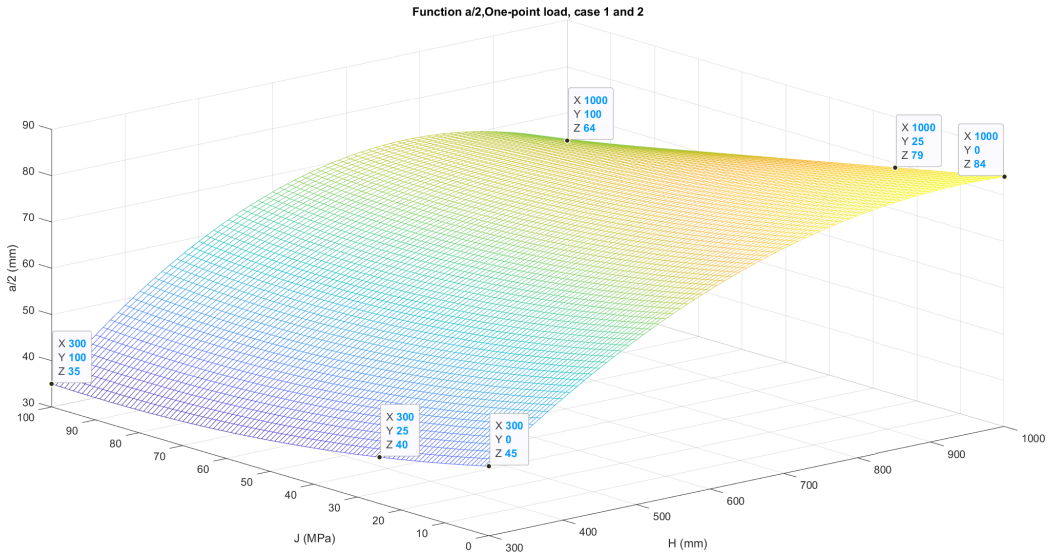

Figure 5.64: Plot of function a/2, one-point load for cases 1 and 2

Figure 5.64 shows the plot of the Equation 5.1 for one-point load with the reinforcement for cases 1 and 2. The coordinates that are marked on the plot are the results of a/2

shown in Table 5.1.

Table 5.3: Parameters for calculating a/2 for all models for cases 1 and 3

	Two-point loads	**Uniform distributed load**	**One-point load**
b	0	0	0
c	0.209	0.25057	0.17829
d	-0.21762	-0.61286	-0.24048
e	-0.00013	-0.00016857	-9.4286e-05
f	-0.00018571	0.00030952	-9.5238e-06
g	0	0	0
h	5.6063e-06	1.4838e-05	8.0825e-06
i	-3.873e-09	-1.3905e-08	-7.6825e-09

Table 5.3 displays the values of b to i for all models for cases 1 and 3, which is the one with a curved prestressed reinforcement and without prestressed reinforcement.

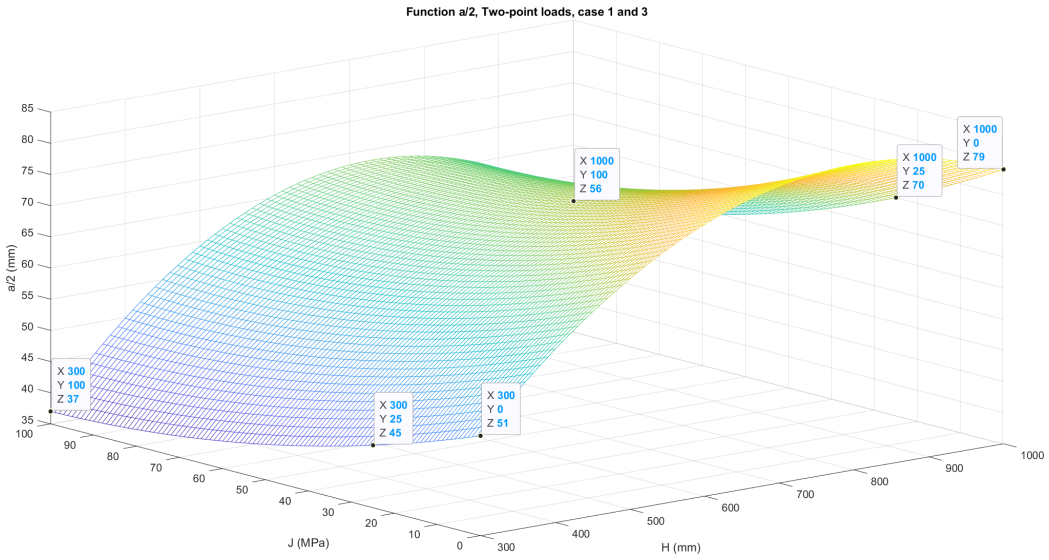

Figure 5.65: Plot of function a/2, two-point loads for cases 1 and 3

Figure 5.65 shows the plot of Equation 5.1 with the parameters from two-point loads with cases 1 and 3 shown in Table 5.3.

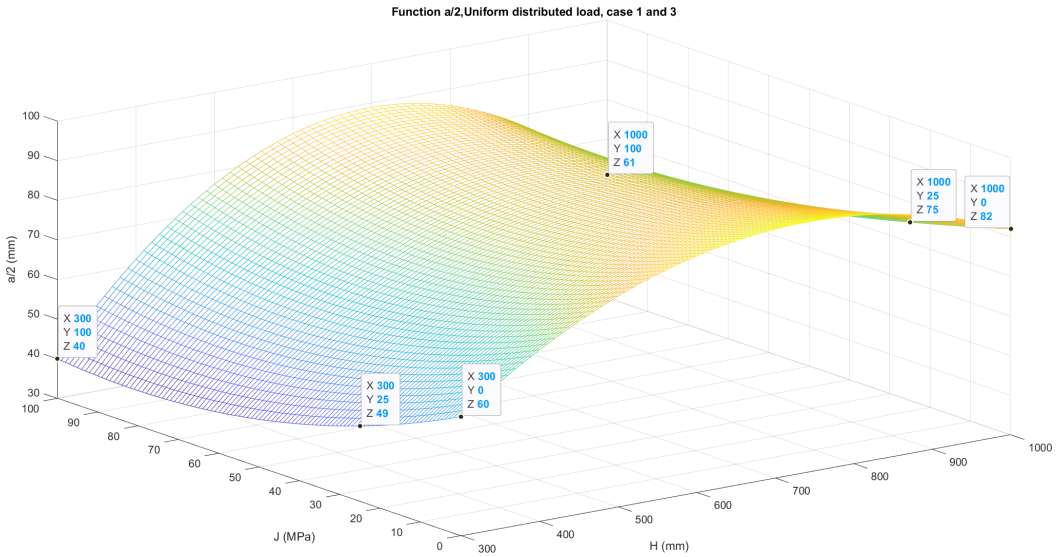

Figure 5.66: Plot of function a/2, uniform distributed load for cases 1 and 3

Figure 5.66 shows the plot of the Equation 5.1 with the parameters for uniform distributed load with cases 1 and 3 shown in Table 5.3.

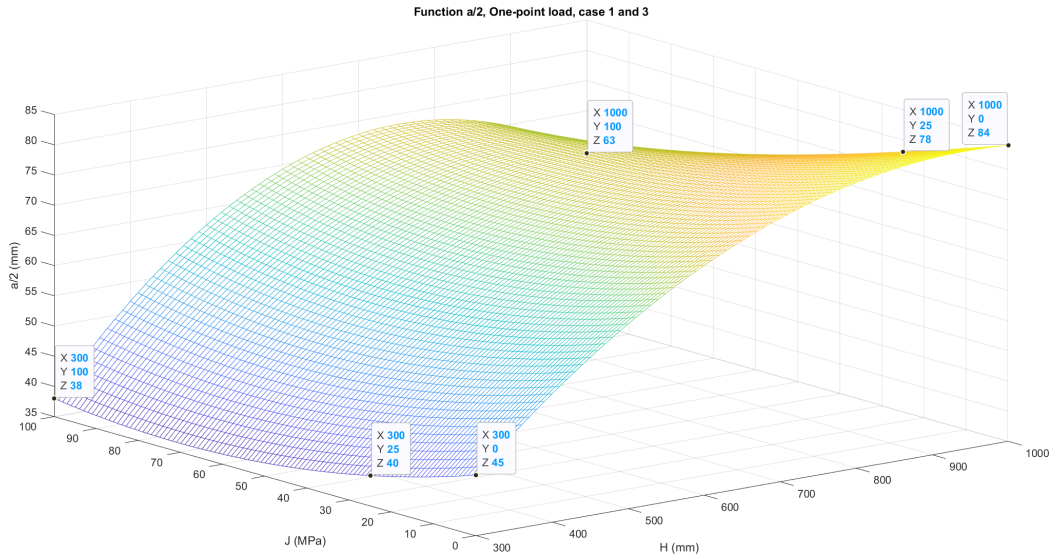

Figure 5.67: Plot of function a/2, one-point load for cases 1 and 3

Figure 5.67 shows the plot of the Equation 5.1 for one-point load with the reinforcement for cases 1 and 3. The coordinates that are marked on the plot are the results of a/2 shown in Table 5.1.

Table 5.4: Table of the distance b/2 for all cases with all models

		b/2 [mm]					
		Model 1.1	Model 1.2	Model 1.3	Model 2.1	Model 2.2	Model 2.3
0 MPa	Case 1	53	260	53	40	22	43
25 MPa	Case 2	53	260	53	40	22	43
	Case 3	53	260	53	40	22	43
100 MPa	Case 2	53	260	53	40	22	43
	Case 3	53	260	53	40	22	43

Table 5.4 shows all the distances between the top strut or node to the top of the beam for the models. The results show no change in the distance b/2 for each model with the same load parameters.

5.6 Case 4

The following results regard Case 4, which is Model 1.1 with different openings. There are three different cases where the positions of the openings change, the different cases contain two openings, and their x-position remains the same but the z-position change. The STM has the same color description as previously, with black representing the models without prestressed reinforcement, red representing 25 MPa prestressing, and green 100 MPa prestressing. The following results of Case 4 show the principal tensile and compressive stress for the models, then a proposed STM is added. The STM is developed similarly to previously, for the principal tensile stress, the red area is measured, and the ties are placed at the center. The same method is used for the principal compressive stress for the placements of struts, where the compressive areas are divided, and the struts are placed. The developed STM is controlled by placing a unit load of 100 kN for the top struts and supporting at the bottom, then the equilibrium of forces is controlled, the calculations are shown in the appendix.

5.6.1 Case 4.1

Case 4.1 are Model 1.1 with two openings, the openings are placed 0.3m from the bottom to the bottom of the opening. Figure 4.19 shows the placement of the two openings.

5.6.1.1 Case 4.1 without prestressed reinforcement

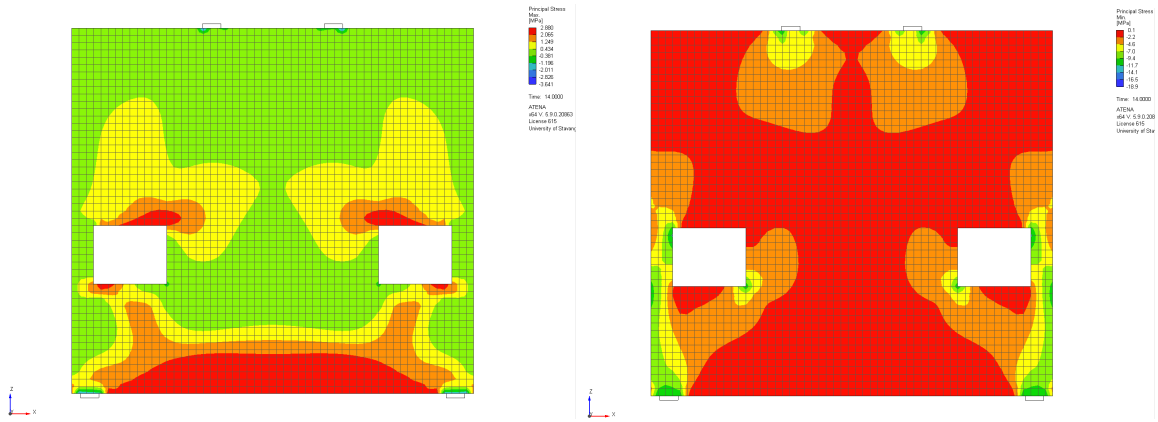

Figure 5.68: Principal tensile (left) and compressive (right) stress for Case 4.1 without prestressed reinforcement

Figure 5.68 shows the principal tensile and compressive stress for Case 4.1 without prestressed reinforcement. The principal tensile stress distribution at the bottom of the beam is similar to the results of Model 1.1. The area around the openings has a concentration of tensile stress, the reason for this is there comes a local deflection in the openings, which results in tensile stresses. The tensile stress distribution under the openings can be explained by the deformation of the deep beam results in a rotation that becomes tensile stress towards the end of the beam and compressive stress towards the middle.

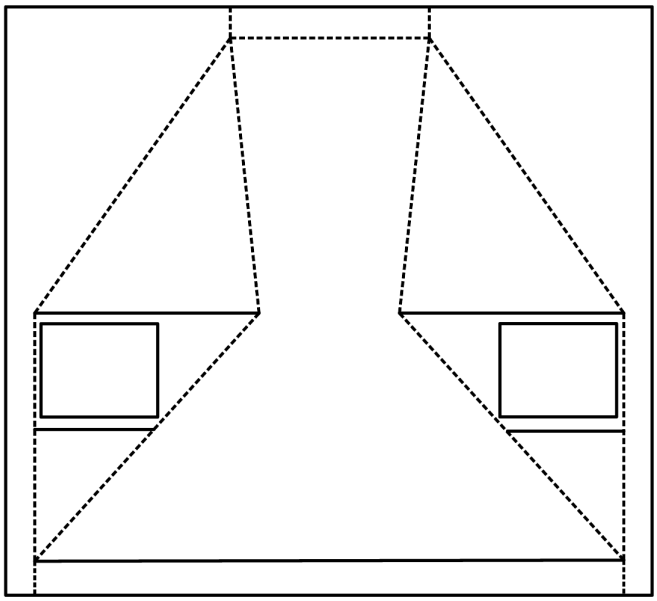

Figure 5.69: Strut and Tie model for Case 4.1 without prestressed reinforcement

Figure 5.69 shows the STM developed from the principal tensile and compressive stress. The struts and ties are placed in the middle of the stress development. As in previous models without openings, a tie is placed towards the bottom of the beam, since there develop tensile stresses around the openings, ties are allowed to be placed there. The struts connect the ties and are placed where there is principal compressive stress distribution.

5.6.1.2 Case 4.1 with 25 MPa prestressed reinforcement

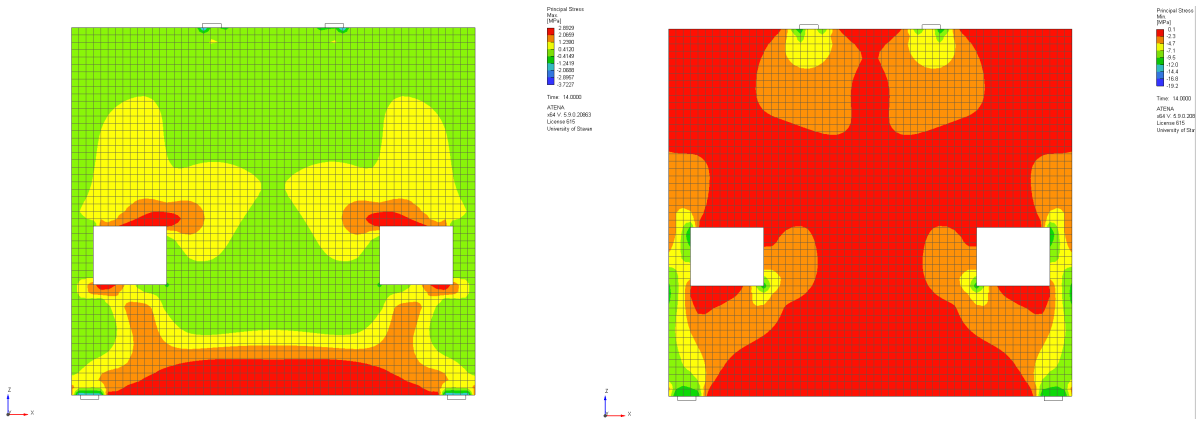

Figure 5.70: Principal tensile (left) and compressive (right) stress for Case 4.1 with 25 MPa prestressing

Figure 5.70 shows the principal tensile and compressive stress for Case 4.1 with 25 MPa prestressed reinforcement. When comparing these results to Figure 5.68 the only notable difference is the height of the principal stress distribution at the bottom of the beam (a). The tensile stress distribution around the openings is similar, and the principal compressive stress distribution is also similar.

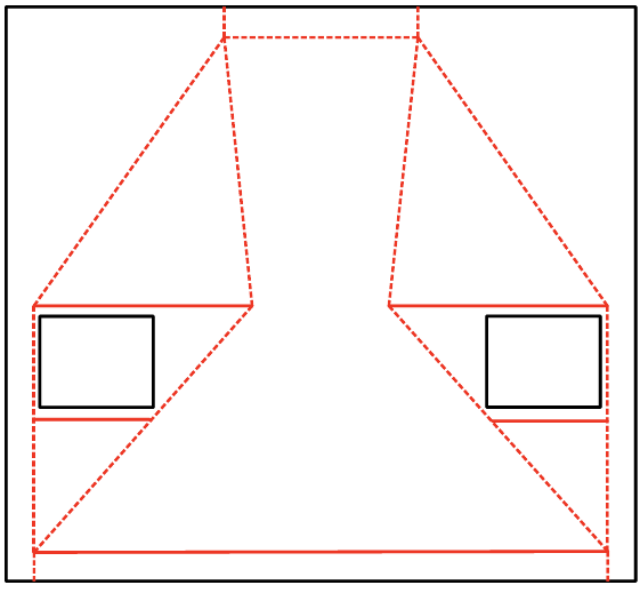

Figure 5.71: Strut and Tie model for Case 4.1 with 25 MPa prestressed reinforcement

The strut and tie model for Case 4.1 with 25 MPa prestressing is shown in Figure 5.71, the difference between this STM and the previous is the distance a/2 which has decreased with 8mm. This also changes the angles between the struts and ties slightly.

5.6.1.3 Case 4.1 with 100 MPa prestressed reinforcement

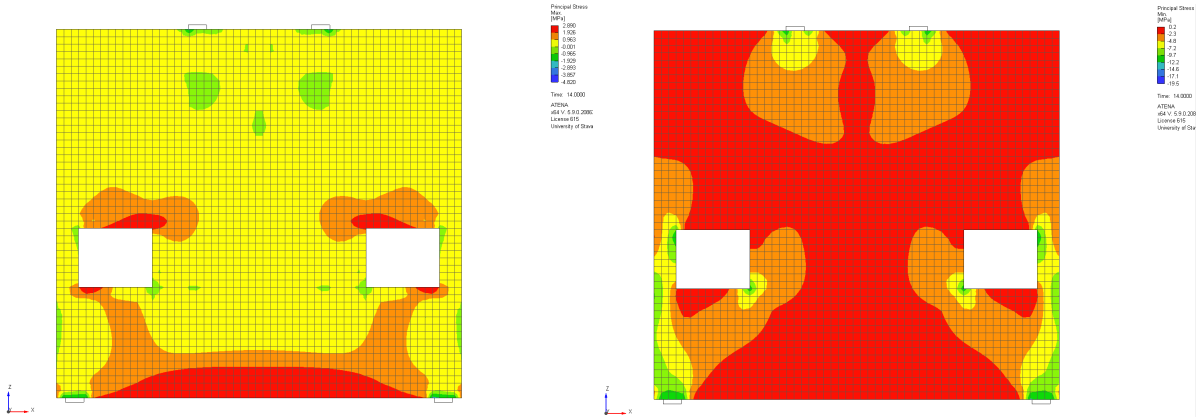

Figure 5.72: Principal tensile (left) and compressive (right) stress for Case 4.1 with 100 MPa prestressing

The principal tensile and compressive stress distribution for Case 4.1 with 100 MPa prestressing has the same change as for Case 4.1 with 25 MPa prestressing compared to the one without prestressing, the principal stresses are shown in Figure 5.72.

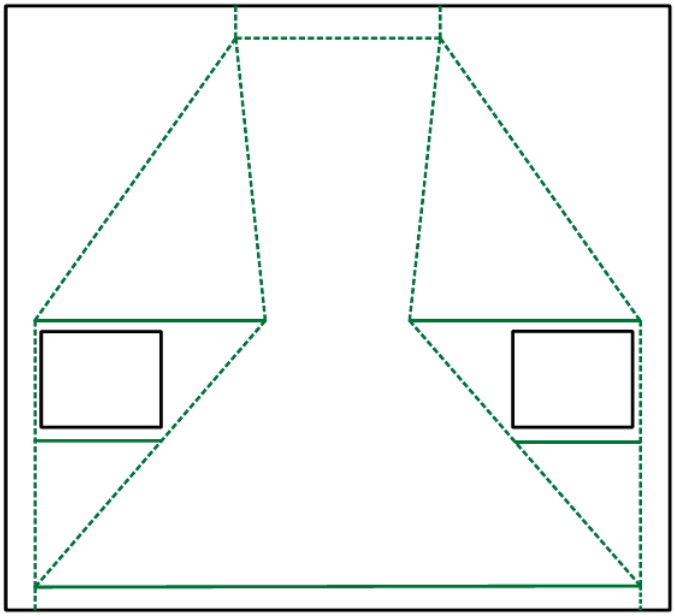

Figure 5.73: Strut and Tie model for Case 4.1 with 100 MPa prestressing

The STM for Case 4.1 with 100 MPa prestressing is shown in Figure 5.73, it is developed the same way as the previous STM. The distance a/2 has decreased by 15mm compared to Case 4.1 without prestressing.

5.6.2 Case 4.2

Case 4.2 has the same openings as Case 4.1 but they are located 0.54m from the bottom of the deep beam compared to Case 4.1 where the openings are located 0.3m from the bottom of the deep beam. The following results are the principal tensile and compressive stress for Case 4.2 and the developed STM for each model, Case 4.2 contains three different models, without prestressing, 25 MPa, and 100 MPa prestressing.

5.6.2.1 Case 4.2 without prestressed reinforcement

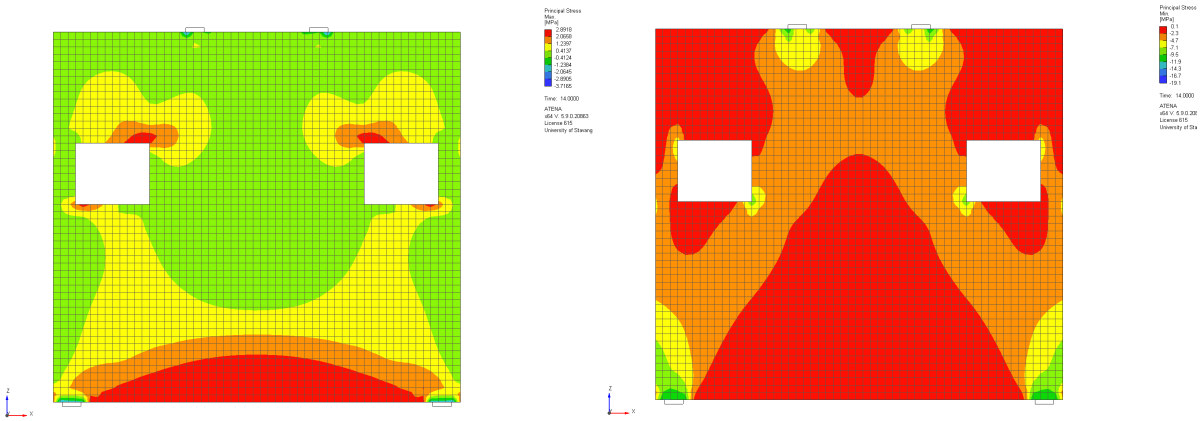

Figure 5.74: Principal tensile (left) and compressive (right) stress for Case 4.2 without prestressed reinforcement

Figure 5.74 shows the principal tensile and compressive stress distribution for Case 4.2 without prestressed reinforcement. The tensile stress distribution is similar to Case 4.1, but the compressive stress distribution is not. When the openings are moved upward the compressive stresses can distribute straight from the external loads to the supports.

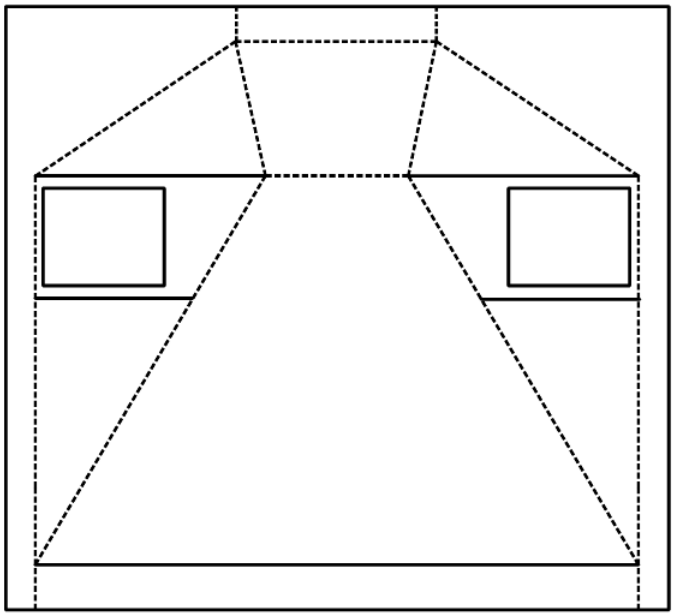

Figure 5.75: Strut and Tie model for Case 4.2 without prestressed reinforcement

The strut and tie model for Case 4.2 without prestressed reinforcement is shown in Figure 5.75, it is symmetrical about the z-axis.

5.6.2.2 Case 4.2 with 25 MPa prestressed reinforcement

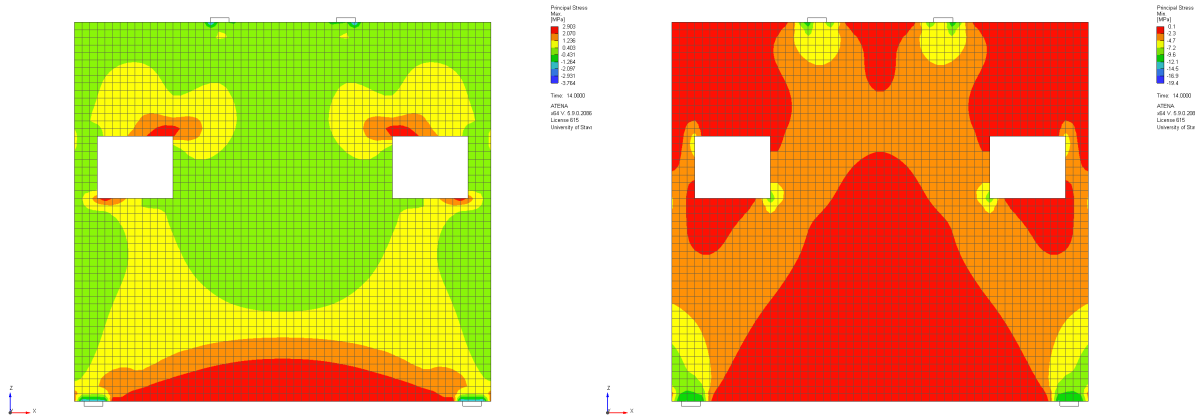

Figure 5.76: Principal tensile (left) and compressive (right) stress for Case 4.2 with 25 MPa prestressed reinforcement

The principal tensile and compressive stress distribution for Case 4.2 with 25 MPa prestressed reinforcement is similar to Case 4.2 without prestressing, the principal stresses are shown in Figure 5.76. The peak of the tensile stress a has decreased by 14mm from Case 4.2 without prestressing. The compressive stress distribution is similar.

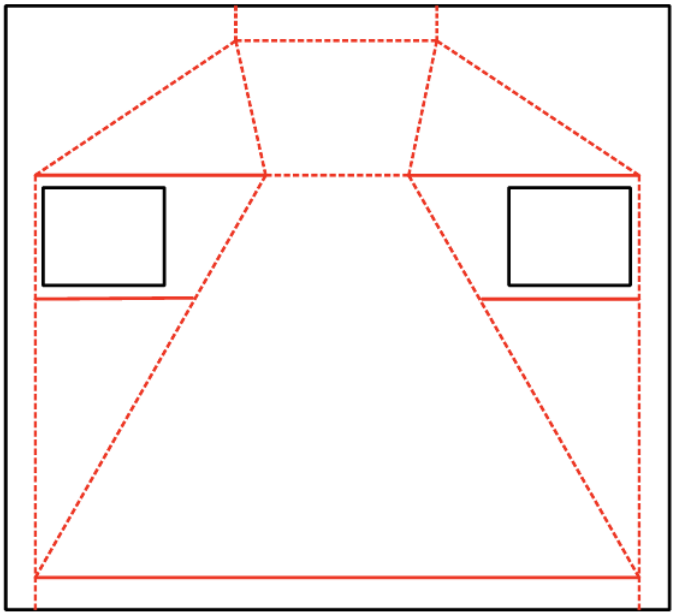

Figure 5.77: Strut and Tie model for Case 4.2 with 25 MPa prestressing

The strut and tie model for Case 4.2 with 25 MPa prestressing is shown in Figure 5.77. It is similar to the STM for Case 4.2 without prestressing, the difference is the placement of the bottom tie, and the distance a/2 has decreased by 9mm.

5.6.2.3 Case 4.2 with 100 MPa prestressed reinforcement

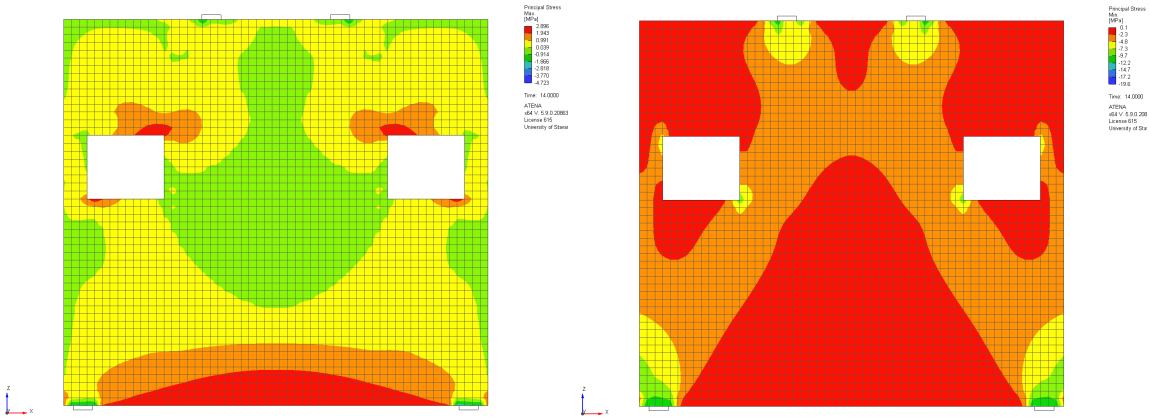

Figure 5.78: Principal tensile (left) and compressive (right) stress for Case 4.2 with 100 MPa prestressed reinforcement

As for Case 4.2 without prestressing and with 25 MPa prestressing, the stress distribution is similar for Case 4.2 with 100 MPa prestressing, the principal tensile and compressive stress are shown in Figure 5.78. The distance a has decreased by 38mm compared to Case 4.2 without prestressing.

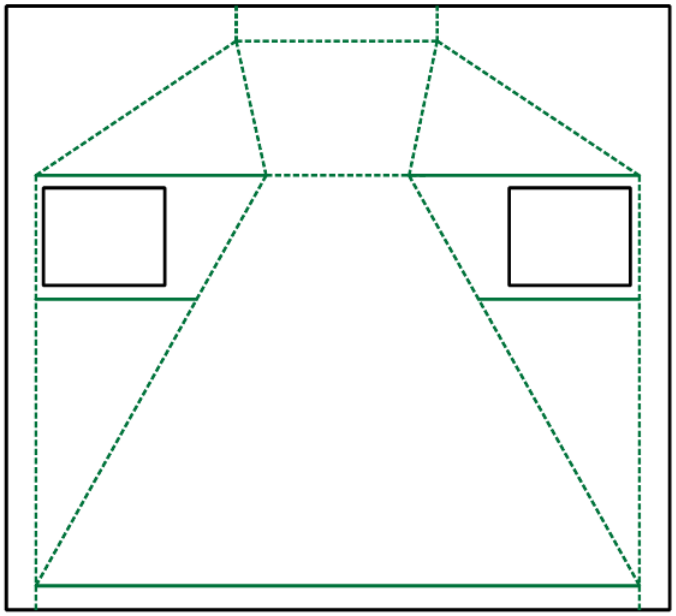

Figure 5.79: Strut and Tie model for Case 4.2 with 100 MPa prestressing

The proposed STM for Case 4.2 with 100 MPa prestressing is displayed in Figure 5.79 and is developed similarly to the others.

5.6.3 Case 4.3

Case 4.3 are Model 1.1 with two openings, the two openings are now placed at different heights from the bottom of the beam to the openings. The opening on the left is placed 0.54m from the bottom of the beam, and the opening on the right is placed 0.3m from the bottom.

5.6.3.1 Case 4.3 without prestressed reinforcement

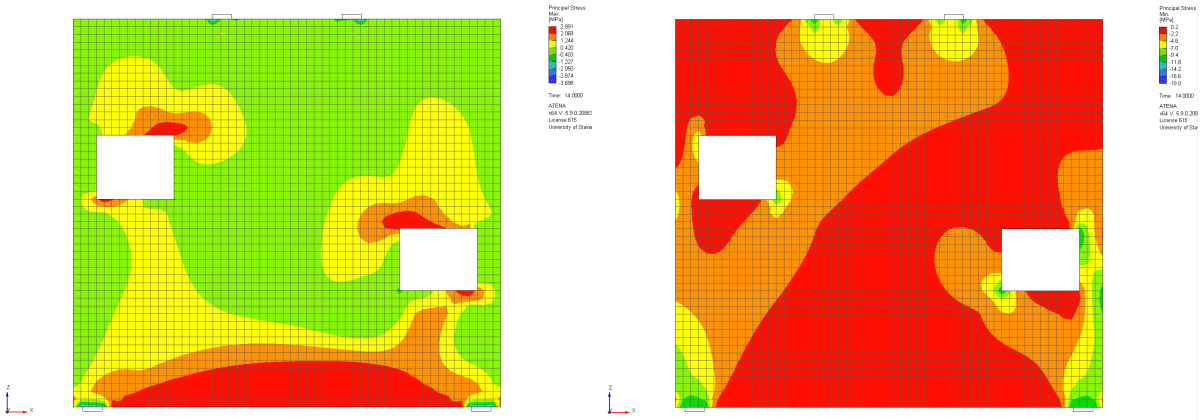

Figure 5.80: Principal tensile (left) and compressive (right) stress for Case 4.3 without prestressed reinforcement

The principal tensile stress distribution is not evenly distributed for Case 4.3 without prestressing as it was for Case 4.1 and Case 4.2, the peak (a) has moved to the right. The tensile stresses around the opening to the right have increased slightly when compared to the stresses around the opening on the left. The principal compressive stress distribution is not evenly distributed, it has a distribution which is similar to the sum of Case 4.1 and Case 4.2. If the beam is divided in half on the x-axis, the stress distribution on the left is similar to Case 4.2, and the right is similar to Case 4.1.

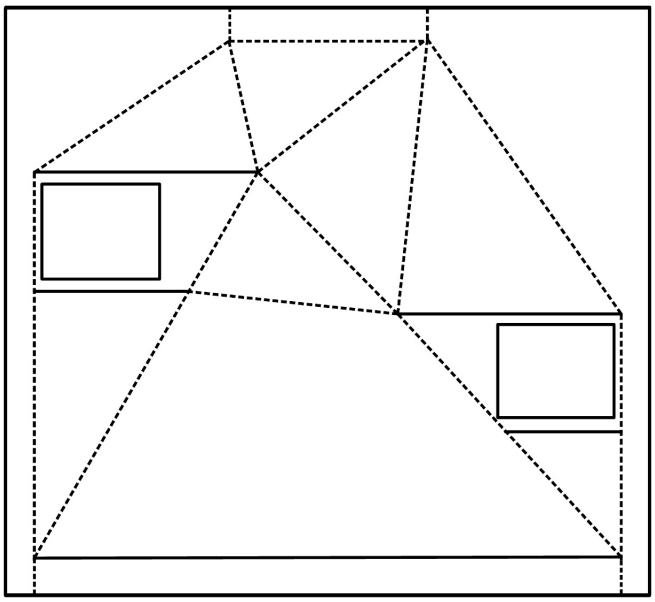

Figure 5.81: Strut and Tie model for Case 4.3 without prestressing

The proposed STM for Case 4.3 without prestressing is shown in Figure 5.81. The STM is the sum of the STM for cases 4.1 and 4.2, there are also added two struts to connect the nodes and follow the principal compressive stress.

5.6.3.2 Case 4.3 with 25 MPa prestressed reinforcement

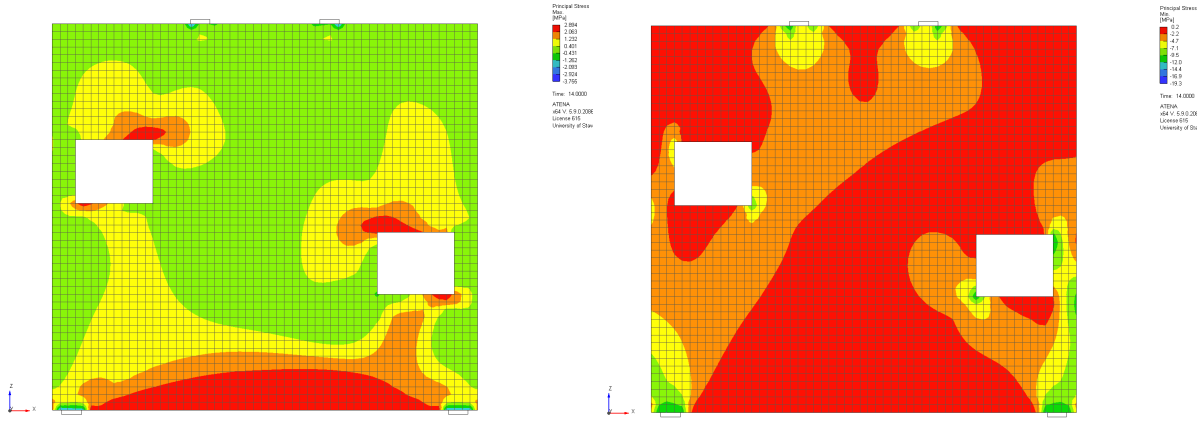

Figure 5.82: Principal tensile (left) and compressive (right) stress for Case 4.3 with 25 MPa prestressing

The principal tensile and compressive stress distribution for Case 4.3 with 25 MPa prestressing is shown in Figure 5.82. The stress distribution is similar to Case 4.3 without prestressed reinforcement, but the distance a has decreased by 14mm.

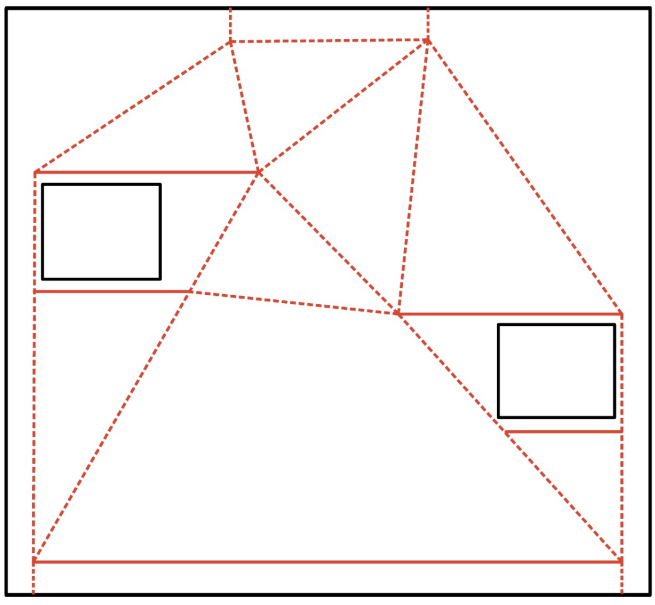

Figure 5.83: Strut and Tie model for Case 4.3 with 25 MPa prestressing

The proposed strut and tie model for Case 4.3 with 25 MPa prestressing is shown in

Figure 5.83, it is developed the same way as the previous cases.

5.6.3.3 Case 4.3 with 100 MPa prestressed reinforcement

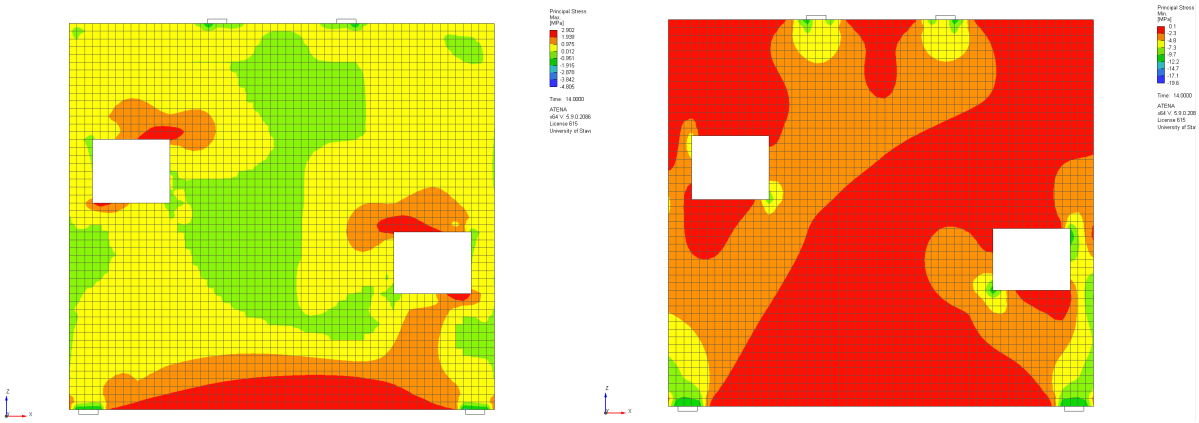

Figure 5.84: Principal tensile (left) and compressive (right) stress for Case 4.3 with 100 MPa prestressing

Figure 5.84 shows the principal tensile and compressive stress for Case 4.3 with 100 MPa prestressing. The stress distribution for both tensile and compressive stresses is similar to Case 4.3 with 25 MPa prestressing. The distance a has decreased by 30mm compared with Case 4.3 without prestressed reinforcement.

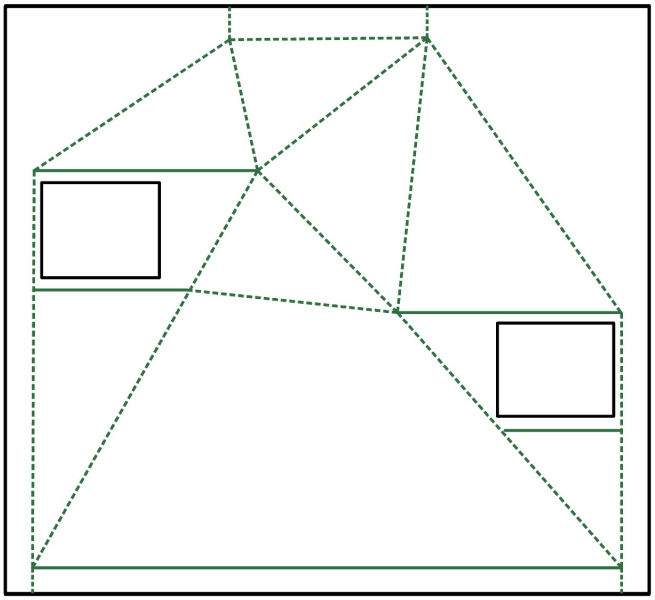

Figure 5.85: Strut and Tie model for Case 4.3 with 100 MPa prestressing

Figure 5.85 shows the proposed STM for Case 4.3 with 100 MPa prestressing.

6 Discussion and Conclusion

The results from the principal tensile stresses show a decrease in the peak of the stresses when adding and increasing the prestressing, the reason for this is that when applying prestressed reinforcement, it applies compressive force. This will decrease the deflection, which reduces the tensile stresses. The amount of change in (a) varies for which load case and the height of the deep beam. Therefore when using prestressed reinforcement and increasing the amount of jacking force, the distance a/2 will decrease.

The results for principal compressive stresses show that there is no change in the peak of the stresses when applying prestressed reinforcement, the reason for this is that the prestressed reinforcement is used at the bottom of the beams where the tensile stresses are.

The results from case 4, where model 1.1 are analyzed with openings, show a similar change in principal tensile stresses at the bottom of the deep beams, where the peak decreases when applying and increasing the prestressed reinforcement. When adding prestressed reinforcement, the tensile stress distribution surrounding the openings remains the same. As for cases 1, 2, and 3, the principal compressive stress distribution remains the same when applying prestressed reinforcement.

The equilibrium of forces for the strut and tie models are calculated and shown in the appendix. The calculations are done for all the models without prestressed reinforcement. The calculations are done with an external load of 100 kN. The placement of the bottom ties changes slightly when applying and increasing the prestressed reinforcement. Since the change in ties is minor, the angle between the struts and ties will not change drastically. Therefore, the calculations are only done for the models without prestressed reinforcement. The equilibrium of forces is close to zero for all the calculations.

The conclusion is; when adding and increasing the prestressed reinforcement, the distance from the bottom of the deep beam to the bottom tie decreases. While the placement of the top strut or node will not change when adding and increasing the prestressed reinforcement.

6.1 Suggestion for further work

The models analyzed in this thesis are meshed with a mesh of 20mm, a suggestion for further work is to change the mesh size to 10mm in order to see if the change is significant or not. It would also be interesting to change the amount of prestressing force to see how significant the difference would be and try different models with different dimensions to find out if Equation 5.1 is still valid.

References

[1] J. K. Wight, "Reinforced concrete : mechanics and design," Upper Saddle River, N.J, 2009.

[2] "Atena program documentation part 1 theory."

[3] "Eurokode 2: Prosjektering av betongkonstruksjoner = eurocode 2: Design of concrete structures. part 1-1: General rules and rules for buildings : Del 1-1 : Allmenne regler og regler for bygninger," Standard Norge, Lysaker, 2008.

[4] F. K. Kong, *Reinforced concrete deep beams*. CRC Press, 1991.

[5] T. English. What is finite element analysis and how does it work? [Online]. Available: https://interestingengineering.com/science/what-is-finite-element-analysis-and-how-does-it-work

[6] A. Cheng, M. Auerbach, E. A. Hunt, T. P. Chang, M. Pusic, V. Nadkarni, and D. Kessler, "Designing and conducting simulation-based research," *Pediatrics*, vol. 133, no. 6, pp. 1091–1101, 2014.

[7] "The blackwell companion to organizations," Malden, Mass, 2002.

[8] S. Norge, "Ns-en 1992-1-1: 2004+ na: 2008: Eurokode 2: Prosjektering av betongkonstruksjoner, del 1-1: Allmenne regler og regler for bygninger," *Brussel: CEN*, 2008.

[9] J. Erochko. An introduction to structural analysis. [Online]. Available: https://learnaboutstructures.com/Bernoulli-Euler-Beam-Theory

[10] S. El-Metwally and W.-F. Chen, *Structural concrete: strut-and-tie models for unified design*. CRC Press, 2017.

[11] T. C. center. Strut and tie. [Online]. Available: https://www.concretecentre.com/Codes/Eurocode-2/Stut-and-Tie.aspx

[12] R. J. Roark, "Roark's formulas for stress and strain," New York, 2002.

[13] K. Dwivedi. Principal stress: Definition, formula, derivation, calculation. [Online]. Available: https://www.mechical.com/2022/06/principal-stress.html

[14] A. T. Committees, "Building code requirements for structural concrete and commentary," 2019.

[15] C. Consulting. Atena. [Online]. Available: https://www.cervenka.cz/products/atena/

[16] V. Červenka and J. Červen, "Atena program documentation part 2-2 user's manual for atena 3d version 5.4.1," 2017.

[17] J. Vladimír Červenka and Z. Janda, "Atena program documentation part 3-2 example manual atena," 2021.

[18] R. I. GILBERT, "Design of prestressed concrete to as3600-2009," Place of publication not identified, 2017.

[19] "Concepts and applications of finite element analysis," New York, 2002.

[20] J. Nocedal, "Numerical optimization," New York, 1999.

[21] S. I. Sørensen, "Betongkonstruksjoner : beregning og dimensjonering etter eurocode 2," Trondheim, 2013.

[22] S. W. Grant, G. L. Hickey, and S. J. Head, "Statistical primer: multivariable regression considerations and pitfalls†," *European Journal of Cardio-Thoracic Surgery*, vol. 55, no. 2, pp. 179–185, 12 2018. [Online]. Available: https://doi.org/10.1093/ejcts/ezy403

Appendix

A1 Principal tensile stress with cracks

The following results are the principal tensile stresses with the crack development before and after yield. The applied load is shown for each model. The cracks are displayed with black lines.

A1 Principal tensile stress with cracks

A1.1 Case 1, without prestressed reinforcement

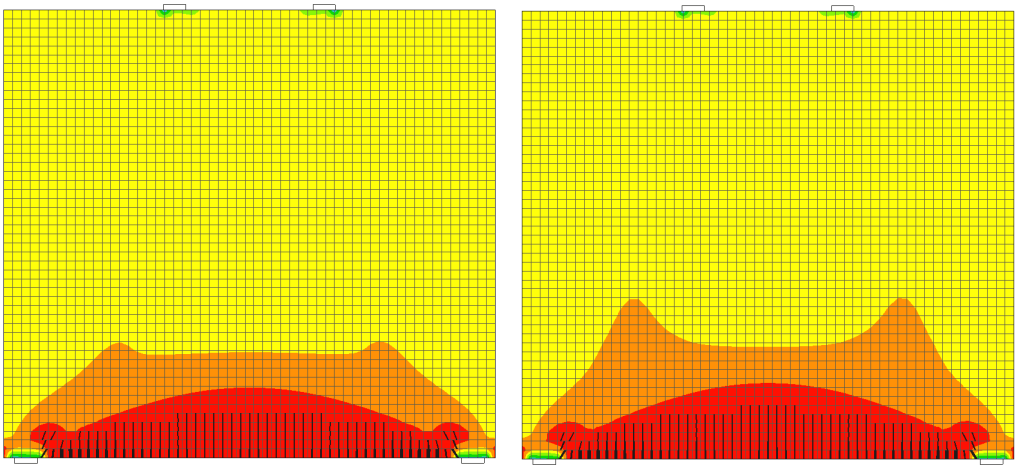

Figure A1.1: Model 1.1 without prestressed reinforcement, before (left) and after (right) yield

Applied load before yield is $254.8kN$ and after $259.7kN$

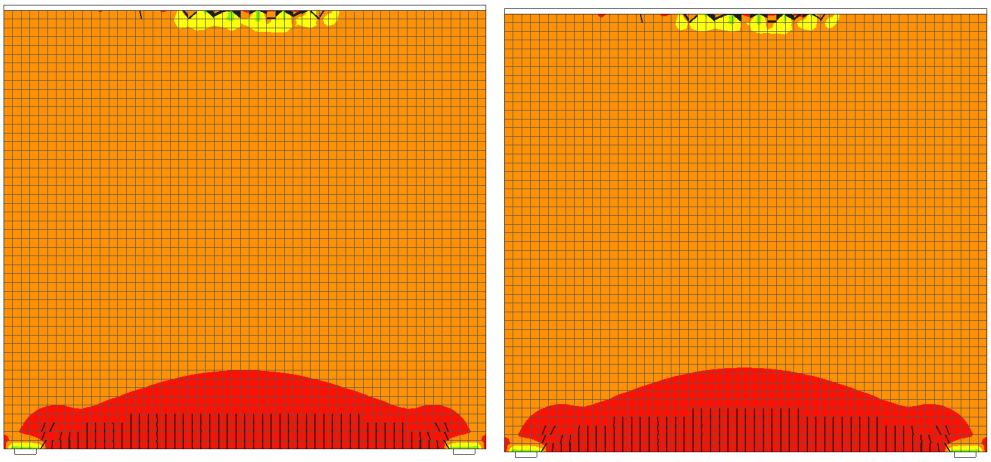

Figure A1.2: Model 1.2 without prestressed reinforcement, before (left) and after (right) yield

Applied load before yield is $226.3kN/m^2$ and after $237kN/m^2$

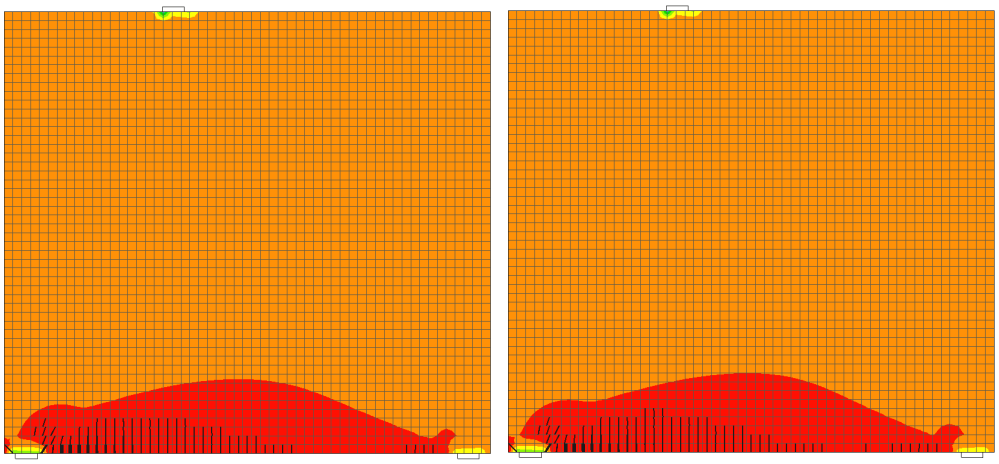

Figure A1.3: Model 1.3 without prestressed reinforcement, before (left) and after (right) yield

Applied load before yield is $208.5kN$ and after $216.4kN$

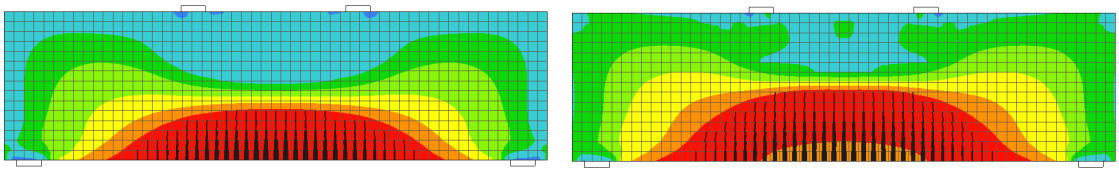

Figure A1.4: Model 2.1 without prestressed reinforcement, before (left) and after (right) yield

Applied load before yield is $48.51kN$ and after $57.45kN$

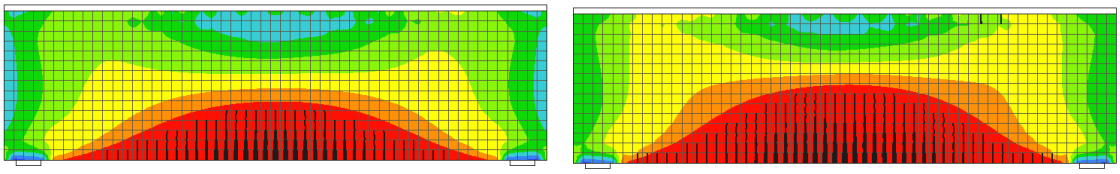

Figure A1.5: Model 2.2 without prestressed reinforcement, before (left) and after (right) yield

Applied load before yield is $110kN/m^2$ and after $125.5kN/m^2$

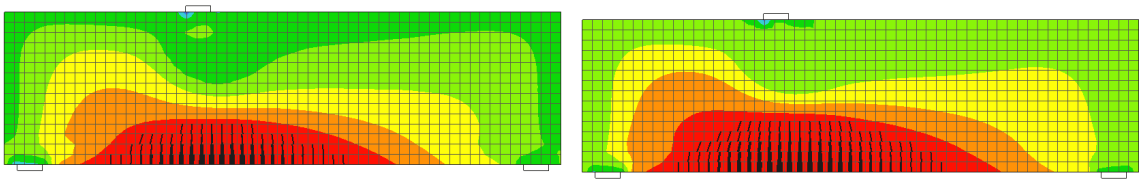

Figure A1.6: Model 2.3 without prestressed reinforcement, before (left) and after (right) yield

Applied load before yield is $53.77kN$ and after $63.14kN$

A1.2 Case 2, straight prestressed reinforcement

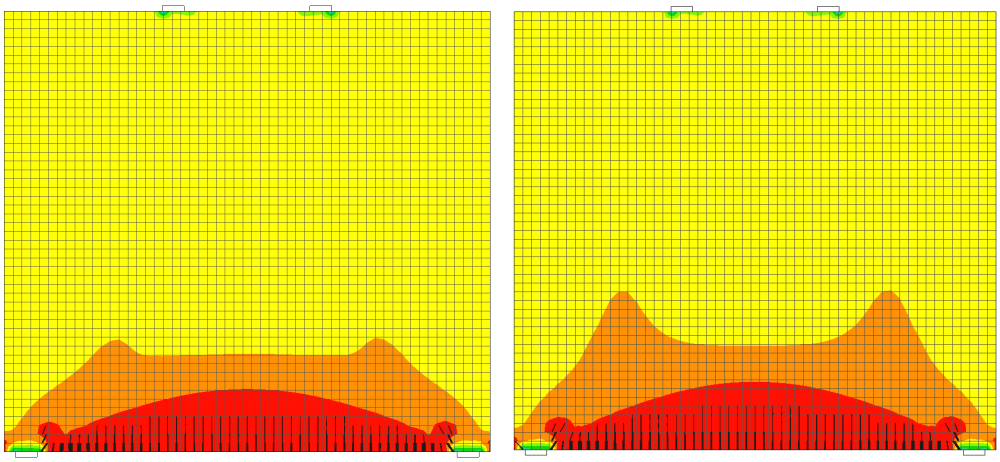

Figure A1.7: Model 1.1 with 25 MPa prestressed reinforcement, before (left) and after (right) yield

Applied load before yield is $259.7kN$ and after $272.2kN$

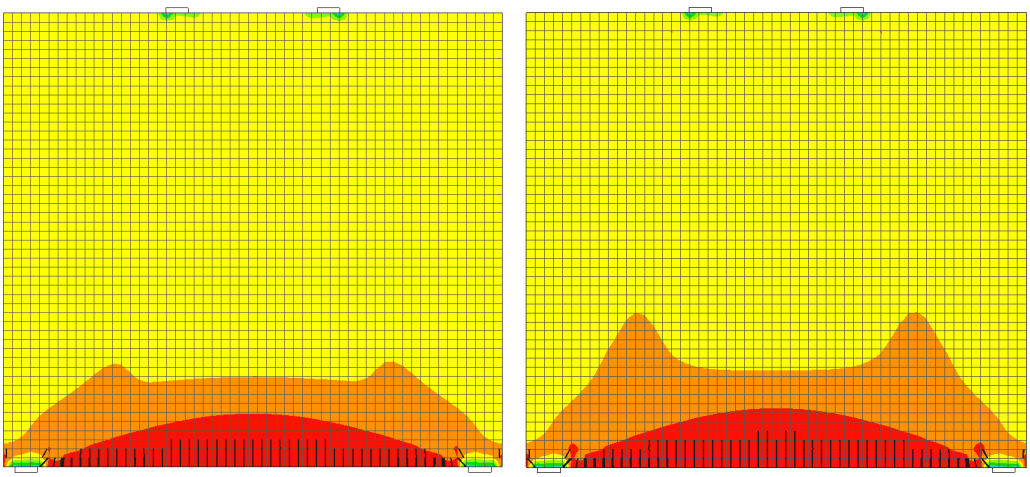

Figure A1.8: Model 1.1 with 100 MPa prestressed reinforcement, before (left) and after (right) yield

Applied load before yield is $265.3kN$ and after $278.6kN$

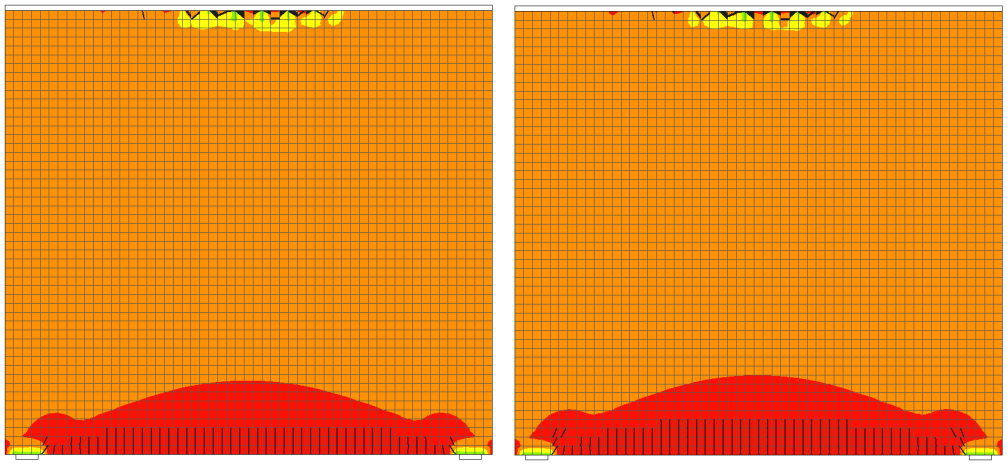

Figure A1.9: Model 1.2 with 25 MPa prestressed reinforcement, before (left) and after (right) yield

Applied load before yield is $230.1kN/m^2$ and after $241.4kN/m^2$

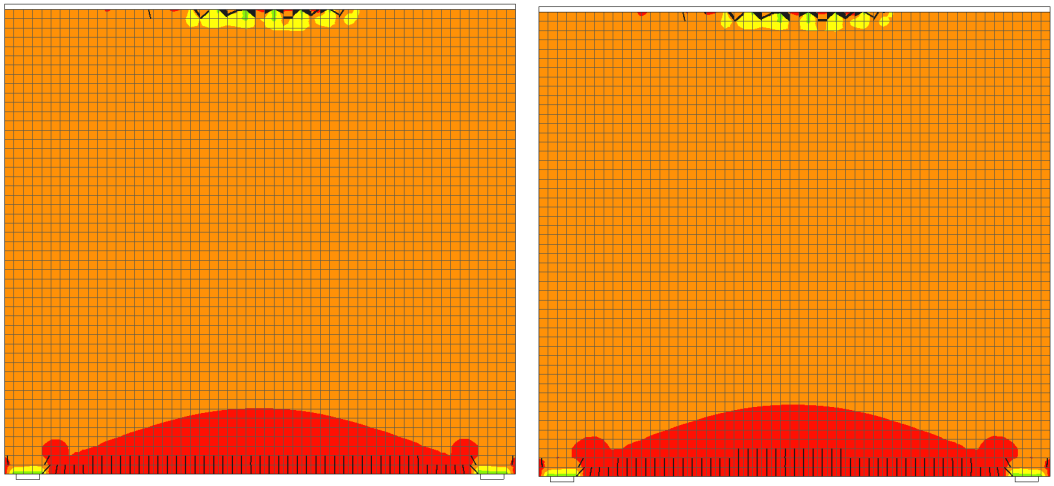

Figure A1.10: Model 1.2 with 100 MPa prestressed reinforcement, before (left) and after (right) yield

Applied load before yield is $234.1kN7m^2$ and after $246.3kN7m^2$

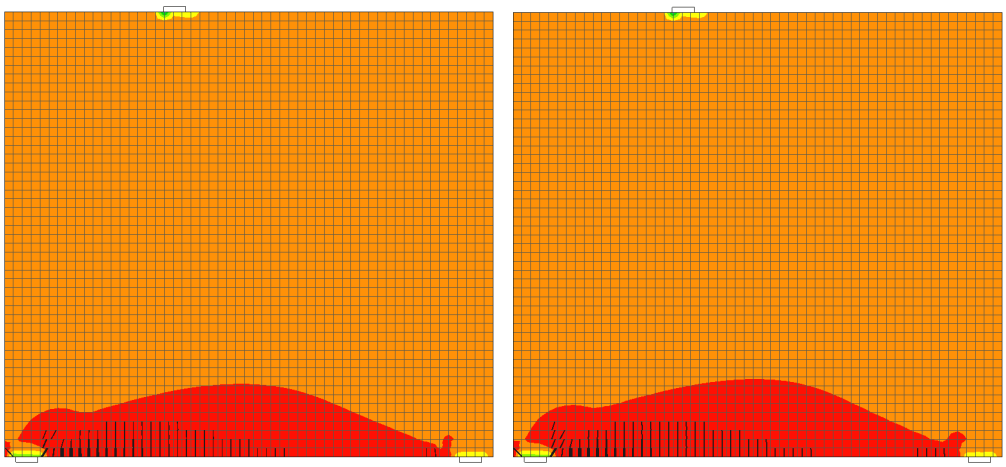

Figure A1.11: Model 1.3 with 25 MPa prestressed reinforcement, before (left) and after (right) yield

Applied load before yield is $209.8kN$ and after $217.9kN$

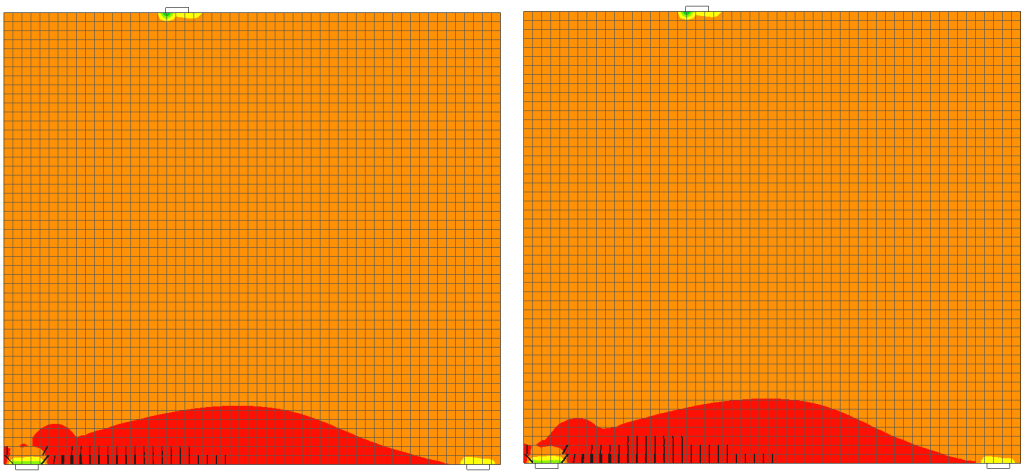

Figure A1.12: Model 1.3 with 100 MPa prestressed reinforcement, before (left) and after (right) yield

Applied load before yield is $215.3kN$ and after $224kN$

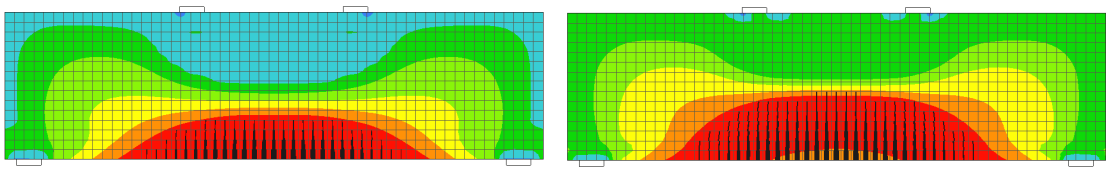

Figure A1.13: Model 2.1 with 25 MPa prestressed reinforcement, before (left) and after (right) yield

Applied load before yield is $50.95kN$ and after $63.19kN$

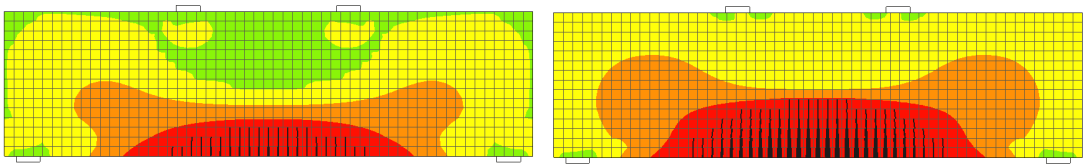

Figure A1.14: Model 2.1 with 100 MPa prestressed reinforcement, before (left) and after (right) yield

Applied load before yield is $54.51kN$ and after $70.54kN$

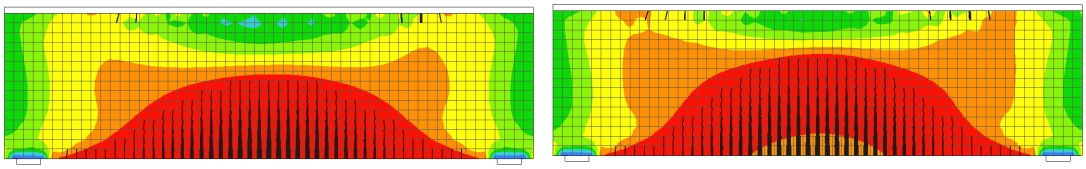

Figure A1.15: Model 2.2 with 25 MPa prestressed reinforcement, before (left) and after (right) yield

Applied load before yield is $144.7kN/m^2$ and after $156.1kN/m^2$

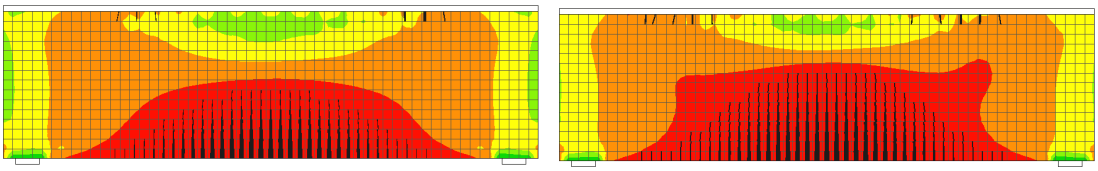

Figure A1.16: Model 2.2 with 100 MPa prestressed reinforcement, before (left) and after (right) yield

Applied load before yield is $151.3kN/m^2$ and after $163.2kN/m^2$

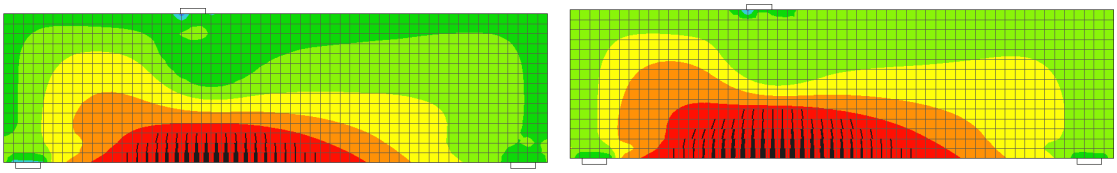

Figure A1.17: Model 2.3 with 25 MPa prestressed reinforcement, before (left) and after (right) yield

Applied load before yield is $54.35kN$ and after $64.53kN$

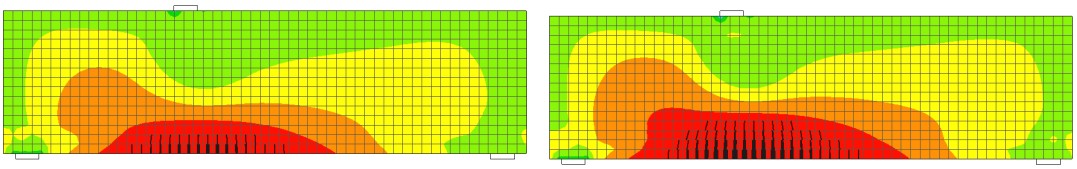

Figure A1.18: Model 2.3 with 100 MPa prestressed reinforcement, before (left) and after (right) yield

Applied load before yield is $55.05kN$ and after $66.42kN$

A1.3 Case 3, curved prestressed reinforcement

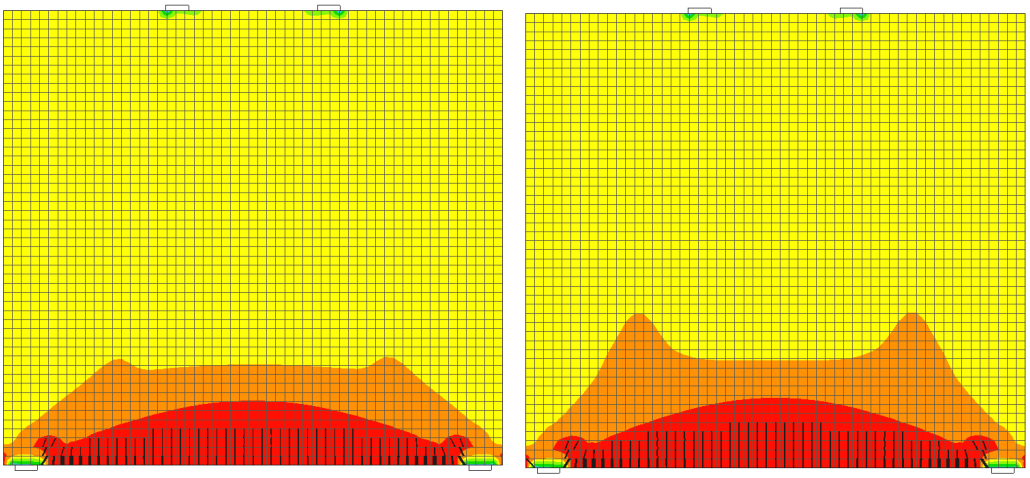

Figure A1.19: Model 1.1 with 25 MPa prestressed reinforcement, before (left) and after (right) yield

Applied load before yield is $258.4kN$ and after $270.8kN$

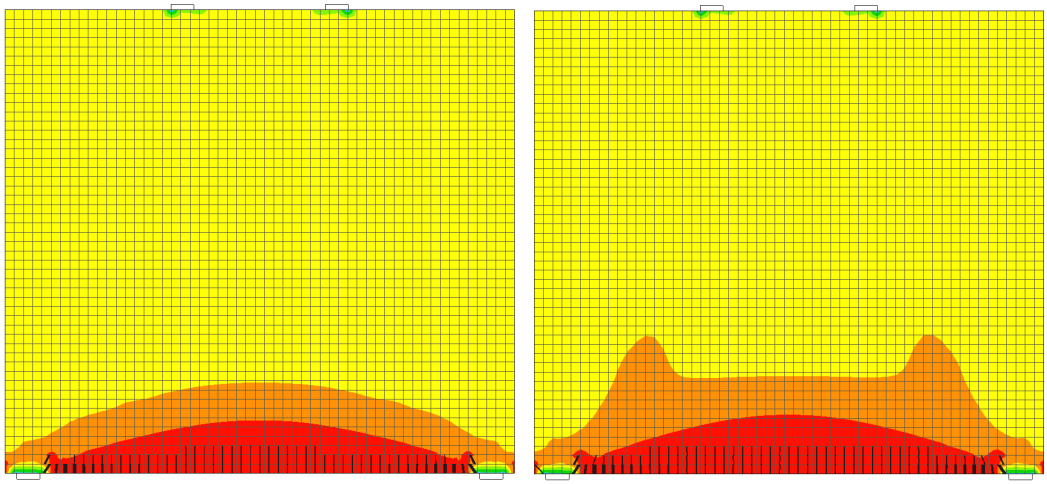

Figure A1.20: Model 1.1 with 100 MPa prestressed reinforcement, before (left) and after (right) yield

Applied load before yield is $263kN$ and after $276.1kN$

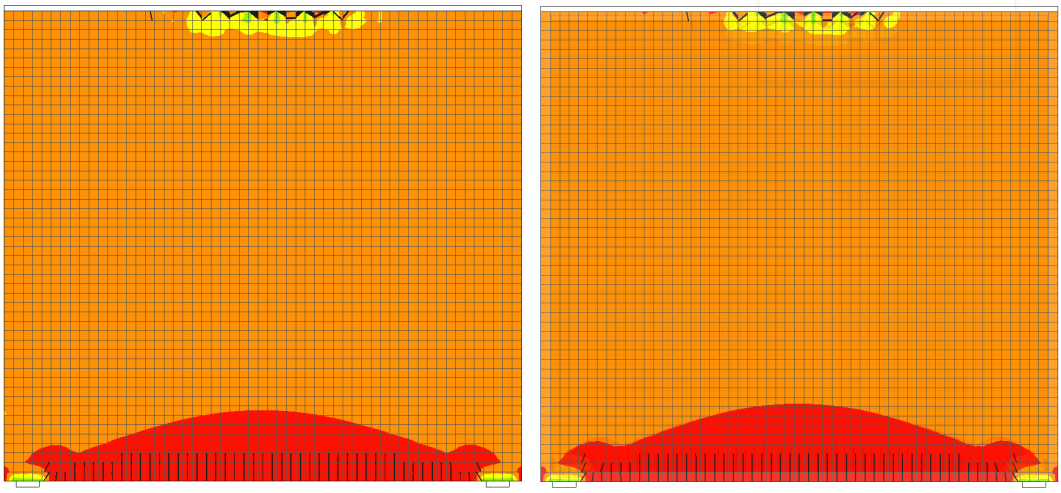

Figure A1.21: Model 1.2 with 25 MPa prestressed reinforcement, before (left) and after (right) yield

Applied load before yield is $229kN/m^2$ and after $240.2kN/m^2$

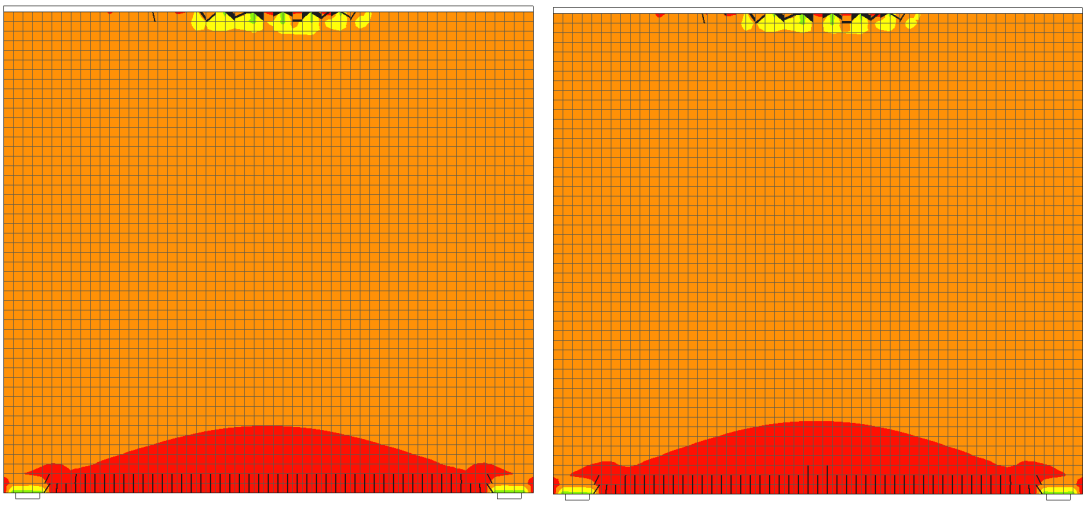

Figure A1.22: Model 1.2 with 100 MPa prestressed reinforcement, before (left) and after (right) yield

Applied load before yield is $232.3kN/m^2$ and after $244.2kN/m^2$

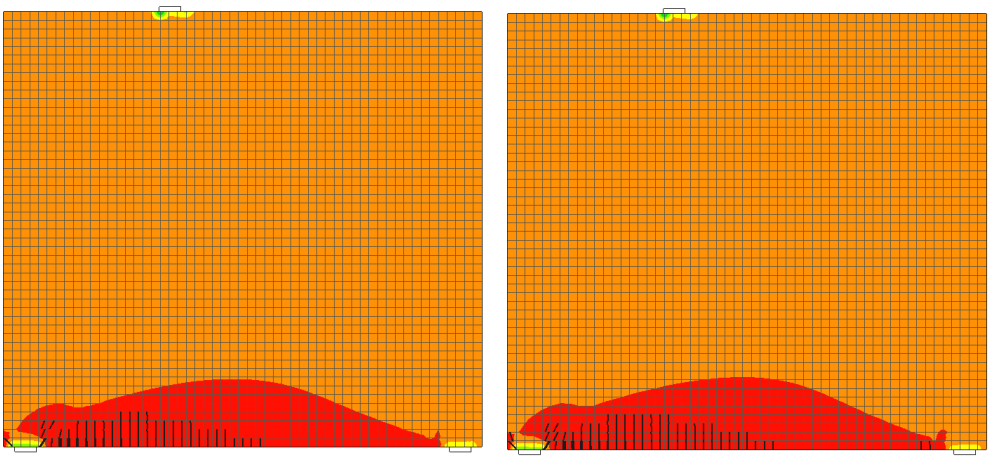

Figure A1.23: Model 1.3 with 25 MPa prestressed reinforcement, before (left) and after (right) yield

Applied load before yield is $210.7kN$ and after $218.8kN$

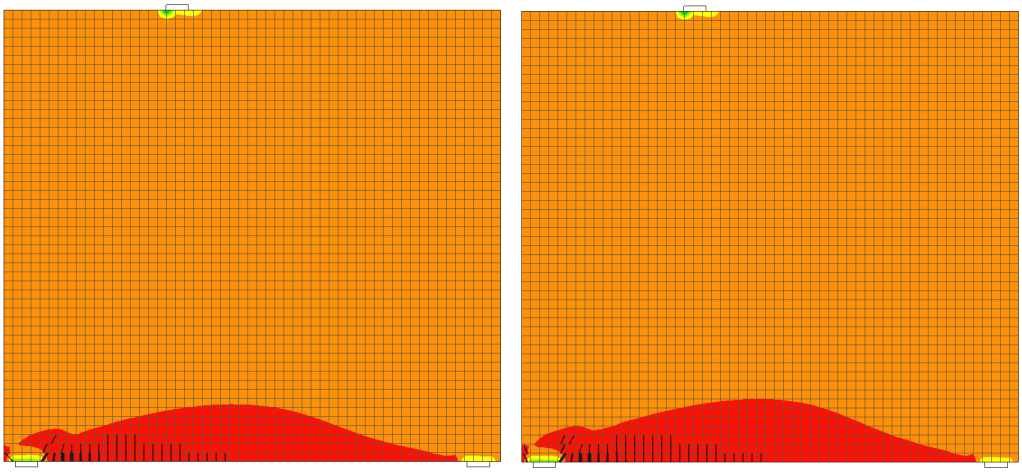

Figure A1.24: Model 1.3 with 100 MPa prestressed reinforcement, before (left) and after (right) yield

Applied load before yield is $213.5kN$ and after $222.1kN$

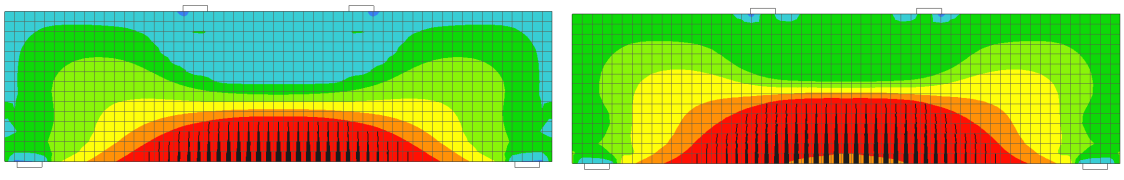

Figure A1.25: Model 2.1 with 25 MPa prestressed reinforcement, before (left) and after (right) yield

Applied load before yield is $50.97kN$ and after $63.32kN$

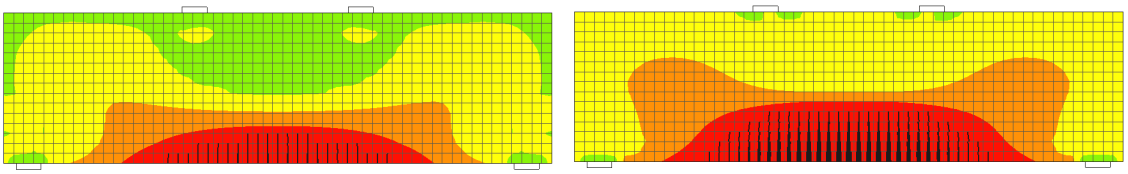

Figure A1.26: Model 2.1 with 100 MPa prestressed reinforcement, before (left) and after (right) yield

Applied load before yield is $54.56kN$ and after $70.83kN$

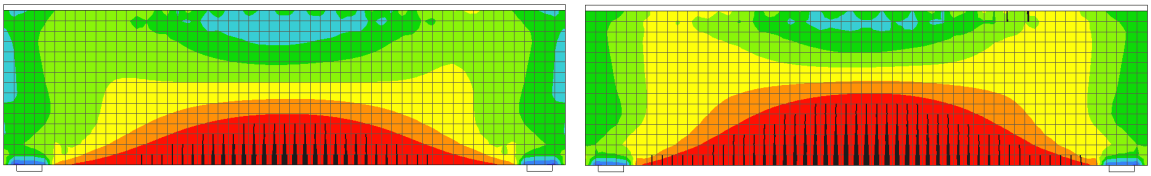

Figure A1.27: Model 2.2 with 25 MPa prestressed reinforcement, before (left) and after (right) yield

Applied load before yield is $113.3kN/m^2$ and after $132.4kN/m^2$

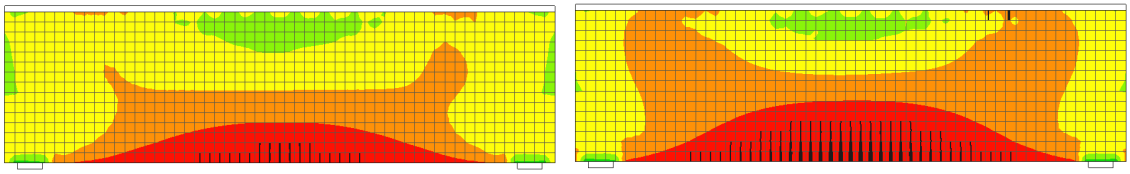

Figure A1.28: Model 2.2 with 100 MPa prestressed reinforcement, before (left) and after (right) yield

Applied load before yield is $117kN/m^2$ and after $142.5kN/m^2$

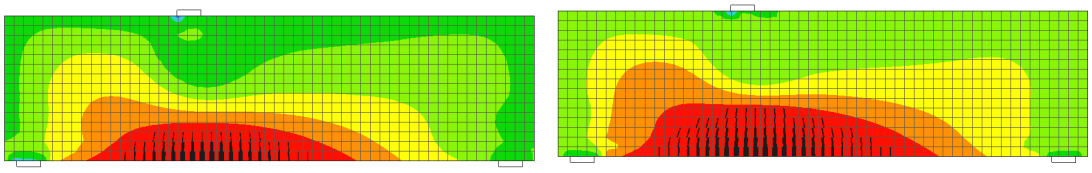

Figure A1.29: Model 2.3 with 25 MPa prestressed reinforcement, before (left) and after (right) yield

Applied load before yield is $54.35kN$ and after $64.62kN$

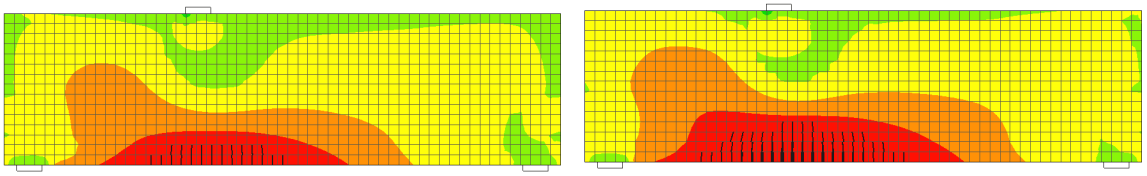

Figure A1.30: Model 2.3 with 100 MPa prestressed reinforcement, before (left) and after (right) yield

Applied load before yield is $55.26kN$ and after $67.56kN$

	Case 1		Case 2				Case 3			
	0 MPa		25MPa		100MPa		25 MPa		100 MPa	
	Before	After	Before	After	Before	After	Before	After	Before	After
Model 1.1 $[kN]$	254,8	259,7	259,7	272,2	265,3	278,6	258,4	270,8	263	276,1
Model 1.2 $[kN/m^2]$	226,3	237	230,1	241,4	234,1	246,3	229	240,2	232,3	244,2
Model 1.3 $[kN]$	208,5	216,4	209,8	217,9	215,3	224	210,7	218,8	213,5	222,1
Model 2.1 $[kN]$	48,51	57,45	50,95	63,19	54,51	70,54	50,97	63,32	54,56	70,83
Model 2.2 $[kN/m^2]$	110	125,5	144,7	156,1	151,3	163,2	113,3	132,4	117	142,5
Model 2.3 $[kN]$	53,77	63,14	54,36	64,63	55,05	66,42	54,34	64,62	55,26	67,56

Table A1.1: Applied force before and after yield for case 1, 2 and 3

A1.4 Case 4

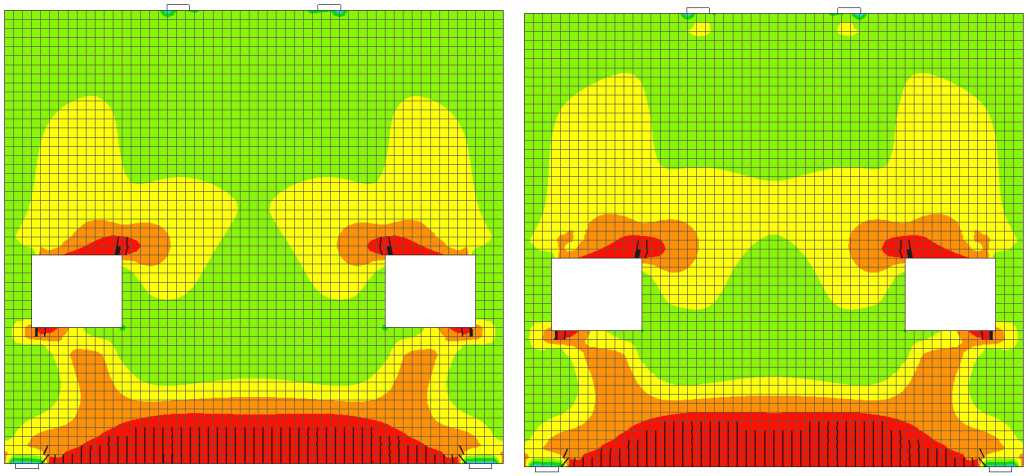

Figure A1.31: Case 4.1 without prestressed reinforcement, before (left) and after (right) yield

Applied load before yield is $181.8kN$ and after $193.5kN$

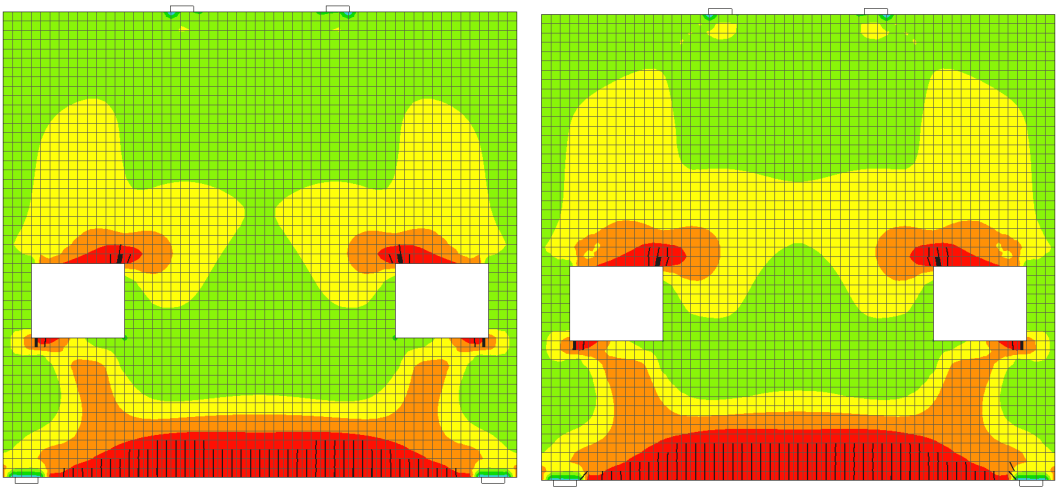

Figure A1.32: Case 4.1 with 25 MPa prestressed reinforcement, before (left) and after (right) yield

Applied load before yield is 185.6kN and after 197.5kN

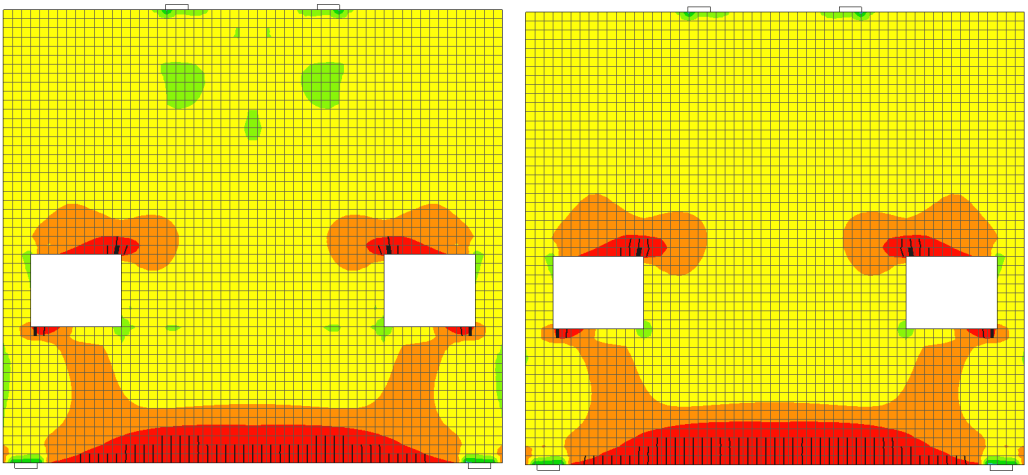

Figure A1.33: Case 4.1 with 100 MPa prestressed reinforcement, before (left) and after (right) yield

Applied load before yield is 189.1kN and after 202.8kN

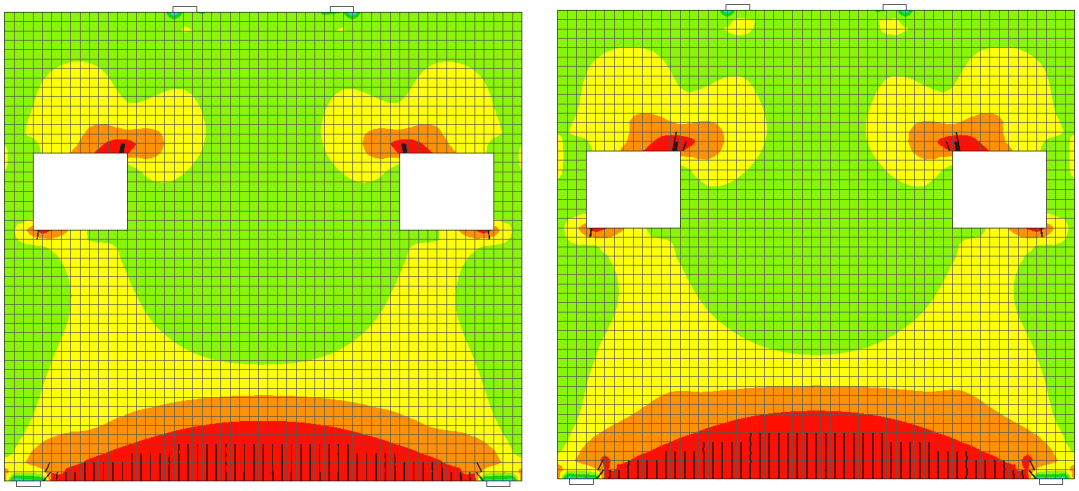

Figure A1.34: Case 4.2 without prestressed reinforcement, before (left) and after (right) yield

Applied load before yield is $185.7kN$ and after $198.3kN$

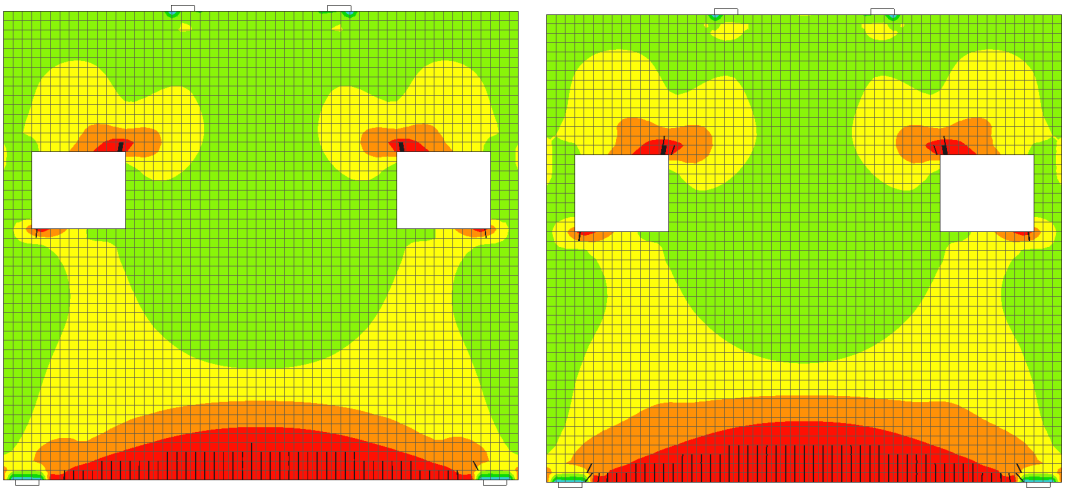

Figure A1.35: Case 4.2 with 25 MPa prestressed reinforcement, before (left) and after (right) yield

Applied load before yield is $188.4kN$ and after $201.8kN$

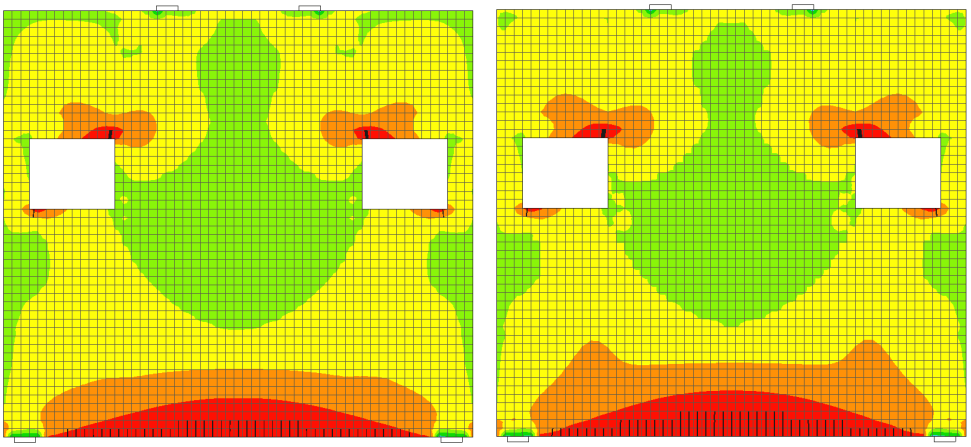

Figure A1.36: Case 4.2 with 100 MPa prestressed reinforcement, before (left) and after (right) yield

Applied load before yield is $191.2kN$ and after $205.7kN$

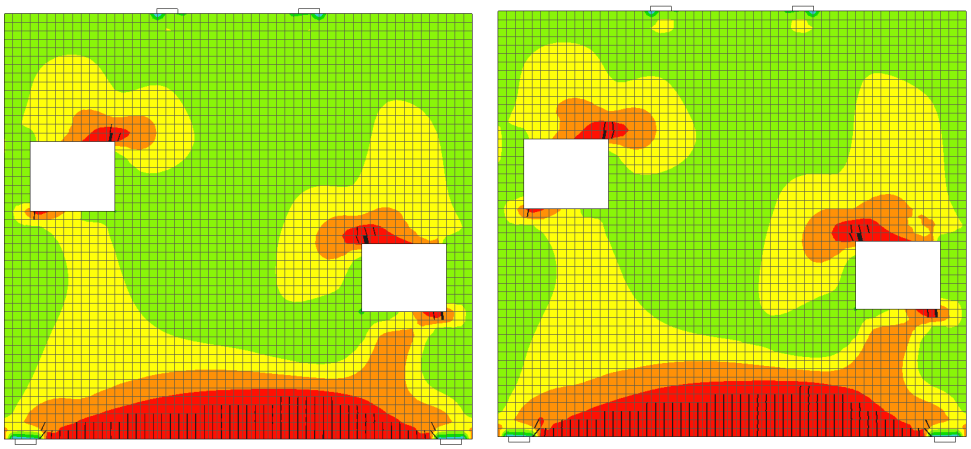

Figure A1.37: Case 4.4 without prestressed reinforcement, before (left) and after (right) yield

Applied load before yield is $183.6kN$ and after $194.8kN$

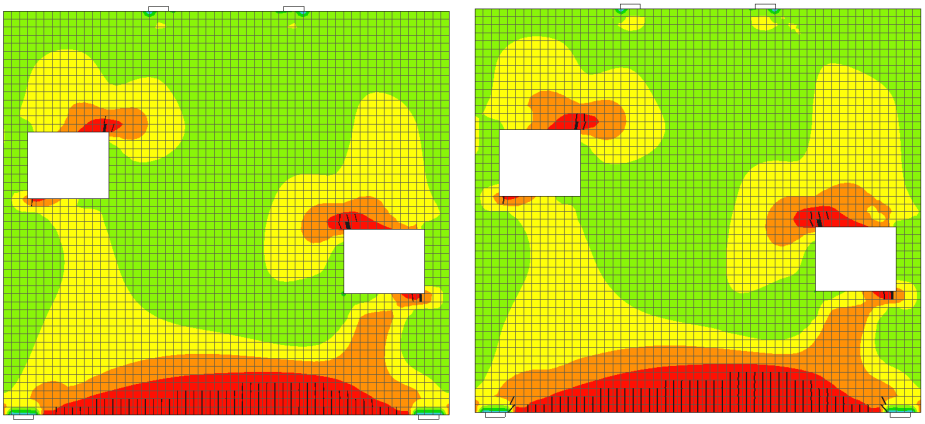

Figure A1.38: Case 4.3 with 25 MPa prestressed reinforcement, before (left) and after (right) yield

Applied load before yield is 186.4kN and after 198.6kN

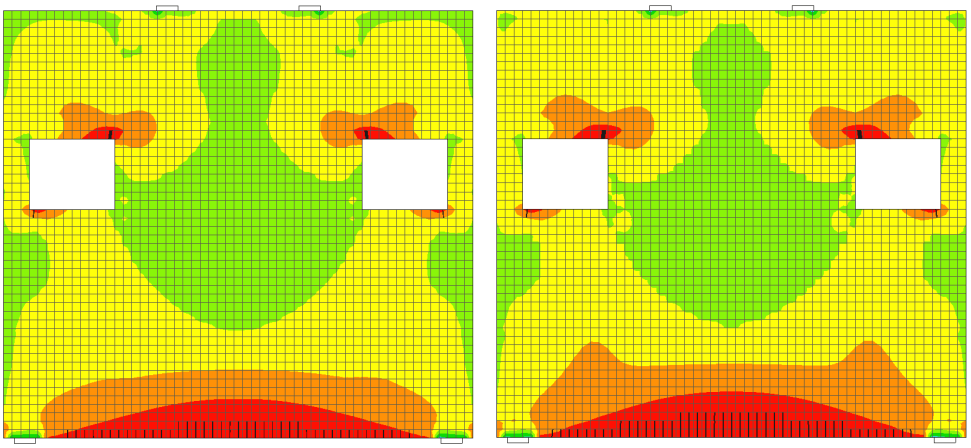

Figure A1.39: Case 4.2 with 100 MPa prestressed reinforcement, before (left) and after (right) yield

Applied load before yield is 189.7kN and after 203.6kN

	Case 4					
	0MPa		25MPa		100MPa	
	Before	After	Before	After	Before	After
Case 4.1	181,8	193,5	185,6	197,5	189,1	202,8
Case 4.2	185,7	198,3	188,4	201,8	191,2	205,7
Case 4.3	183,6	194,8	186,4	198,6	189,7	203,6

Table A1.2: Applied force [kN] before and after yield for Case 4

A2 Equilibrium of forces for the Strut and Tie models

The following calculations are the equilibrium of forces for the strut and tie models. The calculations are done by applying a unit load of 100 kN for models 1.1 and 1.2, for model 1.3 it is 100 kN/m. The results show that the equilibrium is close to zero for all the nodes. The red number represents the nodes, while the green the members.

Equilibrium of Forces

Green number : member
Red number : node

Tension: positive,
compression: negative

Model 1.1

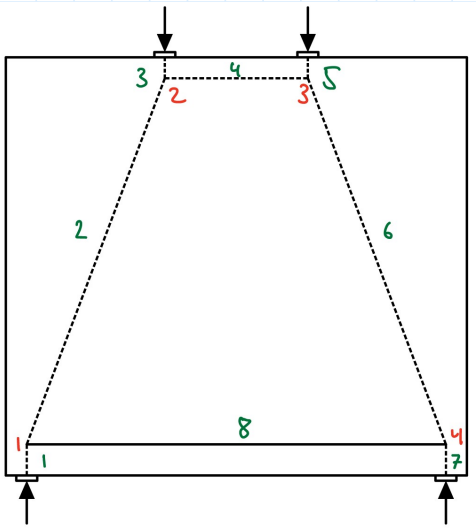

$e1 := 100\ kN$	Compression (C)
$e2 := 107.1\ kN$	C
$e3 := 100\ kN$	C
$e4 := 38.36\ kN$	C
$e5 := 100\ kN$	C
$e6 := 107.1\ kN$	C
$e7 := 100\ kN$	C
$e8 := 38.36\ kN$	Tension

Node 1

$$\theta_1 := \operatorname{atan}\left(\frac{9.47-0.79}{3.83-0.5}\right) = 69.011\ deg$$ Angle between e8 and e2

ΣFy=0 -> $e1 - e2 \cdot \sin(\theta_1) = 0.006\ kN$

$\Sigma Fx=0$ -> $e8 - e2 \cdot \cos(\theta_1) = -0.002\ kN$

Node 2

$$\theta := \operatorname{atan}\left(\frac{9.47-0.79}{3.83-0.5}\right) = 69.011\ deg$$ Angle between e2 and horizontal axis

ΣFy=0 -> $e2 \cdot \sin(\theta) - e3 = -0.006\ kN$

$\Sigma Fx=0$ -> $e2 \cdot \cos(\theta) - e4 = 0.002\ kN$

Model 1.2

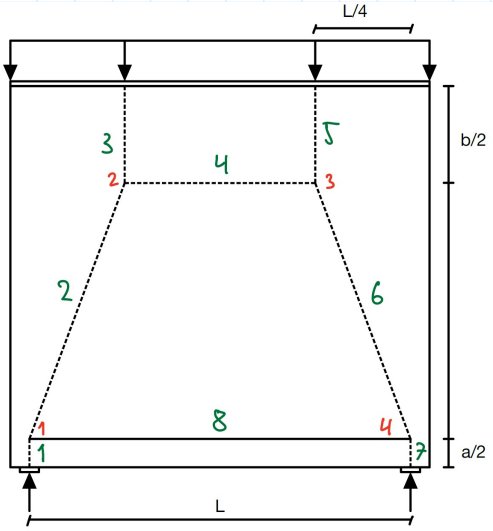

$e1 := 100\ kN$	Compression (C)
$e2 := 106.97\ kN$	C
$e3 := 100\ kN$	C
$e4 := 37.98\ kN$	C
$e5 := 100\ kN$	C
$e6 := 106.97\ kN$	C
$e7 := 100\ kN$	C
$e8 := 37.98\ kN$	Tension

Node 1

$$\theta := \operatorname{atan}\left(\frac{7.4-0.82}{3-0.5}\right) = 69.196\ deg$$ Angle between e8 and e2

ΣFy=0 -> $e1 - e2 \cdot \sin(\theta) = 0.004\ kN$

$\Sigma Fx=0$ -> $e8 - e2 \cdot \cos(\theta) = -0.012\ kN$

Node 2

$$\theta := \operatorname{atan}\left(\frac{7.4-0.82}{3-0.5}\right) = 69.196\ deg$$ Angle between e2 and horizontal axis

ΣFy=0 -> $e2 \cdot \sin(\theta) - e3 = -0.004\ kN$

$\Sigma Fx=0$ -> $e2 \cdot \cos(\theta) - e4 = 0.012\ kN$

Model 1.3

$e1 := 66.7\ kN$ Compression (C)
$e2 := 71.49\ kN$ C
$e3 := 100\ kN$ C
$e4 := 42.08\ kN$ C
$e5 := 33.3\ kN$ C
$e6 := 25.73\ kN$ Tension

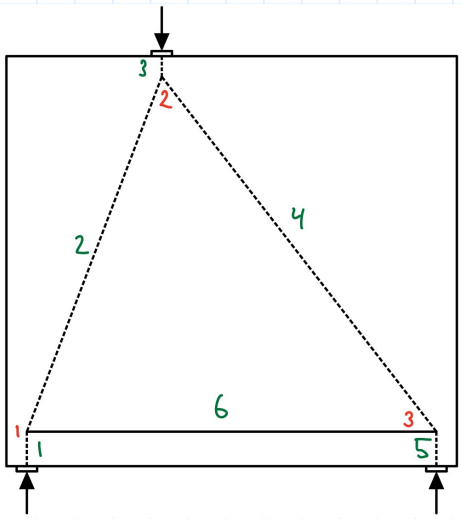

Node 1

$\theta := \operatorname{atan}\left(\frac{9.47-0.84}{3.83-0.5}\right) = 68.9\ deg$ Angle between e6 and e2

ΣFy=0 -> $e1 - e2 \cdot \sin(\theta) = 0.003\ kN$

$\Sigma Fx=0$ -> $e6 - e2 \cdot \cos(\theta) = -0.006\ kN$

Node 2

$\theta_1 := \operatorname{atan}\left(\frac{3.83-0.5}{9.47-0.84}\right) = 21.1\ deg$ Angle between e2 and vertical axis

$\theta_2 := \operatorname{atan}\left(\frac{10.5-3.83}{9.47-0.84}\right) = 37.7\ deg$ Angle between e4 and vertical axis

ΣFy=0 -> $e2 \cdot \cos(\theta_1) - e3 + e4 \cdot \cos(\theta_2) = -0.008\ kN$

$\Sigma Fx=0$ -> $e2 \cdot \sin(\theta_1) - e4 \cdot \sin(\theta_2) = 0.003\ kN$

Model 2.1

$e1 := 100\ kN$	Compression (C)
$e2 := 187.73\ kN$	C
$e3 := 100\ kN$	C
$e4 := 158.88\ kN$	C
$e5 := 100\ kN$	C
$e6 := 187.73\ kN$	C
$e7 := 100\ kN$	C
$e8 := 158.88\ kN$	Tension

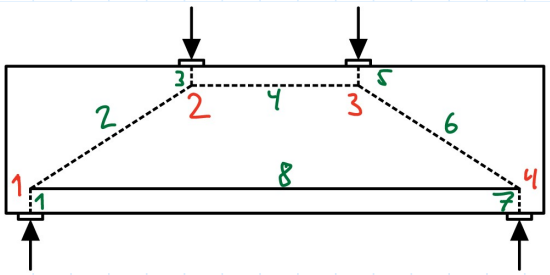

Node 1

$$\theta := \operatorname{atan}\left(\frac{2.6-0.51}{3.83-0.5}\right) = 32.114\ deg$$ Angle between e8 and e2

ΣFy=0 -> $e1 - e2 \cdot \sin(\theta) = 0.203\ kN$

$\Sigma Fx=0$ -> $e8 - e2 \cdot \cos(\theta) = -0.127\ kN$

Node 2

$$\theta := \operatorname{atan}\left(\frac{2.6-0.51}{3.83-0.5}\right) = 32.114\ deg$$ Angle between e2 and horizontal axis

ΣFy=0 -> $e2 \cdot \sin(\theta) - e3 = -0.203\ kN$

$\Sigma Fx=0$ -> $e2 \cdot \cos(\theta) - e4 = 0.127\ kN$

Model 2.2

$e1 := 100\ kN$	Compression (C)
$e2 := 159.82\ kN$	C
$e3 := 100\ kN$	C
$e4 := 124.67\ kN$	C
$e5 := 100\ kN$	C
$e6 := 159.82\ kN$	C
$e7 := 100\ kN$	C
$e8 := 124.67\ kN$	Tension

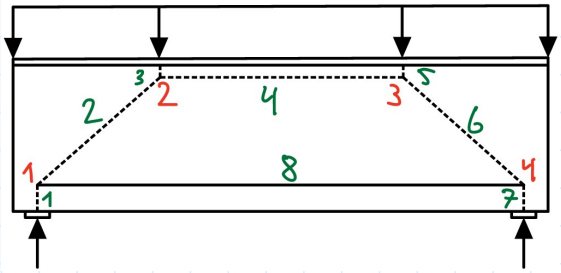

Node 1

$$\theta := \operatorname{atan}\left(\frac{2.6-0.6}{3-0.5}\right) = 38.66\ deg$$ Angle between e8 and e2

ΣFy=0 -> $e1 - e2 \cdot \sin(\theta) = 0.161\ kN$

$\Sigma Fx=0$ -> $e8 - e2 \cdot \cos(\theta) = -0.128\ kN$

Node 2

$$\theta := \operatorname{atan}\left(\frac{2.6-0.6}{3-0.5}\right) = 38.66\ deg$$ Angle between e2 and horizontal axis

ΣFy=0 -> $e2 \cdot \sin(\theta) - e3 = -0.161\ kN$

$\Sigma Fx=0$ -> $e2 \cdot \cos(\theta) - e4 = 0.128\ kN$

Model 1.3

$e1 := 66.7\ kN$	Compression (C)
$e2 := 123.83\ kN$	C
$e3 := 100\ kN$	C
$e4 := 109.5\ kN$	C
$e5 := 33.3\ kN$	C
$e6 := 104.32\ kN$	Tension

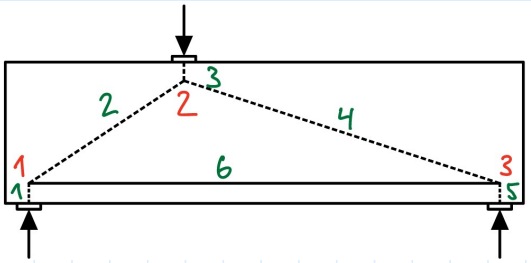

Node 1

$\theta := \operatorname{atan}\left(\frac{2.57-0.45}{3.83-0.5}\right) = 32.482\ deg$ Angle between e6 and e2

ΣFy=0 -> $e1 - e2 \cdot \sin(\theta) = 0.198\ kN$

$\Sigma Fx=0$ -> $e6 - e2 \cdot \cos(\theta) = -0.138\ kN$

Node 2

$\theta_1 := \operatorname{atan}\left(\frac{2.57-0.45}{3.83-0.5}\right) = 32.482\ deg$ Angle between e2 and horizontal axis

$\theta_2 := \operatorname{atan}\left(\frac{2.57-0.45}{10.5-3.83}\right) = 17.632\ deg$ Angle between e4 and horizontal axis

ΣFy=0 -> $e2 \cdot \sin(\theta_1) + e4 \cdot \sin(\theta_2) - e3 = -0.33\ kN$

$\Sigma Fx=0$ -> $e2 \cdot \cos(\theta_1) - e4 \cdot \cos(\theta_2) = 0.102\ kN$

Case 4.1 Equilibrium of forces

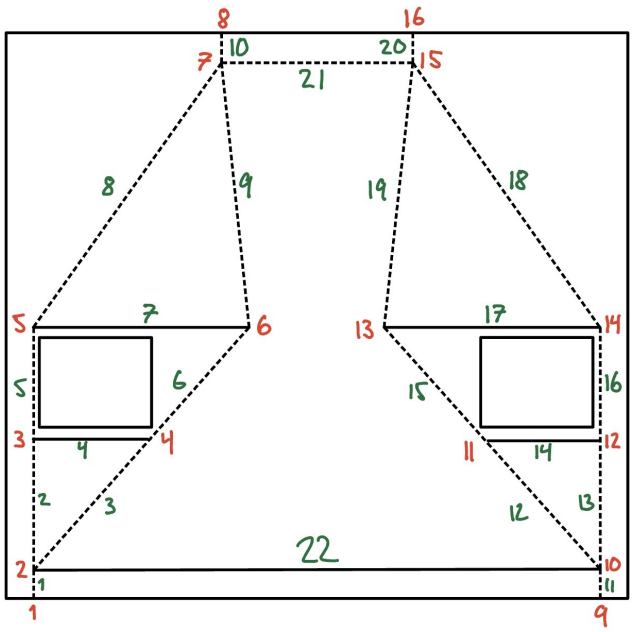

Green number : member
Red number : node

Tension: positive,
compression: negative

$e1 := 100\ kN$	Compression (C)
$e2 := 59.87\ kN$	C
$e3 := 53.06\ kN$	C
$e4 := 0.4\ kN$	Tension (T)
$e5 := 60.28\ kN$	C
$e6 := 53.06\ kN$	C
$e7 := 40.15\ kN$	T
$e8 := 72.32\ kN$	C
$e9 := 39.93\ kN$	C
$e10 := 100\ kN$	C
$e11 := e1$	C
$e12 := e3$	C
$e13 := e2$	C
$e14 := e4$	T
$e15 := e6$	C
$e16 := e5$	C
$e17 := e7$	T
$e18 := e8$	C
$e19 := e9$	C
$e20 := e10$	C
$e21 := 34.84\ kN$	C
$e22 := 34.48\ kN$	T

Node 2

$$\theta := \operatorname{atan}\left(\frac{0.28-0.06}{0.24-0.05}\right) = 49.185 \ \textit{deg}$$

ΣFy=0 -> $e1 - e2 - e3 \cdot \sin(\theta) = -0.027 \ \textit{kN}$

$\Sigma Fx=0$ -> $e22 - e3 \cdot \cos(\theta) = -0.201 \ \textit{kN}$

Node 3

$e6 - e3 = 0 \ \textit{N}$

Node 5

$$\theta := \operatorname{atan}\left(\frac{0.95-0.48}{0.36-0.05}\right) = 56.592 \ \textit{deg}$$

ΣFy=0 -> $e5 - e8 \cdot \sin(\theta) = -0.091 \ \textit{kN}$

$\Sigma Fx=0$ -> $e7 - e8 \cdot \cos(\theta) = 0.331 \ \textit{kN}$

Node 7

$$\theta := \operatorname{atan}\left(\frac{0.95-0.48}{0.36-0.05}\right) = 56.592 \ \textit{deg}$$

ΣFy=0 -> $e5 - e8 \cdot \sin(\theta) = -0.091 \ \textit{kN}$

$\Sigma Fx=0$ -> $e7 - e8 \cdot \cos(\theta) = 0.331 \ \textit{kN}$

Node 10

$$\theta_1 := \operatorname{atan}\left(\frac{0.95-0.48}{0.42-0.36}\right) = 82.725 \ \textit{deg}$$

$$\theta_2 := \operatorname{atan}\left(\frac{0.95-0.48}{0.36-0.05}\right) = 56.592 \ \textit{deg}$$

ΣFy=0 -> $e9 \cdot \sin\left(\theta_1\right) + e8 \cdot \sin\left(\theta_2\right) - e10 = -0.021 \ \textit{kN}$

$\Sigma Fx=0$ -> $e8 \cdot \cos\left(\theta_2\right) - e9 \cdot \cos\left(\theta_1\right) - e21 = -0.077 \ \textit{kN}$

Equilibrium of forces are about zero

Case 4.2 Equilibrium of forces

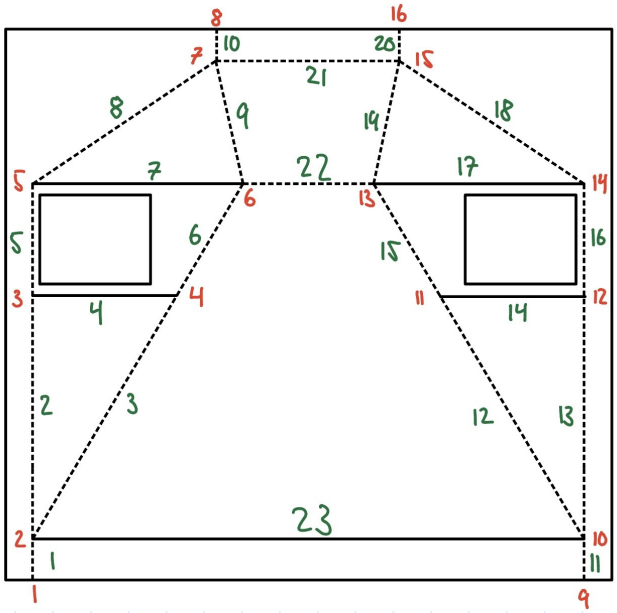

Green number : memeber (e..)
Red number : node

Tension: positive,
compression: negative

$e1 := 100\ kN$	Compression (C)
$e2 := 31.39\ kN$	C
$e3 := 79.27\ kN$	C
$e4 := 0.38\ kN$	Tension (T)
$e5 := 31.72\ kN$	C
$e6 := 79.18\ kN$	C
$e7 := 48.29\ kN$	T
$e8 := 57.54\ kN$	C
$e9 := 69.67\ kN$	C
$e10 := 100\ kN$	C
$e11 := e1$	C
$e12 := e3$	C
$e13 := e2$	C
$e14 := e4$	T
$e15 := e6$	C
$e16 := e5$	C
$e17 := e7$	T
$e18 := e8$	C
$e19 := e9$	C
$e20 := e10$	C
$e21 := 33.77\ kN$	C
$e22 := 6.6\ kN$	C
$e23 := 39.77\ kN$	C

Node 2

$\theta := \operatorname{atan}\left(\frac{5.2-0.7}{3.1-0.5}\right) = 59.982\ deg$ Angle between e23 and e3

ΣFy=0 -> $e1 - e2 - e3 \cdot \sin(\theta) = -0.027\ kN$

$\Sigma Fx=0$ -> $e23 - e3 \cdot \cos(\theta) = 0.113\ kN$

Node 5

$\theta := \operatorname{atan}\left(\frac{9.4-7.2}{3.83-0.5}\right) = 33.451\ deg$ Angle between e7 and e8

ΣFy=0 -> $e5 - e8 \cdot \sin(\theta) = 0.002\ kN$

$\Sigma Fx=0$ -> $e7 - e8 \cdot \cos(\theta) = 0.281\ kN$

Node 6

$\theta_1 := \operatorname{atan}\left(\frac{7.2-5.2}{4.3-3.1}\right) = 59.036\ deg$ Angle between e6 and e7

$\theta_2 := \operatorname{atan}\left(\frac{9.4-7.2}{4.3-3.83}\right) = 77.941\ deg$ Angle between e7 and e9

ΣFy=0 -> $e6 \cdot \sin(\theta_1) - e9 \cdot \sin(\theta_2) = -0.236\ kN$

$\Sigma Fx=0$ -> $e6 \cdot \cos(\theta_1) - e7 - e22 + e9 \cdot \cos(\theta_2) = 0.403\ kN$

Node 7

$\theta_1 := \operatorname{atan}\left(\frac{9.4-7.2}{4.3-3.83}\right) = 77.941\ deg$ Angle between e9 and e21

$\theta_2 := \operatorname{atan}\left(\frac{9.4-7.2}{3.83-0.5}\right) = 33.451\ deg$ Angle between e8 and horizontal axis

ΣFy=0 -> $e8 \cdot \sin(\theta_2) - e10 + e9 \cdot \sin(\theta_1) = -0.15\ kN$

$\Sigma Fx=0$ -> $e8 \cdot \cos(\theta_2) - e9 \cdot \cos(\theta_1) - e21 = -0.317\ kN$

Case 4.3 Equilibrium of forces

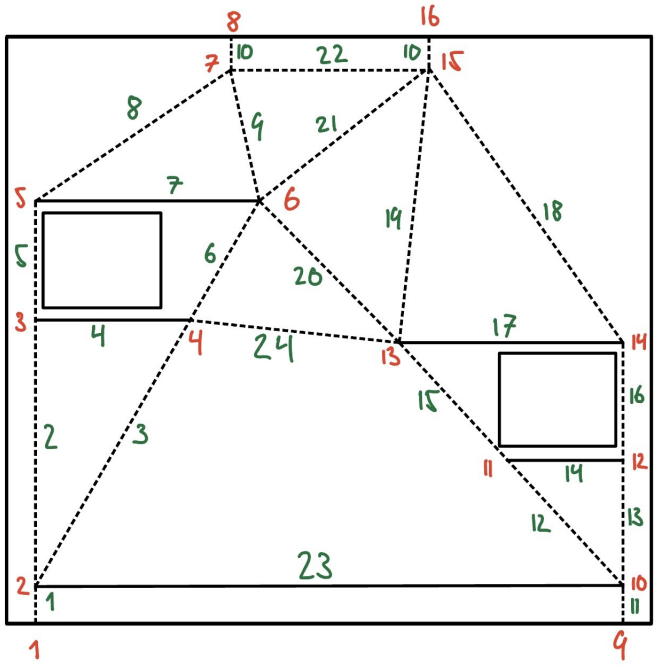

Green number : memeber (e..)
Red number : node

Tension: positive,
compression: negative

$e1 := 100\ kN$	Compression (C)
$e2 := 28.9\ kN$	C
$e3 := 81.69\ kN$	C
$e4 := 0.77\ kN$	Tension (T)
$e5 := 28.49\ kN$	C
$e6 := 83.06\ kN$	C
$e7 := 41.71\ kN$	T
$e8 := 51.02\ kN$	C
$e9 := 73.19\ kN$	C
$e10 := 100\ kN$	C
$e11 := 100\ kN$	C
$e12 := 61.13\ kN$	C
$e13 := 53.78\ kN$	C
$e14 := 0.51\ kN$	T
$e15 := 61.15\ kN$	C
$e16 := 54.18\ kN$	C
$e17 := 39.61\ kN$	T
$e18 := 66.96\ kN$	C
$e19 := 39.14\ kN$	C
$e20 := 10.36\ kN$	C
$e21 := 11.24\ kN$	C
$e22 := 27.28\ kN$	C
$e23 := 40.17\ kN$	T
$e24 := 3.54\ kN$	C

Node 2

$\theta := \operatorname{atan}\left(\frac{5.2-0.6}{3.1-0.5}\right) = 60.524\ deg$ Angle between e23 and e3

ΣFy=0 -> $e1 - e2 - e3 \cdot \sin(\theta) = -0.016\ kN$

$\Sigma Fx=0$ -> $e23 - e3 \cdot \cos(\theta) = -0.026\ kN$

Node 5

$\theta := \operatorname{atan}\left(\frac{9.4-7.2}{3.83-0.5}\right) = 33.451\ deg$ Angle between e7 and e8

ΣFy=0 -> $e5 - e8 \cdot \sin(\theta) = 0.366\ kN$

$\Sigma Fx=0$ -> $e7 - e8 \cdot \cos(\theta) = -0.859\ kN$

$e27 := 48.8\ kN$

Node 6 Angle between e7 and e9

$\theta_1 := \operatorname{atan}\left(\frac{9.4-7.2}{4.3-3.83}\right) = 77.941\ deg$

$\theta_2 := \operatorname{atan}\left(\frac{9.4-7.2}{7.17-4.3}\right) = 37.472\ deg$ Angle between e21 and horizontal axis

$\theta_3 := \operatorname{atan}\left(\frac{7.2-4.8}{6.8-4.3}\right) = 43.831\ deg$ Angle between horizontal axis and e20

$\theta_4 := \operatorname{atan}\left(\frac{7.2-5.2}{4.3-3.1}\right) = 59.036\ deg$ Angle between e7 and e6

ΣFy=0 -> $e6 \cdot \sin(\theta_4) + e20 \cdot \sin(\theta_3) - e21 \cdot \sin(\theta_2) - e9 \cdot \sin(\theta_1) = -0.015\ kN$

$\Sigma Fx=0$ -> $-e7 + e6 \cdot \cos(\theta_4) - e20 \cdot \cos(\theta_3) - e21 \cdot \cos(\theta_2) + e9 \cdot \cos(\theta_1) = -0.079\ kN$

Node 7

$\theta_1 := \operatorname{atan}\left(\frac{9.4-7.2}{4.3-3.83}\right) = 77.941\ deg$ Angle between e22 and 29

$\theta_2 := \operatorname{atan}\left(\frac{9.4-7.2}{3.83-0.5}\right) = 33.451\ deg$ Angle between e8 and horizontal axis

ΣFy=0 -> $-e10 + e8 \cdot \sin(\theta_2) + e9 \cdot \sin(\theta_1) = -0.302\ kN$

$\Sigma Fx=0$ -> $e8 \cdot \cos(\theta_2) - e9 \cdot \cos(\theta_1) - e22 = -0.002\ kN$

Node 15

$\theta_1 := \operatorname{atan}\left(\frac{9.4-7.2}{7.17-4.3}\right) = 37.472\ deg$ Angle between e22 and e21

$\theta_2 := \operatorname{atan}\left(\frac{7.17-6.8}{9.4-6.8}\right) = 8.099\ deg$ Angle between e19 and vertical axis

$\theta_3 := \operatorname{atan}\left(\frac{9.4-4.8}{10.5-7.17}\right) = 54.099\ deg$ Angle between e18 and horizontal axis

ΣFy=0 -> $-e10 + e21 \cdot \sin(\theta_1) + e19 \cdot \cos(\theta_2) + e18 \cdot \sin(\theta_3) = -0.173\ kN$

$\Sigma Fx=0$ -> $e22 + e21 \cdot \cos(\theta_1) + e19 \cdot \sin(\theta_2) - e18 \cdot \cos(\theta_3) = 2.45\ kN$

Node 14

$\theta := \operatorname{atan}\left(\frac{9.4-4.8}{10.5-7.17}\right) = 54.099\ deg$ Angle between e17 and e18

ΣFy=0 -> $e16 - e18 \cdot \sin(\theta) = -0.06\ kN$

$\Sigma Fx=0$ -> $e18 \cdot \cos(\theta) - e17 = -0.345\ kN$

Node 10

$\theta := \operatorname{atan}\left(\frac{2.8-0.6}{10.5-8.6}\right) = 49.185\ deg$ Angle between e23 and e12

ΣFy=0 -> $e11 - e13 - e12 \cdot \sin(\theta) = -0.045\ kN$

$\Sigma Fx = 0$ -> $e12 \cdot \cos(\theta) - e23 = -0.214\ kN$

A3 Input parameters for equations

The following calculations are of the input parameters to the equations to calculate a/2 for each model and cases one to three.

```
clc
clear all
```

Two-point loads, case 1 and 2

Given data

```
H = [1000; 1000; 1000; 300; 300; 300]; % Heights in mm
J = [0; 25; 100; 0; 25; 100]; % Jacking forces in MPa
a = [79; 70; 59; 51; 51; 39]; % Unknown values

% Create the design matrix
X = [ones(size(H)), H, J, H.^2, H.*J, J.^2, H.*J.^2, H.^2.*J.^2];

% Perform the regression analysis
coefficients = X\a;

% Extract the coefficients
b = coefficients(1);
c = coefficients(2);
d = coefficients(3);
e = coefficients(4);
f = coefficients(5);
g = coefficients(6);
h = coefficients(7);
i = coefficients(8);

% Display the coefficients
disp(['b = ' num2str(b)]);
disp(['c = ' num2str(c)]);
disp(['d = ' num2str(d)]);
disp(['e = ' num2str(e)]);
disp(['f = ' num2str(f)]);
disp(['g = ' num2str(g)]);
disp(['h = ' num2str(h)]);
disp(['i = ' num2str(i)]);
```

```
b = 0
c = 0.209
d = 0.23429
e = -0.00013
f = -0.00064762
g = 0
h = -8.5333e-06
i = 1.0667e-08
```

Create a grid of points for H and J

```
[H_mesh, J_mesh] = meshgrid(min(H):10:max(H), min(J):1:max(J));

% Evaluate the quadratic equation using the estimated coefficients
```

```
a_mesh = b + c * H_mesh + d * J_mesh + e * H_mesh.^2 + f * H_mesh .*
 J_mesh + g * J_mesh.^2 + h * H_mesh .* J_mesh.^2 + i * H_mesh.^2 .*
 J_mesh.^2;


% Plot the function
figure;
mesh(H_mesh, J_mesh, a_mesh);
xlabel('H (mm)');
ylabel('J (MPa)');
zlabel('a/2 (mm)');
title('Function a/2, Two-point loads, case 1 and 2');
hold on;

% Plot raw data
scatter3(H, J, a, 'filled');
xlabel('H (mm)');
ylabel('J (MPa)');
zlabel('a/2 (mm)');

grid on;
hold off;
```

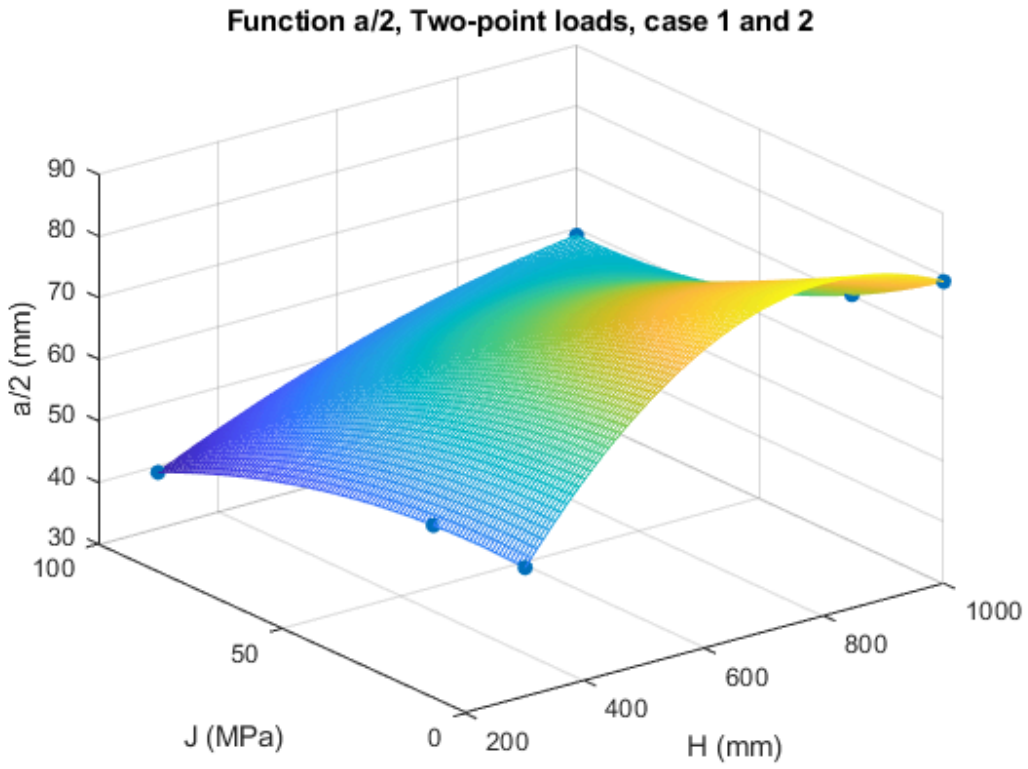

Published with MATLAB® R2021a

```
clc
clear all
```

Uniform distributed load, case 1 and 2

Given data

```
H = [1000; 1000; 1000; 300; 300; 300]; % Heights in mm
J = [0; 25; 100; 0; 25; 100]; % Jacking forces in MPa
a = [82; 76; 64; 60; 59; 54]; % Unknown values

% Create the design matrix
X = [ones(size(H)), H, J, H.^2, H.*J, J.^2, H.*J.^2, H.^2.*J.^2];

% Perform the regression analysis
coefficients = X\a;

% Extract the coefficients
b = coefficients(1);
c = coefficients(2);
d = coefficients(3);
e = coefficients(4);
f = coefficients(5);
g = coefficients(6);
h = coefficients(7);
i = coefficients(8);

% Display the coefficients
disp(['b = ' num2str(b)]);
disp(['c = ' num2str(c)]);
disp(['d = ' num2str(d)]);
disp(['e = ' num2str(e)]);
disp(['f = ' num2str(f)]);
disp(['g = ' num2str(g)]);
disp(['h = ' num2str(h)]);
disp(['i = ' num2str(i)]);
```

```
b = 0
c = 0.25057
d = 0.06381
e = -0.00016857
f = -0.00032381
g = 0
h = -1.6127e-06
i = 2.4127e-09
```

```
% Create a grid of points for H and J
[H_mesh, J_mesh] = meshgrid(min(H):10:max(H), min(J):1:max(J));

% Evaluate the quadratic equation using the estimated coefficients
a_mesh = b + c * H_mesh + d * J_mesh + e * H_mesh.^2 + f * H_mesh .*
 J_mesh + g * J_mesh.^2 + h * H_mesh .* J_mesh.^2 + i * H_mesh.^2 .*
 J_mesh.^2;
```

```
% Plot the function
figure;
mesh(H_mesh, J_mesh, a_mesh);
xlabel('H (mm)');
ylabel('J (MPa)');
zlabel('a/2 (mm)');
title('Function a/2, Uniform distributed load, case 1 and 2');
hold on;

% Plot raw data
scatter3(H, J, a, 'filled');
xlabel('H (mm)');
ylabel('J (MPa)');
zlabel('a/2 (mm)');

grid on;
hold off;
```

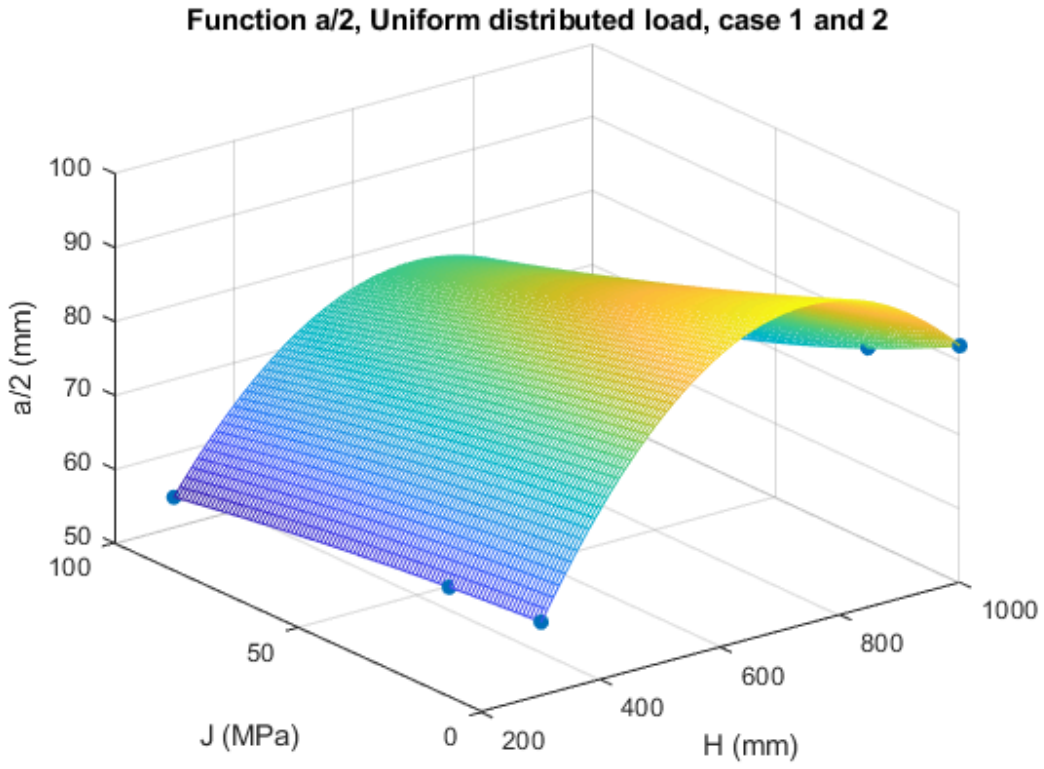

Published with MATLAB® R2021a

```
clc
clear all
```

One-point load, case 1 and 2

Given data

```
H = [1000; 1000; 1000; 300; 300; 300]; % Heights in mm
J = [0; 25; 100; 0; 25; 100]; % Jacking forces in MPa
a = [84; 79; 64; 45; 40; 35]; % Unknown values

% Create the design matrix
X = [ones(size(H)), H, J, H.^2, H.*J, J.^2, H.*J.^2, H.^2.*J.^2];

% Perform the regression analysis
coefficients = X\a;

% Extract the coefficients
b = coefficients(1);
c = coefficients(2);
d = coefficients(3);
e = coefficients(4);
f = coefficients(5);
g = coefficients(6);
h = coefficients(7);
i = coefficients(8);

% Display the coefficients
disp(['b = ' num2str(b)]);
disp(['c = ' num2str(c)]);
disp(['d = ' num2str(d)]);
disp(['e = ' num2str(e)]);
disp(['f = ' num2str(f)]);
disp(['g = ' num2str(g)]);
disp(['h = ' num2str(h)]);
disp(['i = ' num2str(i)]);
```

```
b = 0
c = 0.17829
d = -0.24762
e = -9.4286e-05
f = 4.7619e-05
g = 0
h = 6.3492e-06
i = -6.3492e-09
```

```
% Create a grid of points for H and J
[H_mesh, J_mesh] = meshgrid(min(H):10:max(H), min(J):1:max(J));

% Evaluate the quadratic equation using the estimated coefficients
a_mesh = b + c * H_mesh + d * J_mesh + e * H_mesh.^2 + f * H_mesh .*
 J_mesh + g * J_mesh.^2 + h * H_mesh .* J_mesh.^2 + i * H_mesh.^2 .*
 J_mesh.^2;
```

```
% Plot the function
figure;
mesh(H_mesh, J_mesh, a_mesh);
xlabel('H (mm)');
ylabel('J (MPa)');
zlabel('a/2 (mm)');
title('Function a/2,One-point load, case 1 and 2');
hold on;

% Plot raw data
scatter3(H, J, a, 'filled');
xlabel('H (mm)');
ylabel('J (MPa)');
zlabel('a/2 (mm)');

grid on;
hold off;
```

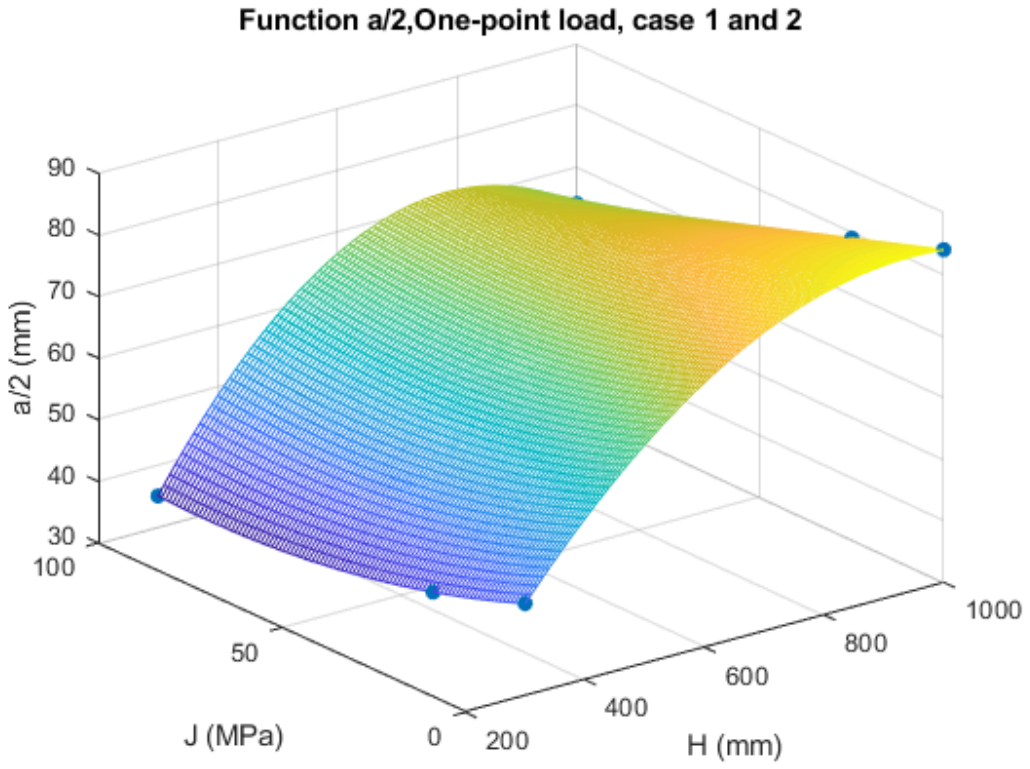

Published with MATLAB® R2021a

```
clc
clear all
```

Two-point loads, case 1 and 3

Given data

```
H = [1000; 1000; 1000; 300; 300; 300]; % Heights in mm
J = [0; 25; 100; 0; 25; 100]; % Jacking forces in MPa
a = [79; 70; 56; 51; 45; 37]; % Unknown values

% Create the design matrix
X = [ones(size(H)), H, J, H.^2, H.*J, J.^2, H.*J.^2, H.^2.*J.^2];

% Perform the regression analysis
coefficients = X\a;

% Extract the coefficients
b = coefficients(1);
c = coefficients(2);
d = coefficients(3);
e = coefficients(4);
f = coefficients(5);
g = coefficients(6);
h = coefficients(7);
i = coefficients(8);

% Display the coefficients
disp(['b = ' num2str(b)]);
disp(['c = ' num2str(c)]);
disp(['d = ' num2str(d)]);
disp(['e = ' num2str(e)]);
disp(['f = ' num2str(f)]);
disp(['g = ' num2str(g)]);
disp(['h = ' num2str(h)]);
disp(['i = ' num2str(i)]);
```

```
b = 0
c = 0.209
d = -0.21762
e = -0.00013
f = -0.00018571
g = 0
h = 5.6063e-06
i = -3.873e-09
```

Create a grid of points for H and J

```
[H_mesh, J_mesh] = meshgrid(min(H):10:max(H), min(J):1:max(J));

% Evaluate the quadratic equation using the estimated coefficients
```

```
a_mesh = b + c * H_mesh + d * J_mesh + e * H_mesh.^2 + f * H_mesh .*
 J_mesh + g * J_mesh.^2 + h * H_mesh .* J_mesh.^2 + i * H_mesh.^2 .*
 J_mesh.^2;

% Plot the function
figure;
mesh(H_mesh, J_mesh, a_mesh);
xlabel('H (mm)');
ylabel('J (MPa)');
zlabel('a/2 (mm)');
title('Function a/2, Two-point loads, case 1 and 3');
hold on;

% Plot raw data
scatter3(H, J, a, 'filled');
xlabel('H (mm)');
ylabel('J (MPa)');
zlabel('a/2 (mm)');

grid on;
hold off;
```

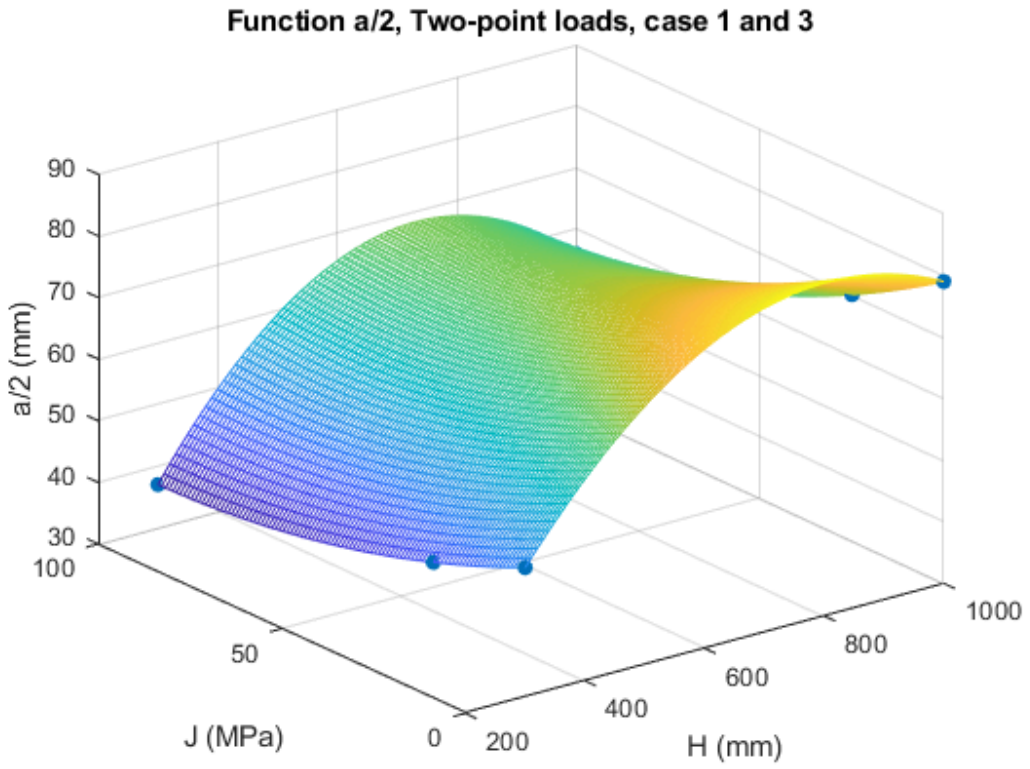

Published with MATLAB® R2021a

```
clc
clear all
```

Uniform distributed load, case 1 and 3

Given data

```
H = [1000; 1000; 1000; 300; 300; 300]; % Heights in mm
J = [0; 25; 100; 0; 25; 100]; % Jacking forces in MPa
a = [82; 75; 61; 60; 49; 40]; % Unknown values

% Create the design matrix
X = [ones(size(H)), H, J, H.^2, H.*J, J.^2, H.*J.^2, H.^2.*J.^2];

% Perform the regression analysis
coefficients = X\a;

% Extract the coefficients
b = coefficients(1);
c = coefficients(2);
d = coefficients(3);
e = coefficients(4);
f = coefficients(5);
g = coefficients(6);
h = coefficients(7);
i = coefficients(8);

% Display the coefficients
disp(['b = ' num2str(b)]);
disp(['c = ' num2str(c)]);
disp(['d = ' num2str(d)]);
disp(['e = ' num2str(e)]);
disp(['f = ' num2str(f)]);
disp(['g = ' num2str(g)]);
disp(['h = ' num2str(h)]);
disp(['i = ' num2str(i)]);
```

```
b = 0
c = 0.25057
d = -0.61286
e = -0.00016857
f = 0.00030952
g = 0
h = 1.4838e-05
i = -1.3905e-08
```

Create a grid of points for H and J

```
[H_mesh, J_mesh] = meshgrid(min(H):10:max(H), min(J):1:max(J));

% Evaluate the quadratic equation using the estimated coefficients
```

```
a_mesh = b + c * H_mesh + d * J_mesh + e * H_mesh.^2 + f * H_mesh .*
 J_mesh + g * J_mesh.^2 + h * H_mesh .* J_mesh.^2 + i * H_mesh.^2 .*
 J_mesh.^2;

% Plot the function
figure;
mesh(H_mesh, J_mesh, a_mesh);
xlabel('H (mm)');
ylabel('J (MPa)');
zlabel('a/2 (mm)');
title('Function a/2,Uniform distributed load, case 1 and 3');
hold on;

% Plot raw data
scatter3(H, J, a, 'filled');
xlabel('H (mm)');
ylabel('J (MPa)');
zlabel('a/2 (mm)');

grid on;
hold off;
```

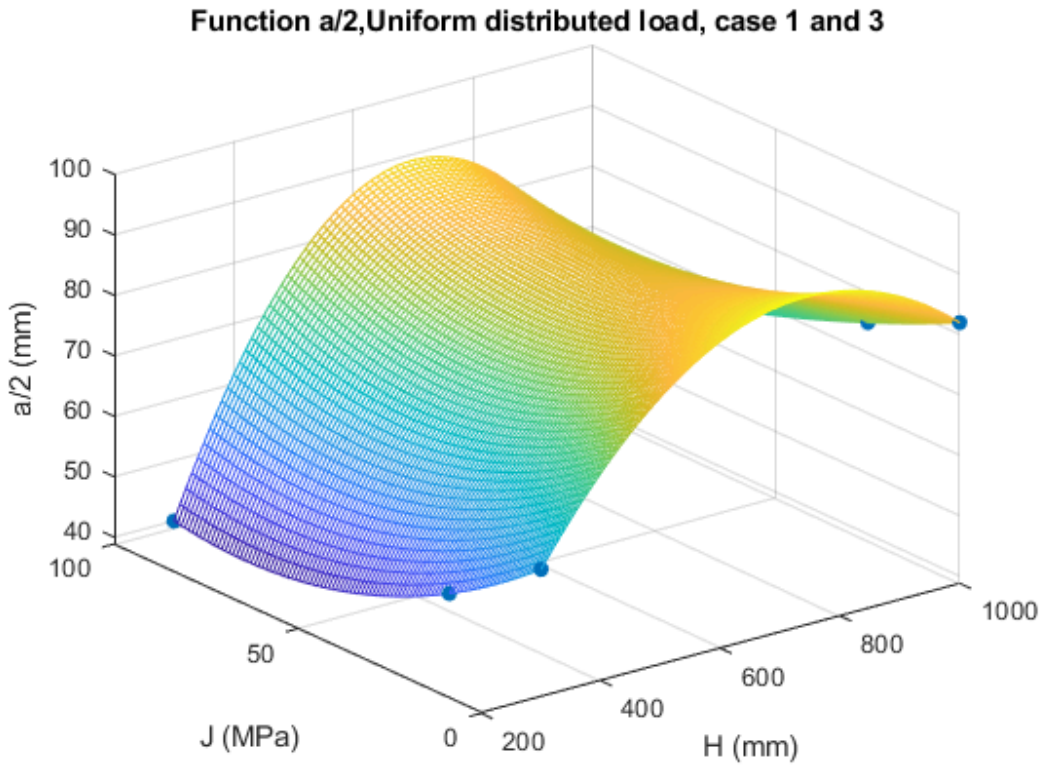

Published with MATLAB® R2021a

```
clc
clear all
```

One-point load, case 1 and 3

Given data

```
H = [1000; 1000; 1000; 300; 300; 300]; % Heights in mm
J = [0; 25; 100; 0; 25; 100]; % Jacking forces in MPa
a = [84; 78; 63; 45; 40; 38]; % Unknown values

% Create the design matrix
X = [ones(size(H)), H, J, H.^2, H.*J, J.^2, H.*J.^2, H.^2.*J.^2];

% Perform the regression analysis
coefficients = X\a;

% Extract the coefficients
b = coefficients(1);
c = coefficients(2);
d = coefficients(3);
e = coefficients(4);
f = coefficients(5);
g = coefficients(6);
h = coefficients(7);
i = coefficients(8);

% Display the coefficients
disp(['b = ' num2str(b)]);
disp(['c = ' num2str(c)]);
disp(['d = ' num2str(d)]);
disp(['e = ' num2str(e)]);
disp(['f = ' num2str(f)]);
disp(['g = ' num2str(g)]);
disp(['h = ' num2str(h)]);
disp(['i = ' num2str(i)]);
```

```
b = 0
c = 0.17829
d = -0.24048
e = -9.4286e-05
f = -9.5238e-06
g = 0
h = 8.0825e-06
i = -7.6825e-09
```

Create a grid of points for H and J

```
[H_mesh, J_mesh] = meshgrid(min(H):10:max(H), min(J):1:max(J));

% Evaluate the quadratic equation using the estimated coefficients
```

```
a_mesh = b + c * H_mesh + d * J_mesh + e * H_mesh.^2 + f * H_mesh .*
 J_mesh + g * J_mesh.^2 + h * H_mesh .* J_mesh.^2 + i * H_mesh.^2 .*
 J_mesh.^2;

% Plot the function
figure;
mesh(H_mesh, J_mesh, a_mesh);
xlabel('H (mm)');
ylabel('J (MPa)');
zlabel('a/2 (mm)');
title('Function a/2, One-point load, case 1 and 3');
hold on;

% Plot raw data
scatter3(H, J, a, 'filled');
xlabel('H (mm)');
ylabel('J (MPa)');
zlabel('a/2 (mm)');

grid on;
hold off;
```

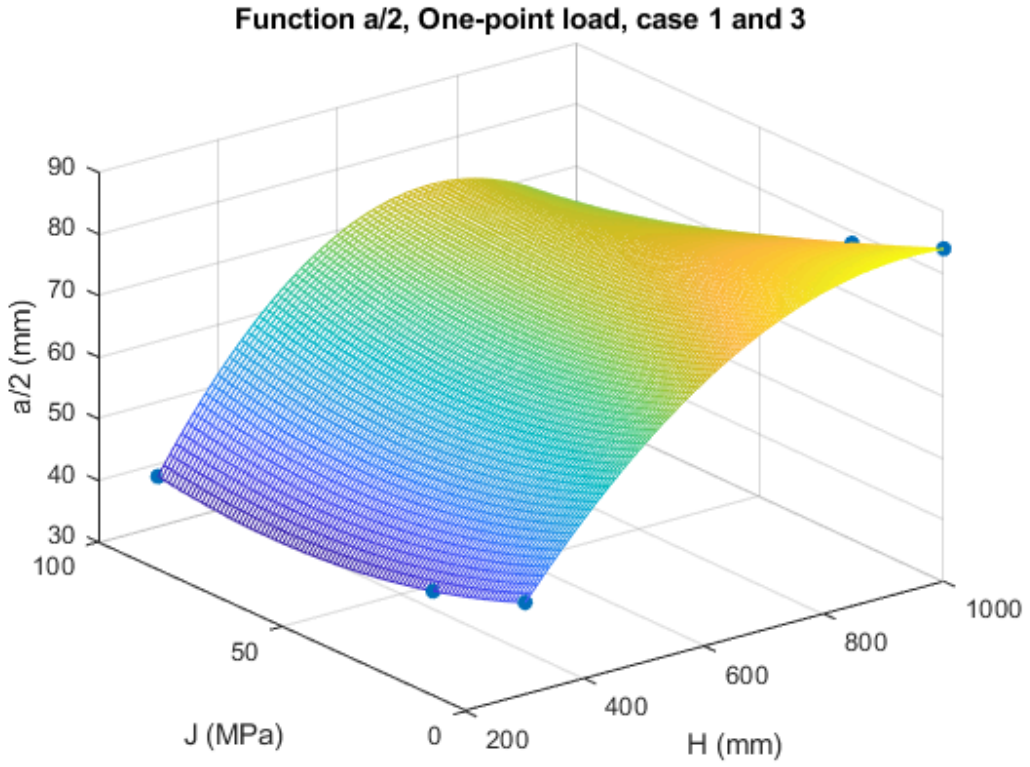

Published with MATLAB® R2021a